University of Kentucky

UKnowledge

Theses and Dissertations--Pharmacy

College of Pharmacy

2012

CLINICAL EVALUATION OF NOVEL METHODS FOR EXTENDING MICRONEEDLE PORE LIFETIME

Nicole K. Brogden
University of Kentucky, nkbrog2@uky.edu

Recommended Citation

CLINICAL EVALUATION OF NOVEL METHODS FOR EXTENDING MICRONEEDLE
PORE LIFETIME

_____

DISSERTATION
_____

A dissertation submitted in partial fulfillment

of the requirements for the degree of Doctor of Philosophy in the

College of Pharmacy

at the University of Kentucky

By

Nicole K. Brogden

Lexington, Kentucky

Director: Dr. Audra L. Stinchcomb, Professor of Pharmaceutical Sciences

Lexington, Kentucky

2012

ABSTRACT OF DISSERTATION

CLINICAL EVALUATION OF NOVEL METHODS FOR EXTENDING MICRONEEDLE
PORE LIFETIME

Microneedles are a minimally invasive method for delivering drugs through the impermeable skin layers, and have been used to deliver a variety of compounds including macromolecules, vaccines, and naltrexone. Microneedles can be applied to the skin once, creating micropores that allow for drug delivery into the underlying circulation from a drug formulation. The utility of this technique, however, is blunted by rapid micropore closure. This research project sought to: 1) characterize micropore lifetime and re-sealing kinetics, and 2) prolong micropore lifetime via inhibition of the skin's barrier restoration processes. Impedance spectroscopy was used as a surrogate technique in animals and humans to measure micropore formation and lifetime. A proof of concept study in humans, using impedance spectroscopy, demonstrated that diclofenac (a topical anti-inflammatory) applied to microporated skin resulted in slower re-sealing kinetics compared to placebo, in agreement with previous animal studies. The clinical feasibility of prolonging micropore lifetime with diclofenac was confirmed via 7-day delivery of naltrexone through microneedle treated skin in humans (compared to 72 hour delivery with placebo). Lastly, naltrexone gels with calcium salts were applied to microneedle treated skin (hairless guinea pigs) to restore the altered epidermal calcium gradient; this method did not significantly extend micropore lifetime.

KEYWORDS: diclofenac, impedance, microneedles, naltrexone, transdermal

Nicole K. Brogden
Student's signature

July 17, 2012
Date

CLINICAL EVALUATION OF NOVEL METHODS FOR EXTENDING MICRONEEDLE
PORE LIFETIME

By

Nicole K. Brogden

Dr. Audra L. Stinchcomb
Director of Dissertation

Dr. Jim Pauly
Director of Graduate Studies

July 17, 2012
Date

DEDICATION

This entire body of work is dedicated to my parents,
who have provided immense support, encouragement, and guidance throughout all of
my academic endeavors.

ACKNOWLEDGEMENTS

Listen to the MUSTN'TS, child,
Listen to the DON'TS,
Listen to the SHOULDN'TS
The IMPOSSIBLES, the WON'TS
Listen to the NEVER HAVES
Then listen close to me –
Anything can happen, child,
ANYTHING can be.

– Shel Silverstein

It is not an overstatement that this work could not have been completed without the expertise and support of a large number of people. I extend my sincerest thanks to Dr. Audra Stinchcomb for the opportunity to be involved in a clinically relevant and human-focused research project. I have grown as both a pharmacist and research investigator through completion of this work. Additionally, Dr. Stinchcomb was extremely generous to support me in completing my studies at University of Kentucky after she relocated for a new faculty position at University of Maryland, Baltimore. Next, I wish to thank the complete dissertation committee, and outside examiner, respectively: Dr. E. Penni Black, Dr. Charles Loftin, Dr. Susan S. Smyth, and Dr. Kimberly Anderson. My committee was extremely supportive throughout my training, particularly after Dr. Stinchcomb began her new position in Baltimore. Dr. Leslie Crofford, as my clinical mentor and study physician on all of the human studies, has been generous beyond words in the support she provided me. She selflessly agreed to mentor me through all of my clinical work, and I am deeply grateful for her continued encouragement and mentoring. The love and support of my parents, Kim and Katherine Brogden, has been unwavering during my long academic training (from pharmacy school through residency

iii

TABLE OF CONTENTS

LIST OF TABLES

LIST OF FIGURES

LIST OF ABBREVIATIONS

w/w	weight per weight
w/v	weight per volume
°C	degrees Celsius
μm	micrometer
ACN	acetonitrile
ANOVA	analysis of variance
APCI	atmospheric pressure chemical ionization
AUC	area under the curve
Cl	clearance
cm	centimeter
C_{max}	Maximum plasma concentration
C_{ss}	Plasma concentration at steady state
COX	cyclooxygenase
FDA	Food and Drug Administration
J	flux
hr	hour
HCl	hydrochloride
HEC	hydroxyethylcellulose
HEPES	4-(2-hydroxyethyl)-1-piperazineethanesulfonic acid
HPLC	high performance liquid chromatography
IACUC	Institutional Animal Care and Use Committee
IS	Impedance spectroscopy
IV	intravenous
kHz	kilohertz
kg	kilogram
LC-MS/MS	liquid chromatography-tandem mass spectroscopy
log $K_{o/w}$	logarithm of octanol-water partition coefficient
logP	logarithm of permeability coefficient
MeOH	methanol
mg	milligram
mHz	millihertz
min	minute
ml	milliliter

mm	millimeter
mM	millimolar
MN(s)	microneedle(s)
MW	molecular weight
n	number
ng	nanogram
NSAID	non-steroidal anti-inflammatory drugs
NTX•HCl	naltrexone hydrochloride salt
NTXol	6-β-naltrexol free base
NTXol•HCl	6-β-naltrexol hydrochloride salt
pH	negative logarithm of hydronium ion concentration
pK_a	acid ionization constant
PGs	prostaglandins
r^2	coefficient of determination
SC	stratum corneum
SD	standard deviation
SDS	sodium dodecyl sulfate
TEWL	transepidermal water loss
T_{lag}	Time until appearance of drug in the plasma
T_{max}	Time of maximum plasma concentration
UV	ultraviolet

Chapter 1
Statement of the problem

Two of the most common routes for drug delivery include oral and injectable formulations. Oral drug delivery is not optimal in many situations for reasons that include gastrointestinal side effects, extensive first-pass metabolism, enzymatic degradation, and poor bioavailability. A common alternative is to deliver the drug via injection with a hypodermic needle, which is painful, invasive, and less convenient for the patient. Transdermal drug delivery is a unique technique that avoids many of the problematic adverse events common to other drug delivery methods. Transdermal systems, by way of patches that adhere to the skin, offer several key advantages over oral and parenteral delivery. Drug patches applied to the skin are convenient and painless for patients to self-administer, allowing for prolonged zero-order drug delivery and avoidance of first pass metabolism. Despite its clear advantages, passive transdermal delivery is restricted to a very small number of drugs (approximately 20 drug compounds) because of the strict physicochemical properties required for a drug to diffuse through the skin [1-3]. The stratum corneum (SC) is the outermost layer of the skin and serves as the primary barrier to passive transdermal drug delivery because of its unique structure. Due to its composition of rigid keratinocytes embedded in a lipid matrix, the SC greatly limits the number of drug compounds that can be transdermally delivered. Favorable candidates for percutaneous delivery are traditionally small in size (molecular weight <500 Daltons), have a $logK_{o/w}$ of ~2, low melting point, and are effective at low doses [1]. In an effort to increase the number of molecules that can be transdermally delivered, a number of physical enhancement techniques have been explored to disrupt the barrier function of the SC; these include such methods as iontophoresis, electroporation, sonophoresis, and microneedles [2-5].

Microneedles (MNs) by definition are small needles of approximately 100 – 1000 μm in length; the MNs assist with the transport of drug molecules across the skin by piercing and creating microchannels (also called micropores) in the SC, thereby increasing its permeability [6]. This physical enhancement technique is minimally invasive, painless, and well tolerated by most patients [7]. In fact, the first MN product was recently introduced to the US market with the Fluzone® intradermal vaccine (Sanofi Pasteur), released for the 2011 – 2012 influenza season [8]. There are several ways that MNs can assist in the transdermal delivery of drug molecules, though arguably the simplest method is known as the "poke (press) and patch" method. This method

involves one-time application of solid MNs to painlessly pierce the skin and create micron-scale channels or pores in the SC. These channels enhance the permeability of various molecules from a drug patch, gel, or solution, by providing a new pathway by which a drug compound can passively diffuse through the SC and into the underlying circulation.

Newer advances using the "poke (press) and patch" method have shown promising results towards the clinical utility of this method of MN application, including the delivery of naltrexone (NTX), an opioid antagonist used as a treatment for alcohol and opioid addiction [9]. Several problems exist with currently available formulations of NTX, including extensive first-pass metabolism and hepatotoxicity associated with the oral formulation (ReVia®), and the high cost and inconvenience of the monthly injectable formulation (Vivitrol®). NTX serves as an excellent compound for development of a MN-assisted delivery system for a variety of reasons. First, a transdermal formulation would be optimal for increasing the clinical usefulness of NTX for opioid and alcohol addiction by avoiding some of the downfalls of the currently available oral and injectable preparations. In that regard, NTX is an ideal candidate for delivery via percutaneous methods. From a practical perspective, however, the physiochemical properties of the molecule, specifically its hydrophilicity, do not allow it to pass through the skin barrier and achieve therapeutic concentrations, rendering NTX an excellent compound for development of physical enhancement techniques. Due to the unique structure of the SC, increasing hydrophobicity generally contributes to better permeability through the skin, and many studies have already been completed in an attempt to increase the hydrophobicity of naltrexone via prodrug methods. One problem that arises, however, is that the aqueous solubility of NTX is desirable to allow the drug to partition into interstitial fluid once it has passed through the skin. This creates a significant challenge for delivering NTX via traditional transdermal delivery approaches. Conversely, these properties make NTX an excellent candidate for studying MN-enhanced delivery, as the newly created micropores allow NTX to pass through the SC, regardless of its hydrophilic nature, where it can readily be measured in the plasma. A recent study described the transdermal delivery of NTX in healthy human subjects following pretreatment with solid MNs [9]. In those subjects pretreated with MNs, application of a NTX patch yielded therapeutic blood levels, while application of the NTX patch without MN pretreatment did not lead to the detection of therapeutic levels. This further confirms that NTX alone does not appreciably permeate the SC, but a MN treatment approach

can help to bypass this problem in a painless and well-tolerated approach.

One of the greatest challenges associated with the poke and patch method is the skin's ability to heal the micropores in a very short period of time following MN placement. If the skin remains exposed to air immediately after MN application, the micropores can heal in as little as 15 minutes; this timeframe can be extended to approximately 2 – 3 days when the skin is occluded with an impermeable membrane or patch [9-14]. The short lifetime of the micropores would severely limit the utility of MN application in a clinical setting, and therefore it is important to develop effective means of extending the lifetime of micropores created by MN insertion (ideal dosing of a transdermal patch is once weekly). For all the reasons mentioned above, NTX is an excellent pharmacokinetic model compound for assessing micropore lifetime under various conditions. Previous work has demonstrated that topical application of diclofenac sodium to MN-treated skin results in transdermal delivery of NTX for 7 days in hairless guinea pigs, as compared to only 2.5 days in the absence of diclofenac sodium [11]. These results suggest that mild, subclinical inflammation may be contributing to the micropore closure process *in vivo,* which can be attenuated via simple application of a non-specific cyclooxygenase inhibitor.

The overall aim of this work was to extend micropore lifetime after one application of a MN array in order to allow for transdermal delivery of a model compound for a 7 day period in human subjects. These methods will be carried out with NTX as an ideal model compound, but the methods developed herein could ultimately be extrapolated to other compounds as well. The underlying hypothesis of this research is that the lifetime of the micropores in the SC can be prolonged by inhibiting early stages of the wound healing process, focusing most specifically on local subclinical inflammation. Achievement of the aims in this work will not only be advantageous for delivering NTX, but may also permit the development of once-weekly MN-assisted transdermal systems that are patient friendly and clinically advantageous for a variety of drug compounds.

Chapter 2
Research hypotheses

The objective of this research project was twofold:

1) Characterize the lifetime of micropores and kinetics of re-sealing, using impedance spectroscopy as an *in vivo* surrogate technique and pharmacokinetic analysis to define drug delivery parameters; and

2) Prolong the lifetime of the micropores via inhibition of various components of the skin's normal wound healing and barrier restoration processes.

Under these primary objectives, the research was driven by the following hypotheses.

Hypothesis 1: MN treatment of healthy skin disrupts the permeability barrier of the stratum corneum, resulting in significantly lower impedance to the flow of electrical current between the body and external environment.

It is important to develop an appropriate *in vivo* model for studying the kinetics of micropore closure following MN treatment in animal models and human subjects. One means of measuring skin permeability barrier function is impedance spectroscopy, which can be used as a complementary or alternative technique to transepidermal water loss (TEWL, a commonly used technique for evaluating permeability barrier function). The SC serves as the skin's barrier to movement of ions (i.e. flow of electrical current), such that the impedance spectrum of the skin changes with disruption of the SC. The impedance decreases if the skin is damaged, and this has been demonstrated as a reliable method of evaluating barrier function. Accurate measurements can be collected in a clinical environment without any computers, software, or need for a highly controlled environment, making this a valuable tool for various environments. Impedance measurements of the SC using various methods and techniques have been described previously, but there are limited publications describing the use of this technique to evaluate micropore lifetime following MN treatment (in animal models or human subjects). A methods development study is necessary to optimize the techniques and electrode types required to minimize variability and optimize reproducibility.

Hypothesis 2: The processes involved in the skin's normal healing and barrier restoration following injury also govern micropore re-sealing, and inhibition of these normal paradigms will result in a clinically relevant extension of micropore lifetime following one-time application of a MN array.

The physiological processes underlying micropore closure following MN treatment are not currently understood, and elucidation of the specific pathways involved would provide therapeutic targets for prolonging the lifetime of the micropores. The skin follows a well-defined sequence of events following injury, and local inflammation (through activation of the arachidonic acid pathway) is one of the first steps. It is possible that subclinical inflammation at a microscopic level may also contribute to the micropore closure process, which could be inhibited via topical application of diclofenac sodium (a non-specific inhibitor of the cyclooxygenase enzymes involved in the arachidonic acid pathway). Additionally, a calcium gradient exists in the unperturbed epidermis, such that high concentrations of extracellular Ca^{2+} are found in the upper epidermis. Following barrier disruption, increased water movement within the SC dissipates the gradient, and this change appears to be one of the primary signals for restoring barrier function. Following disruption via MN application, the Ca^{2+} gradient would likely be disrupted and thus may serve as an additional target to investigate for prolonging micropore lifetime.

Hypothesis 3: Local concentrations of diclofenac in MN-treated skin will not be significantly different in the presence or absence of naltrexone, allowing for co-application of a locally delivered anti-inflammatory and a systemically delivered model compound.

The diclofenac sodium formulation in these studies is delivered from a commercially available preparation called Solaraze®, which consists of 3% diclofenac in a 2.5% hyaluronate sodium vehicle. Following topical application, this unique vehicle creates a depot of diclofenac in the epidermis, providing an ideal situation for locally inhibiting any inflammation that may be involved in micropore closure. A pharmacokinetic study in humans will be completed to characterize the delivery of naltrexone HCl in the presence or absence of diclofenac sodium, but it is important to confirm that the local concentrations of diclofenac are maintained despite the flux of naltrexone HCl through the skin into the systemic circulation in the dermis. These

studies will allow for calculation of an appropriate dose and schedule for co-applying diclofenac and naltrexone HCl for a human pharmacokinetic study.

Hypothesis 4: Inhibition of subclinical inflammatory processes involved in micropore re-sealing will allow a therapeutically relevant dose of naltrexone to be delivered through the skin for up to 7 days in healthy human subjects.

While the overall intent of this research is to prolong the dosing interval following one application of a MN array, extending micropore closure kinetics is only clinically significant if a drug can be delivered to a therapeutically relevant concentration for the duration of the micropore lifetime. A pharmacokinetic study is the best way to characterize the drug diffusion window for the micropores. Naltrexone HCl is an excellent model compound to study because previous work allows for comparison of a drug delivery window under conditions of occlusion without co-application of any active moiety to prolong micropore lifetime. In contrast, inhibition of the skin's inflammatory responses should prolong the drug delivery window by allowing the micropores to remain viable for up to 7 days.

Hypothesis 5: A good correlation exists between *in vitro* flux data and *in vivo* plasma concentrations of naltrexone in human subjects

The plasma concentrations of naltrexone HCl obtained from a pharmacokinetic study in human subjects with MNs should have a strong correlation with the *in vitro* flux data that is used to calculate the patch number and estimate the plasma concentrations over 7 days. This will validate the *in vitro* diffusion studies and provide parameter estimates for future pharmacokinetic studies.

Chapter 3
Research plan

3.1 Develop an impedance spectroscopy technique as a surrogate marker to monitor micropore formation and lifetime

Several methods exist for monitoring barrier disruption in the SC, though many of these techniques are highly sensitive to environmental humidity and skin hydration, or require sophisticated instrumentation and software that makes use in a clinical environment cumbersome. Impedance spectroscopy avoids these pitfalls, and is a reliable method for monitoring the skin's barrier function. The SC is relatively non-conductive and does not permit the movement of electrical current. As such, the impedance of intact skin is very high (indicating an intact barrier) but perturbation of the barrier results in a decrease in the impedance. Impedance has been described to monitor the lifetime of micropores in the skin of human volunteers under occluded and non-occluded conditions, demonstrating its usefulness in this type of physical enhancement [14]. Several types of electrodes and impedance setups exist, and it is necessary to develop an experimental setup that introduces the least amount of error and variability to measure micropore formation. The objective of this study is to develop an impedance spectroscopy setup that can monitor SC barrier function and micropore re-sealing with the least amount of variability. Healthy human volunteers will be treated with 100 MN insertions per site (50 MN array applied twice) at 6 sites on the upper arm following an overnight pre-hydration period. Impedance measurements will be made pre- and post-MN using an impedance meter (EIM-105 Prep-Check Electrode Impedance Meter; General Devices, Ridgefield, NJ) connected by lead wires to reference and measurement electrodes and modified by a 200 kΩ resistor in parallel (IET labs, Inc., Westbury, NY). Three sites will be evaluated with dry Ag/AgCl electrodes (10 mm active electrode diameter; 25 mm x 25 mm total area; Thought Technology T-3404; Stens Corporation, San Rafael, CA), and the other sites will be evaluated with gel Ag/AgCl electrodes (10 mm active electrode diameter; 50 mm diameter; S&W Healthcare Corporation, Brooksville, FA). Measurements will be made in triplicate at each site, and two application pressures will be examined: light pressure (to simply hold the electrode o the surface of the skin) or direct pressure applied by the thumb of the investigator (to create greater contract between the skin and the electrode surface).

3.2 Characterize the kinetics of micropore closure following topical application of diclofenac to microneedle-treated skin in healthy human volunteers

While the specific physiologic processes contributing to micropore closure are not well defined, one of the underlying hypotheses of this project is that local subclinical inflammation at the micropores may contribute to the rapid re-sealing time. Thus, the objective of this study is to demonstrate prolonged micropore lifetime in the presence of diclofenac sodium (a non-specific COX inhibitor) vs. placebo conditions. Ten volunteers will be treated on the arm with a MN array ± diclofenac sodium or placebo gel; control sites will also be included. The kinetics of micropore lifetime under various timeframes of skin pre-hydration (0, 24, or 72 hours) will be measured with impedance spectroscopy as a surrogate *in vivo* technique. Measurements will be taken at baseline, post-MN, and daily thereafter for a total of 5 days (2 subjects will be treated for a full 7 day period and will only have one measurement at 96 hours into the study, rather than daily). Impedance of the micropores will be calculated assuming 3 parallel and independent pathways in the impedance setup (Z_{skin}, Z_{box}, and Z_{pores}), and the micropore impedance will be converted to admittance ($1/Z_{pores}$), to more closely mimic the trends observed with transepidermal water loss (another commonly utilized technique for monitoring skin barrier function). Area under the admittance-time curve will be calculated and the kinetics of micropore closure between diclofenac sodium and placebo treatment sites will be compared (paired t-test). In 6 subjects, skin irritation potential of the treatments will also be assessed via tristimulus colorimetry readings, taken in triplicate at each time point. The Δa^* value will be calculated from baseline (representing a change in the red-green axis) to quantify any local erythema.

3.3 Quantify *in vitro* diclofenac skin concentrations in Yucatan miniature pig skin following one-time microneedle treatment and application of diclofenac ± naltrexone

It is important to determine the local concentration of diclofenac sodium in MN-treated skin in conditions similar to those conditions described above in Research Plan 3.2, as this helps to estimate the amount needed to inhibit micropore closure. Additionally, diclofenac skin concentrations in other situations in which diclofenac sodium and naltrexone HCl gels are both applied to the skin should be examined, as this will mimic the setting for the *in vivo* pharmacokinetic study (described below in Research Plan 3.4). Yucatan miniature pig skin will be treated 20 times with a 5 MN array

(dimensions: 750 µm long, 200 µm wide, and 75 µm thick), to create a grid of 100 non-overlapping micropores. A PermeGear In-Line flow-through diffusion system (Hellertown, PA, USA) will be used. The receiver solution will consist of nanopure water with 20% EtOH, adjusted to a pH of 7.4. The experiments will be started by charging the cells with 100 – 200 µl of Solaraze®, ± 500 µl of an 11% naltrexone HCl gel. Samples will be collected at 6 hour intervals over a 7 day period, and stored at 4°C until analysis on HPLC. Skin will be taken down at 24 to 48 hour intervals for determination of skin diclofenac concentration. The skin will be rinsed 3 times with deionized water and blotted gently with Kimwipes® to remove excess drug from the skin surface. Skin samples will be tape stripped twice and the skin weight recorded. The skin will be suspended in acetonitrile and shaken in a 32°C water bath overnight. Diclofenac concentration will be analyzed by HPLC.

3.4 Determine *in vitro* microneedle-enhanced transdermal flux of naltrexone across Yucatan miniature pig skin in the presence of diclofenac

In order to calculate an appropriate number of patches suitable for a human pharmacokinetic study, it is necessary to determine the transdermal flux of naltrexone hydrochloride across MN-treated Yucatan miniature pig skin in the presence of diclofenac sodium delivered from Solaraze® (3% diclofenac sodium and 2.5% hyaluronate sodium). A PermeGear In-Line flow-through diffusion system (Hellertown, PA, USA) will be used for skin diffusion studies. The physiological receiver solution will consist of HEPES-buffered Hank's balanced salts with gentamicin, maintained at a flow rate of 1.5 ml/min and a temperature of 37° C. Yucatan miniature pig skin will be treated 20 times with a 5 MN array to create a grid of 100 non-overlapping micropores. The experiments will be started by charging the cells with 100 – 200 µl of Solaraze® and 500 µl of 11% naltrexone HCl gel. Samples will be collected at 6 hour intervals over a 7 day period, and stored at 4°C until analysis on HPLC. The cumulative quantity of NTX collected in the receiver solution will be plotted as a function of time and the flux determined from the slope of the line at steady state.

3.5 Establish the tolerability of a combination of a 3% diclofenac gel and an 11% naltrexone gel on microneedle-treated skin in hairless guinea pigs

In order to advance the optimal *in vitro* treatment conditions (determined in Research Plans 3.4 and 3.5) to human subjects, the skin irritation potential and

tolerability of the combination of diclofenac sodium and naltrexone HCl must be assessed. Hairless guinea pigs will be utilized for these studies, as these animals are typically more sensitive than humans to topical xenobiotics, providing a conservative model for assessing irritation potential to human skin. The hairless guinea pigs will be treated on the dorsal surface with arrays of 50 MNs applied twice to create 100 non-overlapping micropores. The microporated skin will be treated with 100 μl of Solaraze® and 500 μl of a 11% naltrexone HCl gel and covered by an occlusive, air-impermeable patch that is secured to the skin with Bioclusive medical tape. Tristimulus colorimetry will be used to assess local erythema at MN-treatment sites; non-MN sites will be used as controls. Measurements will be taken in triplicate at baseline and every 48 hours after application of the gels; fresh gels will be re-applied at each time point. The Δa* value will be calculated from baseline (representing a change in the red-green axis) to quantify local erythema.

3.6 Pharmacokinetic evaluation of microneedle/COX inhibitor-enhanced transdermal 7-day delivery of naltrexone in healthy human volunteers

The first pharmacokinetic study in humans with MN-assisted transdermal delivery demonstrated therapeutic plasma concentrations of naltrexone hydrochloride for 48 – 72 hours after one MN treatment [9]. This study, while confirming the ability of the "poke and patch" method to allow delivery to therapeutic drug concentrations, also demonstrated the relatively short period of drug delivery (2 – 3 days) after one application of MN arrays. Conversely, another study showed enhanced permeation of naltrexone for 7 days in hairless guinea pigs treated with MNs and diclofenac sodium, confirming that topical application of a non-specific COX inhibitor to microporated skin can extend the drug delivery window to a therapeutically relevant timeframe [11]. The objective of the current study is to characterize the clinical utility of extending micropore lifetime (with diclofenac sodium) by measuring plasma naltrexone concentrations in healthy human subjects over 7 days. Subjects will be treated with 50 MN arrays at 8 sites (to create a total of 800 micropores), followed by application of 100 μl of 3% diclofenac sodium gel and 500 μl of a 11% naltrexone hydrochloride gel (gels will be replaced every 48 hours). To confirm the formation (and monitor lifetime) of micropores in the SC, impedance spectroscopy measurements will be taken at baseline, immediately post-MN treatment, and 7 days post-MN. Blood samples will be taken at 9 time points on Day 0 (day of MN treatment), and daily thereafter, up to 7 days. Two

groups of control subjects will also be evaluated: a non-MN group (gels applied to intact skin), and a placebo group (diclofenac sodium gel replaced with a placebo gel formulation containing no anti-inflammatory moiety). All plasma samples will be analyzed for naltrexone and 6-β-naltrexol with LC-MS/MS (positive mode atmospheric pressure chemical ionization [APCI+]). All plasma samples and standards (200 μl volume) will be extracted with 1 ml of ethyl acetate:acetonitrile (1:1, v/v), resulting in protein precipitation. The samples in ethyl acetate:acetonitrile mixture will be vortexed for 15 seconds and centrifuged for 20 minutes at 12000xg. The supernatant will be transferred to a glass tube and evaporated under nitrogen. The resulting residue will be reconstituted in 200 μl acetonitrile, vortexed for 15 seconds, and sonicated for 10 minutes. Samples will be transferred into low volume inserts in HPLC vials and injected onto the LC-MS/MS system.

3.7 Pharmacokinetic evaluation of microneedle-enhanced transdermal 7-day delivery of naltrexone following restoration of the Ca^{2+} epidermal gradient in hairless guinea pigs

Dissipation of the epidermal Ca^{2+} gradient is one of the skin's primary signals for restoring barrier function after disruption via chemical or physical means. Restoration of the gradient would prevent the skin from re-sealing the micropores after one-time application of a MN array. The objective of these studies is to characterize the percutaneous delivery of naltrexone HCl through MN-treated skin in hairless guinea pigs, from gels containing various calcium salts (chloride, citrate, gluconate). The guinea pigs will be treated at 2 sites on the dorsal surface with a 50 MN array applied twice at each site (to create a total of 200 micropores), followed by application of a 11% naltrexone HCl gel containing a calcium salt. Plasma samples will be taken over a 7 day period and assessed via LC-MS/MS with the methods described above in Research Plan 3.6.

Chapter 4

Background and literature review

4.1 Introduction

The skin could be mistakenly viewed as a simple cover to contain the body and internal organs. Conversely, skin is a metabolically active, complex tissue that serves as a 2-way barrier between the body and the external hostile environment. As the largest organ in the body, the skin is an excellent target for drug delivery purposes. Transdermal drug delivery has several distinct advantages over other common drug delivery routes (oral and intravenous), including avoidance of first-pass metabolism, allowing for a constant zero-order delivery profile for up to 7 days from one dose, and ease of application that enhances patient compliance. Despite these advantages, the unique structure and barrier of the skin presents significant challenges for the passive diffusion of most drug molecules, except for those drug molecules that possess a very specific combination of physicochemical characteristics that permit penetration through the outer layers of the skin.

4.2 Structure and function of the skin

The skin is the largest organ in the human body, and serves a multitude of functions. It represents the body's first defense against a hostile external environment, and as such it provides defenses against noxious chemical and microbial external insults and UV radiation. In addition, it provides critical homeostatic functions through the regulation of body temperature, blood pressure, and preventing excessive water loss [15, 16]. The skin is

Figure 4.1 Structure of the skin, adapted from: http://www.natural-skin-health.com/skinstructure.html.

composed of multiple layers, each with distinct characteristics that contribute to the overall function of this intricate organ. From the outside in, the layers of the skin include the stratum corneum (the outermost layer of the epidermis), viable epidermis, and the dermis.

4.2.1 Stratum corneum

The true interface between the body and the hostile external environment is the outermost layer of the skin, known as the stratum corneum (SC), or horny layer [15, 16]. It was believed to be a metabolically inactive tissue, similar to a plastic film, until the mid-1970s [15]. It is now known to be a biosensor with limited metabolic activities that can respond to external cues and insults. The SC is a multicellular layer that is approximately 10 to 15 μm thick over most of the body, though it is much thicker on the friction surfaces of the skin (palms and soles). This outermost layer of the skin serves many critical functions, as it prevents excessive water loss to the outside environment while protecting the body from external xenobiotics and microbes. Structurally, the SC has been described as a "brick and mortal" model, composed of fully differentiated keratinocytes ("bricks") embedded in a continuous lipid matrix ("mortar"). Mechanical strength of the barrier is provided by the keratinocytes, while the lipids serve as the barrier to water and electrolyte movement [15, 17]. This layer of the skin is structurally distinct from all other layers, imparting its unique barrier properties to the skin as a whole.

The mechanical strength of the SC is provided by the keratinocytes (corneocytes). Over most parts of the body, the SC is composed of approximately 10 – 15 layers of flattened keratinocytes (each with a mean thickness of about 1 μm) [15]. The individual keratinocytes are composed of keratin that fills up the cell, and a substance known as natural moisturizing factor, a mixture of amino acids and their derivatives, that helps to maintain the normal hydration of the SC (approximately 20% water under normal conditions) [18]. Natural moisturizing factor acts as a humectant by absorbing atmospheric water, thus allowing the SC to remain hydrated and not lose its moisture to the outside environment; maintaining this free water helps facilitate biochemical events within the SC [18]. The keratinocytes in the SC are encapsulated by a cornified envelope (CE) that is composed of insoluble proline-rich proteins (loricrin and involucrin) [15]. The CEs of neighboring keratinocytes are linked together by intercellular protein structures called corneodesmosomes [19]. These structures must be enzymatically degraded in order for the outermost layer of cells to be shed, in a process known as desquamation [19]. The entire SC is replaced and turned over every 2 weeks in healthy adults [15, 16].

The intercellular lipid matrix makes up approximately 15 - 20% of the SC volume, and provides the barrier to water and electrolyte movement [15-17]. These lipids are

notably different from other biological membranes, in that there is very little phospholipid present [15, 17]. The composition of the lipid species found in the SC is always in an equimolar ratio as follows: ceramides (50% by mass), cholesterol (25% by mass), and free fatty acids (10 - 20% by mass) [15, 17, 19]. These lipids are secreted as lamellar bodies from the keratinocytes. Lamellar bodies are unique to the epidermis (first seen in the stratum spinosum layer), and are membrane bilayer-encircled secretory organelles [17]. These lamellar bodies contain the lipids that serve as precursors to the SC extracellular lipids, and after secretion, these lipids are metabolized by enzymes that are also secreted in the lamellar bodies [17]. This sequence of events is known as "lipid processing" and is a critical step for the formation of a normal permeability barrier [17].

The extracellular processing of lipids has important effects with regard to the barrier function of the SC (in fact, many of the key functions of the SC are somewhat derived from the extracellular processing of lipids) [17]. For example, maintenance of the SC hydration is partly maintained by the glycerol formed by the breakdown of phospholipids [17]. Free fatty acids contribute to the acidic pH of the SC (the pH of the skin surface ranges from ~5 to 5.5 in humans and animals), and this acidity is very important for regulating activity of many of the SC enzymes [17]. If the pH is increased, the lipid processing is impaired, thereby decreasing the permeability barrier function [17].

4.2.2 Viable epidermis

The viable epidermis (often simply referred to as the 'epidermis', which includes the SC) is contained between the SC and the underlying dermis (it deserves note that the epidermis is often described as two distinct layers: the viable epidermis and the SC). The epidermis is approximately 50 – 100 µm thick and is completely avascular. From the perspective of drug delivery this section of the skin is viewed as one single diffusional field, though under microscopic evaluation it can be seen that multiple strata make up the epidermis (representing progressive differentiation of the cells towards the external skin surface). From outward in, the layers of the epidermis consist of the stratum corneum, stratum granulosum, stratum spinosum, and stratum basale [16, 19]

The cells of the basement layer of the epidermis (stratum basale) give rise to the cells that eventually comprise the SC; for this reason the stratum basale is often referred to as the germinative layer. The cells flatten and begin to internally synthesize lipids and proteins that will ultimately characterize a fully differentiated SC layer. Several distinct cell types are found within the epidermis, though the primary cells are keratinocytes.

Langerhans cells serve as the primary antigen presenting cells; melanocytes synthesize the pigment that gives unique colorations across different human races and these cells also produce the suntanning effect in response to ultraviolet radiation [16]. Additional cell types include lymphocytes and migrant macrophages, which are especially evident following skin trauma.
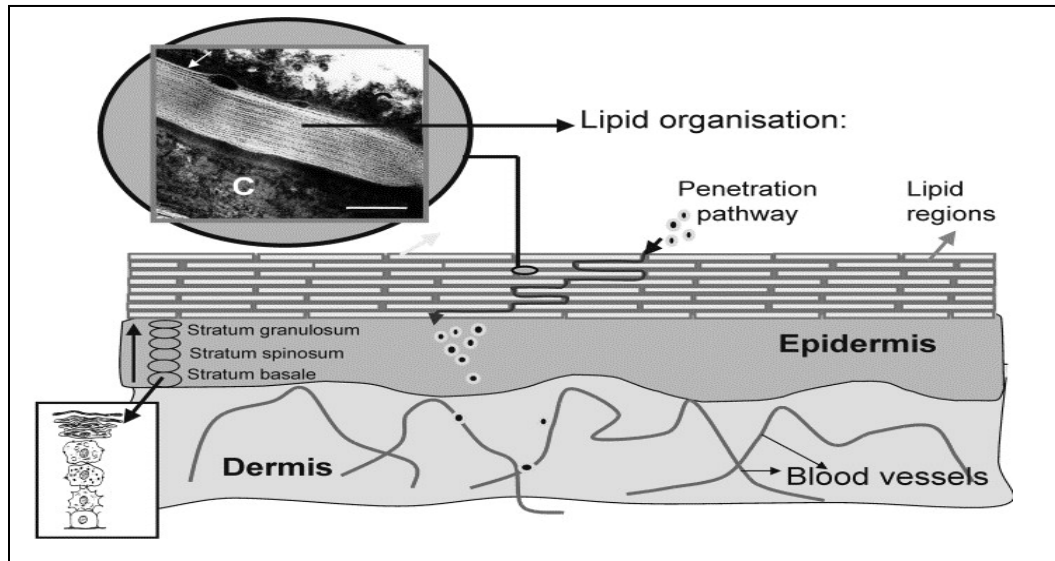
Figure 4.2 Cross-section of the skin depicting the various layers of the epidermis and dermis and the intercellular pathway of penetration for a xenobiotics.
Bouwstra *et al*, 2003. The epidermis is composed of several layers, including (from outside in): the stratum corneum, stratum granulosum, stratum spinosum, and stratum basale. The skin vasculature can be observed at the junction of the dermis and epidermis. Reprinted from *Progress in Lipid Research* with permission from Elsevier.

4.2.3 Dermis and microvasculature

The dermis lies sandwiched between the epidermis and the underlying subcutaneous tissue and is approximately 1 – 2 mm thick. This layer of the skin is quite complex and it provides the mechanical support of the skin structure [16, 19]. The structure of the epidermis is comprised of multiple components including collagen (75%), elastin (4%), reticulin (0.4%), and ground substance (20%, made of mucopolysaccharide gel), all woven into a mesh with structural fibers [16]. Various cell types are found in the

dermis, including: nerve cells and endings (sensors of the skin); endothelial cells that form the vessels of the vasculature; blood cells; fibroblasts that produce the structure fiber network; and mast cells responsible for production of ground substance and release of histamine following aggravation. The appendages of the skin arise in the dermis, including sebaceous glands, hair follicles, eccrine and apocrine sweat glands. Of particular importance, the dermis is highly vascularized, providing the circulation that serves all of the skin. The first point of entry for a drug into the systemic circulation occurs within the papillary plexus (a delicate capillary structure in the upper dermis). A rich lymphatic system is also present, in addition to a network of sensory nerves for pain, pressure, and temperature.

4.3 Transdermal drug delivery

Transdermal (percutaneous) drug delivery, by definition, is the delivery of drugs through the skin in order to elicit systemic effects [16, 20]. Transdermal delivery offers several unique advantages over oral and non-oral drug delivery. The skin provides a large surface area (1 – 2 m^2) that is readily available for drug absorption [1]. Transdermal systems can provide the option for a sustained release system, which is particularly beneficial for drugs with short elimination half-lives and frequent dosing requirements. Controlled kinetics for drug input can be achieved, while avoiding the peak and valley effects seen with oral and IV administration, and removal of the patch allows for easy termination of drug input. These are especially attractive qualities for delivering drugs possessing narrow therapeutic indices [1]. Applying a patch to the skin for drug delivery purposes is non-invasive, allowing for better patient acceptance and ease of application without need for a healthcare professional. The combination of all these factors would likely contribute to an increase in patient compliance, which would be the ultimate goal of any drug delivery system.

In spite of its clear and unique advantages, transdermal delivery is not suitable for all drugs and therapeutic indications. For example, a drug that already exhibits high bioavailability following oral administration, especially with infrequent dosing requirements would not necessarily warrant the use of percutaneous delivery. Additionally, any therapeutics that require a rapid bolus dosing or need to achieve high concentrations quickly would not be appropriate, as transdermal delivery generally provides a slower and sustained release profile over longer timeframes [1] . As such, there still remains a large number of drugs and biologics that would benefit from delivery

through the skin, but as of yet it has not been entirely feasible to commercially develop such systems.

4.3.1 Optimal properties of transdermally delivered drugs

One of the challenges associated with transdermal delivery is that only a small number of drugs can be delivered via this route, as there are several physicochemical properties that a molecule must possess in order to be a reasonable candidate (with currently available passive delivery methods). To be a viable contender for delivery via the transdermal route, the drug molecule should be relatively small in size (generally not more than a few hundred Daltons), have a low melting point (good solubility properties), and be highly skin permeable (octanol-water partition coefficients that favor lipids, ($logK_{oct}$ of ~2)). The structure should not contain a large number of pendant H groups, as the number of H groups reflects the ability of the drug moiety to interact with the polar head groups of the lipids in the SC. Additionally these types of molecules tend to be quite hydrophilic and therefore have a K_{oct} that is lower than optimal.

Generally unionized species will partition better into the skin (relating to the pKa, or ionization potential) [1, 21]. In order to be systemically delivered, a molecule must also be able to cross the viable epidermis and dermis to reach the blood vessels below. These regions of skin beneath the SC are a more hydrophilic environment than the lipid milieu of the SC. Thus, the drug compound must be hydrophilic enough to interact with this environment, but must be lipophilic enough to diffuse through the lipids of the SC. Models now exist to predict the maximum flux (J_{max}) of a compound based on three factors: 1) logarithm of the octanol-water partition coefficient, melting point, and molecular weight [22].

The drug should be potent in its effects (requiring doses of milligrams/day or less), and the drug compound itself should not pose any unwanted cutaneous actions [2, 16]. Other miscellaneous criteria (not related to the physicochemical properties of the molecule) that would make a drug an ideal candidate for development of a transdermal delivery system would include drugs that are subject to extensive first-pass hepatic metabolism, have an undesirable oral or intravenous dosage schedule, or drugs for which the currently available delivery systems have problems associated with compliance or adverse reactions.

4.3.2 Routes of skin penetration

With passive delivery techniques, there are 3 steps that must occur for a drug to be successfully delivered from the vehicle and through the skin. First, the drug must diffuse out of the vehicle and reach the vehicle-SC interface. Following this, the drug must partition into and diffuse through the SC to reach the viable epidermis below. The final step is the diffusion of the drug through the dermis and then into the microcirculation [20]. Based on the general structure of the skin, there are 3 major diffusion pathways that a drug molecule can take through the skin: 1) through the continuous lipid matrix in the SC (intercellular route); 2) directly through the keratinocytes (transcellular route); or 3) appendageal route (hair follicles and sweat glands) [16, 23, 24]. The various routes of skin penetration are displayed in Figure 4.3.

4.3.2.1 Intercellular: The lipid matrix of the SC in which the keratinocytes are embedded provides the only continuous phase throughout the SC, and this is thought to be the primary pathway of percutaneous delivery for most compounds. This creates a very tortuous route through the skin, and as such, generally only low molecular weight and moderately lipophilic drug compounds can transverse this environment successfully.

4.3.2.2 Transcellular: The transcellular path of delivery would include delivery through the keratinocytes, requiring that a drug compound transverse through the keratin-filled corneocytes as well as the intercellular lipid matrix, with several transfers between the corneocytes and the lipid matrix between them [24]. As such, it is thought that this pathway would be generally unfavorable and would not likely contribute substantially to the overall delivery of most drug compounds through the SC.

4.3.2.3 Appendageal: The appendageal route of transport simply refers to the pathway of hair follicles and sweat ducts, which can be seen as a mean of bypassing the permeability barrier of the SC. For this reason, appendageal transport is often known as a "shunt pathway", as it provides a pathway of lesser resistance as compared to the tortuous lipid pathway of the SC. However, the area available for appendageal transport is very small (about 0.1%), and thus this route typically can be considered negligible in its contribution to drug flux at steady state [25].
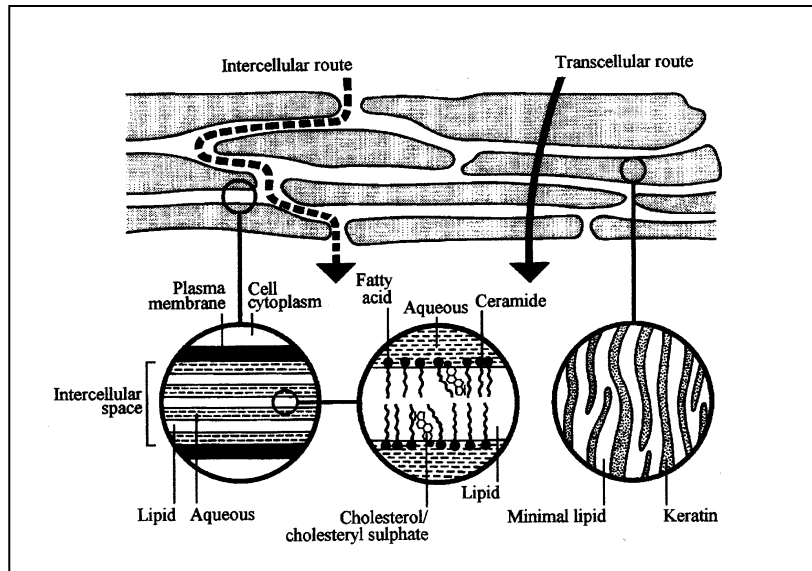
Figure 4.3 Depiction of the intercellular and transcellular routes of penetration through the skin. (Barry 2001) The appendageal route is not displayed. Reprinted from *European Journal of Pharmaceutical Sciences* with permission from Elsevier.

4.3.3 Mathematical models of passive diffusion through the skin

Despite the complex structure of the skin, passive percutaneous delivery can be relatively well described with simple mathematical models of passive diffusion. To use a model of passive diffusion, several assumptions are intrinsically present. It is assumed that steady state conditions have been achieved, and that the compound is permeating via simple diffusion; it is also inherently assumed that the SC is a homogenous layer. As such, Fick's first law of diffusion can be employed:

$$\frac{1}{A}\left(\frac{dM}{dt}\right) = J_{ss} = P\Delta C$$

Equation 4.1

where J_{ss} is the steady state flux, ΔC is the concentration gradient across the skin, and P is a constant that describes a compound's ability to transverse through the barrier of the SC. P can be further broken down into components of the diffusional path length (h), a dimensionless drug partition coefficient and a diffusion coefficient of the drug.

Permeation at steady-state conditions can also be analyzed in terms of the cumulative amount that permeates through the skin into the receiver solution as a

function of time. Thus, the amount of drug appearing in the receiver can be described as:

$$M = PAC\,(t - t_{lag})$$

Equation 4.2

Here, M represents the cumulative amount of drug permeated, P is the permeability coefficient, A is the diffusional area, C is the concentration of drug in the vehicle, t is time and t_{lag} is the lag time. For a homogenous membrane (one of the assumptions about the SC in this mathematical model of diffusion), the lag time can be estimated based on the thickness of the membrane (h) and the diffusivity of the drug in that membrane (D), according to the relationship:

$$t_{lag} = \frac{h^2}{6D}$$

Equation 4.3

As shown in Figure 4.4, the cumulative amount permeated (M) can be plotted against time, and the slope of the line at steady state corresponds to the steady state flux in units of mass/distance^2/time. Back extrapolation of the steady state line to the X axis (time) can provide an estimate of the lag time.
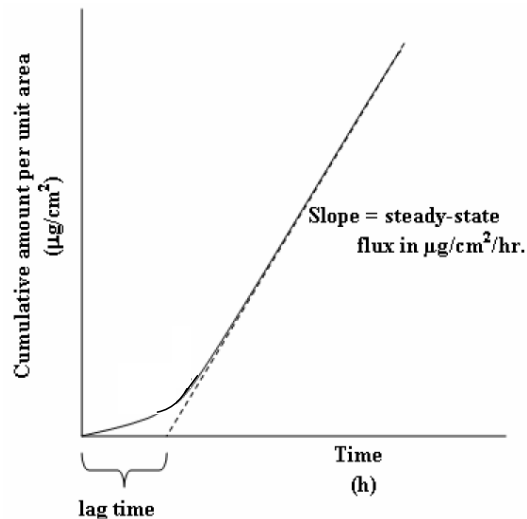
Figure 4.4 Representation of a typical *in vitro* drug permeation profile from a saturated donor solution following topical application.

For situations in which the time dependence of flux of cumulative amount of solute permeated must be solved, Fick's 2nd law of diffusion can be utilized:

$$\frac{\delta C}{\delta t} = \frac{\delta^2 C}{\delta x^2}$$
Equation 4.4

where C is the concentration of drug in the barrier, t is time, and x is a spatial coordinate. Thus, at a point in a diffusional field, the change in concentration over time is proportional to the rate of change in the concentration gradient at that point.

4.4 Enhancement methods in transdermal drug delivery

Due to the effective barrier that the SC presents to the permeation of xenobiotics and most drug moieties, multiple methods of permeation enhancement have been studied, in attempt to extend the benefits of transdermal delivery to a wider variety of compounds. These methods can be broken down into chemical and physical methods for disrupting the barrier of the SC.

4.4.1 Chemical permeation enhancers

Chemical enhancement can be described as a means of facilitating or enhancing absorption of a penetrant across the skin barrier by temporarily diminishing the skin barrier. Several classes of chemical permeation enhancers (CPEs) exist, including fatty esters, fatty acids, terpenes, alcohols, amides, sulfoxides, pyrrolidones, and surfactants [23, 26]. Some CPEs can be obtained naturally (i.e. fatty acids, menthol), while others are synthesized artificially (DMSO, Azone®). CPEs can enhance the permeation of drugs through a variety of mechanisms. Some CPEs disrupt the lipid organization of the SC, resulting in increased permeability [2, 23, 26]. The enhancer inserts into the lipid bilayers, forming microcavities that increase available free volume for drug diffusion [23]. Examples of such CPEs include azone, alcohols, terpenes, fatty acids, and DMSO. Protein modifying CPEs interact closely with the keratin found in the corneocytes (keratinocytes), thus loosening the tight protein structure and allowing for an alternative intracellular pathway of delivery; DMSO and ionic surfactants possess these characteristics. Finally, some CPEs are able to enter the SC and change the chemical environment, which ultimately increases a second molecule's partitioning [23]. Both ethanol and propylene glycol are utilized for these properties. Finally, many of the CPEs possess some combination of these 3 mechanisms. Despite the potential advantage

21

gained in terms of increasing the permeability of drugs across the SC, the biggest challenge that CPEs have faced is skin irritancy and toxicity, as they affect underlying viable cells beneath the SC.

<u>4.4.2 Physical methods</u>

A wide variety of physical methods have been explored to temporarily disrupt the SC, designed to make a physical breach of the barrier without harming the underlying tissues, ultimately to provide a temporary permeation enhancement. In addition to investigation of the individual methods, much research has also been devoted recently to trying to achieve additive effects from combining multiple techniques (Figure 4.5).

4.4.2.1 Thermal ablation: Thermal ablation selectively heats the skin surface for a short period of time to generate micron-scale perforations in the SC, thus increasing skin permeability [5, 6]. This method localizes heat transfer to the skin surface without allowing heat to propagate to and damage the viable tissue below. The heating period is very brief (<< 1 second), generating local temperatures reaching hundreds of degrees Celsius [2, 6]. The short pulses are typically on the time scale of milliseconds or shorter, allowing for limitation of the heat to the SC; longer heating times results in damage to deeper underlying tissue. Several drugs (for example, testosterone, granisetron HCl, and diclofenac) and vaccines have been delivered via this route, while interstitial fluid has also been extracted from human subjects [3]. The PassPort™ system (Altea Therapeutics) has been tested in clinical trials for delivery of insulin using this type of physical enhancement.

4.4.2.2 Laser ablation: Lasers can be used to thermally ablate, and thereby create pores, in the SC. Similar to other poration techniques, this allows a drug to bypass the SC and transverse through the aqueous pathway of the pores and into the underlying epidermis and dermis. It can also be used to increase delivery of both hydrophilic and lipophilic compounds, and can also allow for extraction of interstitial fluids. This method does carry with it a high cost and complicated equipment.

4.4.2.3 Jet injections: Jet injectors can be broken down into two types: liquid and powder. The same principle of delivery applies to both types, in which a high-speed jet is used to puncture the skin and deliver drugs (in either liquid or powder formulations) without using a needle [6]. Acceptance of jet injectors has been somewhat variable, mostly due to the wide variety of reactions that have been observed at the administration sites. Varying levels of pain, bleeding and hematomas have been reported with the

liquid injectors, while powder injectors have seen reports of hyperpigmentation, flaky skin, and erythema at treatment sites.

4.4.2.4 Dermabrasion: Microdermabrasion is a common technique for cosmetic purposes (to treat scars, acne, and dermatologic conditions), primarily to remove or alter the skin tissue. Increased permeability to small drugs like 5-flurouracil has been demonstrated following abrasion of the skin [27].

4.4.2.5 Sonophoresis: Sonophoresis is the term used to describe ultrasound methods that are used to enhance skin permeability. High frequency ultrasound (therapeutic ultrasound, f > 1 MHz) was originally a popular choice for sonophoresis, but it is now known that low frequency ultrasound (f <100 kHz) is much more effective for enhancing transdermal delivery [3]. While there are several possibilities that have been explored as to the exact mechanism of sonophoresis for enhancing skin permeability, perhaps now the most accepted mechanism is acoustic cavitation. This refers to the formation, oscillation, and collapse of "microbubbles" in the tissue. The violent collapse of the bubbles is thought to create aqueous pathways (water channels) within the lipid bilayers of the SC, thus disrupting the structure and allowing for enhanced drug delivery [3, 28, 29].

An interesting feature of sonophoresis delivery systems is that the skin remains in a state of high permeability for hours after a short application of ultrasound, which allows for a pretreatment scenario in which the patient does not need to wear the device for the duration of the drug delivery window [28]. Sonophoresis has been used to successfully deliver a large range of molecules, including macromolecules (insulin and erythropoietin) and smaller molecules such as lidocaine and calcein [30]. In 2004 the FDA approved SonoPrep®, a commercially available tool to accelerate local anesthesia with lidocaine; it has since been proven effective for enhancing anesthesia from application of EMLA® cream prior to intravenous cannulation in children [31].

4.4.2.6 Iontophoresis: The underlying principle of iontophoresis is to provide an electrical driving force to assist the transport of molecules across the SC [1-3, 23]. Iontophoretic delivery has already been well described for clinical applications, including pilocarpine sweat tests for diagnosing cystic fibrosis, lidocaine delivery for local anesthesia, and tap water to treat hyperhidrosis [2]. This method involves the passage of a small current through a drug-containing electrode that is in contact with the skin [23]. The efficiency of transport depends on the polarity, valency, and mobility of the species of interest [1, 23]. Three primary mechanisms of drug transport have been described,

including electroosmosis, electrophoresis, and increased skin permeability resulting from the flow of electric current [1, 4]. Drugs that carry a charge will be moved across the skin via electrophoresis, which drives the compound across the skin via direct interaction with the electric field [2, 3]. Species with smaller molecular mass and greater charge are generally favored and delivered more rapidly with iontophoresis techniques [3]. As such, drug delivery in clinical studies has been limited to smaller molecules including fentanyl and lidocaine [32-34].

Commercial products have been previously marketed in the United States (Iontocaine® and Lidosite®) and IONSYS™ (never marketed in the US). The products marketed in the US were subsequently removed due to safety concerns and corrosion of a component of the device, in the case of the IONSYS™ system. These market withdrawals illustrate perhaps the biggest drawback of iontophoresis, in that it requires a relatively complex and expensive delivery device to be effective.

4.4.2.7 Electroporation: Electroporation (also known as electropermeabilization) involves the application of transient high-voltage electrical pulse to the skin, resulting in a rapid and reversible disruption of the stratum corneum. Lipid bilayer structures are disrupted and a reversible polar pathway is created in the skin (it is generally accepted that rearrangements in the lipid structure creates temporary aqueous pores/pathways) [2, 3, 23, 35]. The main mechanisms of molecular transport derived from this method are enhanced diffusion via skin poration (both during and after the pulses), electrically driven transport that occurs during the pulses, and electroosmosis [4, 23, 35]. Electroporation acts directly on the skin and induces a change in the tissue permeability [36]. The properties of drugs that can be delivered via electroporation are vast, including small and large molecules, hydrophilic or lipophilic, and charged or neutral molecules. Molecules that have been successfully delivered via electroporation include ions, calcein, metoprolol, fentanyl, sulforhodamine, peptides, and macromolecules [37-39].
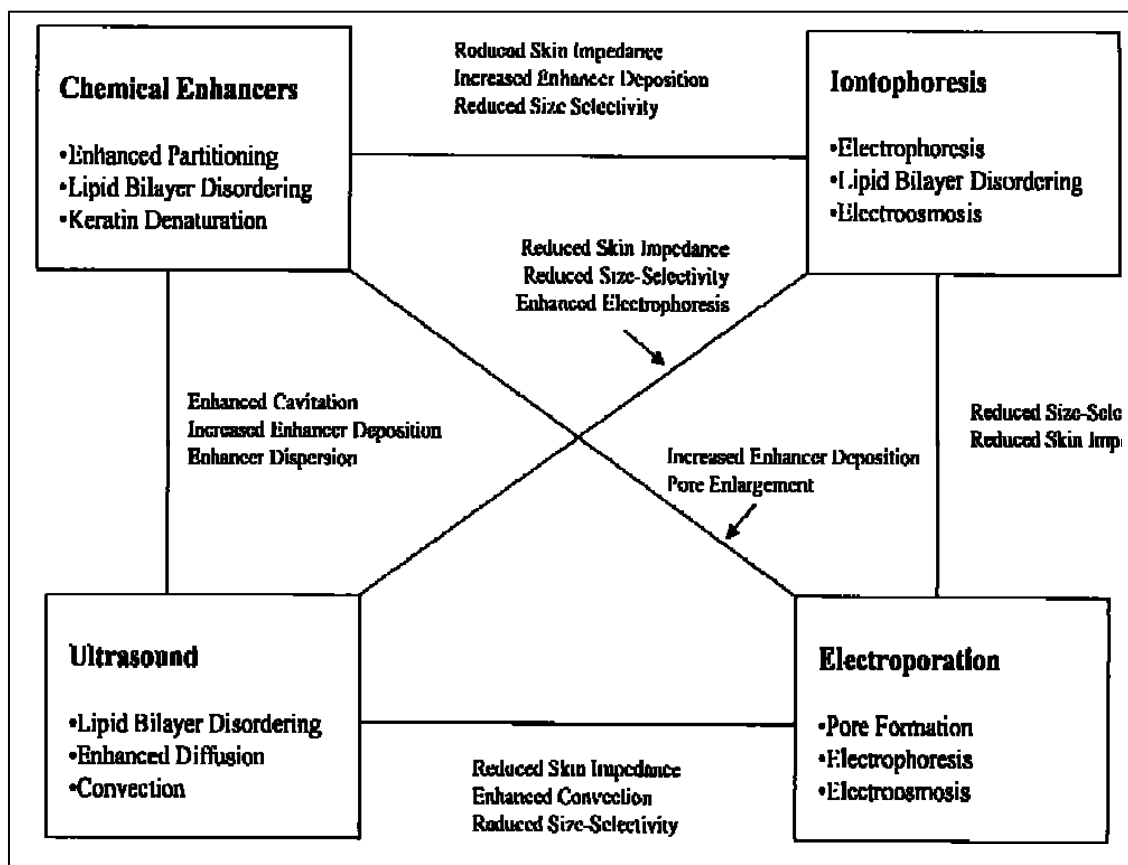
Figure 4.5 Effects of combined physical enhancement methods on the barrier of the stratum corneum. Mitragotri *et al*, 2000. Reprinted from *Pharmaceutical Research* with permission from Springer.

4.4.2.8 Microneedles: As suggested by the name, microneedles (MNs) are needles or projections of micron-scale, designed to aid in drug and vaccine delivery through the skin. The first realization that MNs could be employed to bypass the barrier of the SC (thereby allowing for drug delivery through the skin) occurred in the 1970s but progress in the field was limited by the lack of suitable technology to producing structures of such small dimensions. The use of MNs offers a great deal of advantages over other physical enhancement techniques, as several options are available for tailoring the delivery method to meet specific therapeutic needs.

One of the greatest advantages of MN technologies is removal of restrictions on the size of drug molecules that can be delivered through the skin. Traditional transdermal delivery is limited to small compounds, but this is not the case with

microporated skin. The newly created micropores are micron in scale but are still notably larger than drug molecules. As such, it is feasible to deliver proteins, macromolecules, and DNA through microporated skin. MN treatment also allows for hydrophilic compounds to be delivered into the skin, whereas traditional passive transdermal delivery is restricted to hydrophobic compounds [40]. There is a wide range of flexibility with the geometry and composition of the needles and the arrays. MNs have been made from a variety of materials, including stainless steel, titanium, polymers, silicon, glass, sugars, and palladium [3, 5]. The length of the needles can range from 100 up to 1500 μm, and the number of needles applied can range anywhere from a single needle (in the case of vaccines) all the way up to a roller possessing 192 needles (DermaRoller®).

Four primary methods of drug delivery with MNs have been described (depicted in Figure 4.6): 1) pretreatment of the skin with solid MNs, 2) drug-coated MNs, 3) MNs that dissolve upon insertion into the skin, and 4) hollow MNs [5, 41]. The varying methods all have different mechanisms to allow for drug delivery, each with specific advantages and disadvantages.

The use of solid MNs is typically viewed as a pretreatment paradigm, in which MNs are inserted into the skin and immediately removed, leaving behind micron-scaled pores (micropores) [5, 6, 41]. The creation of such micropores in the SC can increase skin permeability by up to 4 orders of magnitude [42-44], and application of a drug or vaccine over the newly permeable skin allows for delivery into or through the skin [6]. This treatment process is often referred to as the "poke (press) and patch" approach. Solid MNs can be made from a variety of materials, including metals (stainless steel, titanium or nickel), silicon, ceramics, maltose, and polymers (both degradable and non-degradable) [6, 41].   The solid MNs are typically designed as flat substrates such that the needles are all pressed into the skin at the same time. However, a rollers of MNs are now commercially available that can treat larger areas of the skin. Some examples of drug molecules that have been successfully delivered with solid MN technologies include naltrexone [9], calcein [44], docetaxel [45], phenylephrine [46], and insulin [47].

In addition to simply piercing the skin to create aqueous micropores to aid in drug delivery, solid MNs can be coated with drug formulations that can be delivered quickly into the tissue upon insertion of the MNs into the skin (the "coat and poke" approach). Multiple methods exist for coating the MNs, including dipping and spraying techniques [41]. While this technique does limit the amount of drug that can be delivered (due to the

small volume that can be coated onto the needle surfaces), this mode of MN application has proven to be versatile in its applications and the drugs that can be successfully delivered. Peptides [48], vaccines [49-51], and antigens [52] have all been successfully coated onto MNs.

Dissolving MNs are quite different from the 2 MN techniques already discussed, in that these needles are composed of degradable, water-soluble materials (often polymers and sugars) that completely dissolve within the skin following insertion. These needles do offer the possibility of being used as a pretreatment, but often a drug is encapsulated within the polymer, allowing for slow release into the skin. Dissolvable MNs often require up to 5 minutes of insertion time to completely dissolve; in contrast, biodegradable polymers remain in the skin for several days to provide controlled-release degradation. Human growth hormone [53], erythropoietin [54], and influenza vaccine [55] have all been successfully delivered with this approach.

Finally, hollow MNs provide a defined pathway for drug delivery through the needles into the skin. This allows for a liquid drug formulation to be delivered via pressure-driven flow (similar to a hypodermic needle), which creates a system in which the flow rate can be adjusted to meet a specific therapeutic need. The greatest advancement with hollow MNs has been the successful delivery of insulin to both animals and humans [56, 57].
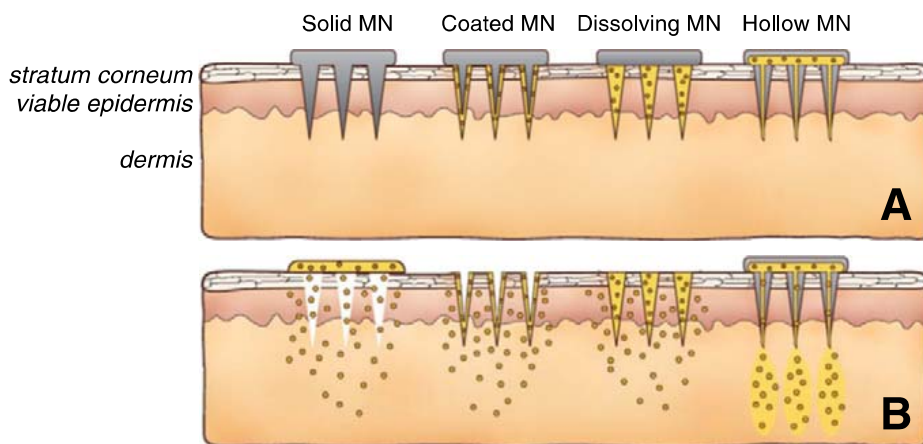
Figure 4.6 Four methods of microneedle-enhanced drug delivery to the skin. Kim *et al*, 2012. Reprinted from *Advanced Drug Delivery Reviews* with permission from Elsevier.

4.5 Tolerability and safety of microneedles

In order to be clinically feasible as a drug delivery technique, it is important that MN treatment is both well tolerated by patients and safe with regards to infection potential/risk. It has been demonstrated through multiple studies that application of MNs to the skin is painless and well tolerated. Using visual analog scales (VAS), MN application is reported to be significantly less painful than a hypodermic needle [7, 58, 59], while other reports have not specifically used VAS methods, but have still reported lack of pain with MN insertion [60, 61]. Subjects perceive MN insertion as a "pressure" or "heavy" sensation, but not painful [7]. The perception of pain increases with two factors: 1) MN length and 2) number of MNs. The MN tip angle, width, and thickness do not significantly affect pain [58].

One of the first criticisms mentioned with regard to MN treatments is the potential for increased risk of local infection once the micropores have been created. In fact, it has been demonstrated that *in vitro* microbial penetration is less after MN application (when compared to a hypodermic needle) for Gram negative, Gram positive, and Yeast species [62]. Additionally, there have been no reports of infection following MN application, despite the increasing numbers of human trials in this area.

4.6 Micropore lifetime after microneedle treatment

The utility of MN treatments for enhancing drug delivery through the SC is dependent on 2 primary factors: the efficiency of micropore formation, and the lifetime during which a drug compound can diffuse through the micropores (in other words, the effective lifetime of the micropores). This has become a topic of great recent interest in the MN delivery field, and several studies in animals and human have been published addressing the topic of micropore closure kinetics and determination of a viable drug delivery window after one-time MN application [10-14]. A variety of experimental techniques are available for assessing both formation and the lifetime of the micropores, including methylene blue staining [7, 63, 64], india ink staining [12], calcein imaging [63, 65], histology techniques [63, 65], optical coherence tomography [13], confocal laser microscopy [10, 63, 65], transepidermal water loss [7, 11, 63, 65], impedance spectroscopy [9, 14], and drug diffusion (pharmacokinetic) studies [9, 11, 12]. Through these various techniques of evaluating micropore formation it is now understood that multiple factors contribute to the degree of perturbation that MNs create in the skin and how long the micropores will remain viable, including: local skin occlusion, geometry and

physical properties of the MNs, and physiological processes involved in barrier restoration. A summary of the studies that have examined the effect of these parameters on micropore re-sealing kinetics is found in Table 4.1, below.

4.6.1 Effects of occlusion

Occlusion of the skin with an impermeable membrane blocks the insensible loss of water from the skin's surface, thereby resulting in a local increase in skin hydration. In typical transdermal delivery systems, the skin remains occluded under a patch for a period of hours to days. This would also be the situation with a "poke (press) and patch" MN application, when the micropores are occluded with a drug formulation. The steep water gradient that results from damage to the skin (in this case, from the creation of micropores) is one of the first signals for the skin to initiate the cascades of events contributing to barrier restoration, as this affects ion gradients in the skin that ultimately trigger repair mechanisms [66-68]. Blocking the formation of the water gradient thus blocks initiation of repair mechanisms. This could also be considered an advantageous attribute of the occlusion of the "poke (press) and patch" system, as the micropores would be expected to heal more slowly under conditions of limited (or absent) airflow to the external environment. This concept has been demonstrated by several groups who have examined the effect of occlusion on micropore re-sealing kinetics.

When unoccluded, the micropores heal quickly: TEWL measurements demonstrated a return to baseline within a range of 2 hours [14, 69], 4 hours [63, 65], or by 24 hours [7]. Other techniques demonstrate similar timeframes. Bal *et al* viewed the micropores with confocal laser scanning microscopy and reported that no dye was present on the skin surface at 15 minutes, suggesting rapid re-sealing of the micropores at the SC [10]; using optical coherence tomography, Enfield and colleagues described that micropores were still visible at 85 minutes post-treatment, though the micropore size had decreased [13]. Methylene blue binding studies have displayed evidence of repair at 8 and 24 hours post-MN [7], while calcein imaging techniques have exhibited closure over a range of 12 to 18 hours [63, 65].

Under occluded conditions, the timeframe of micropore re-sealing is extended to a notable degree. TEWL measurements demonstrate that baseline barrier function is not achieved by 72 hours under occlusion with a blank patch or buffers of pH 4 or 7, confirming that the pH of the local environment does not affect micropore closure rates this was confirmed with calcein imaging in which the micropore could be visualized at 72

29

hours [65]. Gupta *et al* described impedance measurements of micropores under occluded conditions and a range of re-sealing times was observed, from 3 to 40 hours [14].

4.6.2 Geometry and physical properties of the microneedles

A wide range of geometries are available for MN arrays, and several reports have demonstrated that MN length and number significantly affect the amount of barrier perturbation and the rates at which the micropores heal. A positive correlation between TEWL and MN length has been observed *in vitro* when Dermarollers® of varying MN lengths were applied (150 – 1500 µm length) [69]. Additionally, MN geometry was found to significantly affect the permeation of a fluorescent dye *in vivo* into human skin [70].

Under the hypothesis that increasing MN length causes more perturbation to the skin, it has been postulated that treatment with longer needles would result in prolonged liftime of the micropores; in fact, this has been demonstrated via evaluation of micropore lifetime with a variety of techniques. A difference in re-sealing time of 12 hours vs. 18 hours has been demonstrated with TEWL measurements following treatment with MNs lengths of 370 µm and 770 µm, respectively [63]. Gupta *et al* examined the lifetime of micropores (using impedance spectroscopy) under occluded vs. non-occluded conditions [14]. When unoccluded, the micropores all returned to baseline impedance values by 2 hours after treatment, demonstrating re-sealing of the micropores. In contrast, the differing geometries resulted in significantly different re-sealing times under occlusion. An array of 50 MNs, 500 µm length results in a recovery time of ~20 hours, whereas an array of 50 MNs of 750 µm takes up to 40 hours to heal.
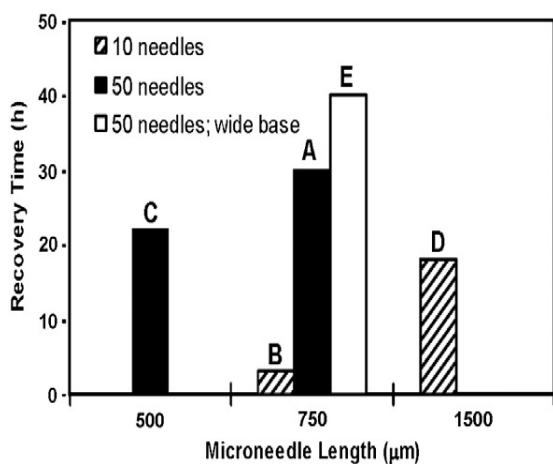
Figure 4.7 Timeframes required for complete return to baseline barrier function under occluded conditions following application of MNs of varying geometries, determined by impedance spectroscopy. Gupta *et al*, 2011. Reprinted from *Journal of Controlled Release* with permission from Elsevier.

4.6.3 Drug delivery window following microneedle treatment

All of the aforementioned studies examining micropore formation and closure kinetics utilized "surrogate" markers to assess the re-sealing time of micropores under various conditions. However, the ultimate goal of characterizing micropore lifetime is to determine the window during which drug can be delivered through the micropores to a therapeutic level. The first study to examine this concept in human subjects described the delivery of naltrexone (NTX), an opioid antagonist, using the "poke (press) and patch" method in healthy human volunteers. Subjects were treated once with MN arrays at 4 patch sites, for a total of 400 micropores (arrays of 50 MNs each, 620 μm in length). A 16% NTX•HCl patch was applied to each MN-treated skin site, and remained on the skin for the full 72 hours of the study. NTX was delivered to a therapeutic plasma concentration (2.5 ± 1.0 ng/ml) for 48 hours; 2 subjects demonstrated delivery up to 72 hours [9]. This delivery window is in very good agreement with impedance, TEWL, and calcein imaging data that demonstrated viability of micropores in a window ranging from 40 hours to 72 hours under occlusion, following treatment with MNs of similar geometries (500 or 750 μm length) [14, 63]. A very similar drug delivery window was observed when hairless guinea pigs were treated on the dorsal surface with MNs (50 MN arrays, 750 μm in length) followed by application of a 21.7% gel patch of 6-β NTXol (the active metabolite of NTX) that remained in place for the duration of the study. Concentrations of NTXol in the plasma were consistent (21.3 ± 6.9 ng/ml) up to 48 hours, after which the plasma levels began to vary. TEWL was employed as a concurrent surrogate technique, which confirmed that the micropores were no longer viable after 48 hours [12]. Furthermore, in a study by Banks *et al* studying the effect of diclofenac sodium on micropore closure, control animals were treated once with MN arrays (50 MN arrays, 750 μm in length) followed by application of a 16% NTX•HCl gel patch. Consistent with the other studies, NTX was detected in the plasma up to approximately 60 hours post-MN (3.4 ± 1.3 ng/ml), after which the plasma levels were undetectable [11]. All of these studies confirm 2 important concepts: first, under occluded conditions drug delivery can be achieved through micropores for a timeframe of approximately 48 – 72 hours (assuming a MN length of ≥ 500 μM); second, the lifetime of micropores predicted by surrogate techniques (e.g. calcein imaging, TEWL, impedance) correlates closely with plasma concentrations of drugs delivered under similar conditions.

Table 4.1 Timeframes of micropore re-sealing, as measured by various research groups. Multiple methods of evaluation and varying MN geometries have been examined.

Reference	Model	Length of MN (µm)	Method of evaluation	Kinetics of micropore closure
[10]	Humans (n = 6)	300	Confocal laser scanning microscopy	No dye present on skin surface at 15 minutes
[13]	Humans (n = 1)	280	Optical coherence tomography	Micropores still visible at 85 minutes
[7]	Humans (n = 13)	180 280	TEWL, methylene blue staining	TEWL: returned to baseline by 24 hours Staining: showed evidence of repair at 8 and 24 hours
[65]	Hairless rats	500	TEWL, calcein imaging	TEWL: returned to baseline by 4 hours (unoccluded), but still not achieved by 72 hours under occlusion. Imaging: closure by 15 hours (unoccluded); channels still visible at 72 hours but not 120 hours (occluded).
[63]	Hairless rats	370 770	TEWL, calcein imaging	TEWL: Returned to baseline by 4 to 5 hours (irrespective of MN length) Imaging: Closure by 12 hours (370 µm) or 18 hours (770 µm)
[69]	*Ex vivo / in vitro*	150 500 1500	TEWL	Returned to baseline by 2 hours (irrespective of MN length)
[14]	Humans (n = 10)	500 750 1500	Impedance spectroscopy	Unoccluded: All sites returned to baseline by 2 hours Occluded: recovery to baseline dependent upon MN length and number: 500 µm, 50 MNs: 22 hours 750 µm, 10 MNs: 3 hours 750 µm, 50 MNs: 30 hours 750 µm, 50 MNs: 40 hours* 1500 µm, 10 MNs: 18 hours * needles were thicker than the other 750 µm arrays

Table 4.1, cont.

[9]	Humans (n = 9)	620	Pharmacokinetic analysis of naltrexone plasma concentrations	Therapeutic plasma concentrations of naltrexone delivered for 48 to 72 hours
[12]	Hairless guinea pigs	750	TEWL, India ink staining, pharmacokinetic analysis of 6-β-naltrexol plasma concentrations	TEWL: Returned to baseline by 48 hours (occluded) Staining: Apparent staining present at 48 hours, but only slightly at 72 hours (occluded) Plasma concentrations: delivery achieved for 48 to 72 hours
[11]	Hairless guinea pigs	620	Pharmacokinetic analysis of naltrexone plasma concentrations	Therapeutic concentrations of naltrexone delivered for 48 hours in control animals

4.7 Extending micropore lifetime

While it is now established that micropores can remain viable for up to 48 to 72 hours following one-time treatment, it would be ideal to extend this timeframe up to 7 days total. Once weekly dosing of a transdermal patch is ideal and would help increase patient compliance and satisfaction with therapy. It becomes necessary, then, to explore means of trying to extend the viable window of drug delivery by prohibiting micropore closure during the period in-between the normal timeframe of closure (48 to 72 hours) and the target dosing interval (7 days). A logical place to start for developing such a system is to target the physiologic events that contribute to the skin's ability to restore its barrier following acute insult.

4.7.1 Processes involved in wound healing and barrier restoration

The SC barrier function can be acutely disrupted by a variety of experimental means (physical, chemical, or physiological), including solvents (i.e. acetone), mechanical forces (i.e. tape stripping), or detergents such as sodium dodecyl sulfate (SDS) [17, 71]. Following the disruption, the skin initiates a homeostatic repair response in order to recover the barrier function. There are several known pathways involved in wound healing and barrier restoration following insult to the skin, and it could be proposed that these processes would also be involved in restoring the barrier following

MN treatment, including 1) lipid synthesis; 2) cationic ion gradients in the skin; and 3) the arachidonic acid pathway.

4.7.1.1 *Lipid synthesis pathway:* The lipids of the SC are the primary determinant of the permeability barrier, affecting water transport, movement of electrolytes, and drug penetration [17, 72]. This has been demonstrated by an inverse correlation that has been noted between penetration of solutes and the weight of SC lipids [72]. In addition to the extreme hydrophobicity of the extracellular lipids, the critical molar ratio (1:1:1) of the 3 key species also contributes to the barrier function [73]. Under basal conditions, epidermal lipid synthesis is highly active and generally independent of systemic influences, though it can be modified by external influences that alter the SC barrier function [73]. Acute disruption of the barrier function stimulates a characteristic sequence of recovery events that contributes to restoration of normal function within approximately 48 – 72 hours [17, 73]. Within minutes of the insult, contents of the lamellar bodies in the stratum granulosum cells are secreted, and this leads to a notable decrease in the number of lamellar bodies that are found in the stratum granulosum [17]. Newly formed lamellar bodies will begin to appear shortly in the stratum granulosum cells, and this accelerated rate of secretion will continue until the barrier function is returned to normal [17]. Of note, this process can be inhibited via application of an impermeable membrane that artificially restores the barrier function [17].

The sequence of events that is initiated to repair barrier function includes accelerated synthesis of epidermal cholesterol, sphingolipids, and fatty acids [17, 72]. The timeframe of these events differs slightly in that the increase in cholesterol and fatty acid synthesis occurs shortly after the barrier disruption (within 1 – 2 hours), whereas the increase in sphingolipid synthesis is slightly delayed (6 – 9 hours) [17, 72]. These events provide the basis for metabolic inhibitors as a potential means to inhibit barrier recovery, thereby increasing SC permeability and improving transdermal delivery of drug molecules [17, 21, 72]. In fact, it has been demonstrated that repair response can be modulated via the use of pharmacological agents aimed specifically at inhibiting some component of epidermal lipid synthesis [17, 21, 72]. In support of this concept, topical HMG CoA reductase inhibitors (specifically lovastatin and fluvastatin) have been shown to cause a delay in barrier recovery when applied to adult hairless mice. In these studies, the kinetics of barrier recovery were delayed, while a barrier defect was also noticed after several days of repeated daily application [17, 21, 72, 74, 75]. Co-

34

application of mevolanate (rate limiting step in the cholesterol synthesis pathway) or cholesterol (distal product of the pathway) reverses the inhibition of barrier restoration, thus suggesting that the delay is not related to nonspecific toxicity effects of the inhibitors themselves [21, 73, 74]. When combined with the assessment of transdermal delivery of the model compound lidocaine, the barrier disruption associated with the topical application of fluvastatin correlated linearly with the extent of lidocaine disruption, further supporting the notion of utilizing these pharmacologic agents to enhance transdermal delivery techniques [72].

4.7.1.2 Cationic ion gradients: Calcium (Ca^{2+}) is known to have several roles in the skin. High concentrations of Ca^{2+} regulate differentiation of cultured keratinocytes, and are involved with late epidermal differentiation events including conversion of profilaggrin to filaggrin and activation of serine proteases and transglutaminase. Under normal conditions, a steep gradient of Ca^{2+} ions exists in the epidermis, with concentrations of ~180 mg/kg in the basal layer, and increasing to a peak of ~460 mg/kg in the outer layers of the stratum granulosum. This gradient falls off steeply at the SC, where the lowest levels of Ca^{2+} are present in the skin [76].

Following disruption of the permeability barrier (acetone treatment, tape stripping, application of 2% SDS), the steep gradient of Ca^{2+} is dissipated, resulting in lower Ca^{2+} concentrations in the outermost layers of the skin. The peak of Ca^{2+} normally found in the stratum granulosum layer falls by almost 4 fold, to ~128 mg/kg [76]. Concurrently, the amount of Ca^{2+} in the epidermis actually increases slightly, suggesting that the skin restores the gradient from below by moving Ca^{2+} up from deeper layers in the skin. The decreased Ca^{2+} in the upper layers of the skin results in a characteristic sequence of responses to repair the permeability barrier. These responses include: 1) secretion of preformed lamellar bodies from the stratum granulosum cells; 2) increased assembly and further secretion of lamellar bodies from stratum granulosum cells; 3) increased synthesis of epidermal cholesterol, fatty acids, and sphingolipids; and 4) and increase epidermal DNA synthesis.

Several bodies of evidence support the involvement of Ca^{2+} in maintaining or repairing skin homeostasis. Following barrier disruption (via acetone treatment or tape stripping), submersion of the skin in an isomolar sucrose or isotonic NaCl solution with mM concentrations of calcium chloride ($CaCl_2$) delays barrier recovery (measured with TEWL). When submersion is performed with phosphate buffered saline solution with added Ca^{2+}, no increase in HMG CoA reductase activity is observed. Application of 1

µM ionomycin (a Ca^{2+} iontophore) to barrier disputed skin also delays barrier recovery [77]. There was also no secretion of lamellar bodies, no localization of neutral lipids, and a very thin stratum corneum/stratum granulosum domain.

In addition to the above mentioned studies demonstrating the role of extracellular Ca^{2+} concentrations towards initiating barrier restoration processes, many of these studies also suggest that high intracellular Ca^{2+}, or at least high flux of Ca^{2+} into cells, prevents lamellar body secretion. When verapamil or nifedipine (L-type, voltage sensitive Ca^{2+} channel blockers) are added to the Ca^{2+}- containing submersion solutions, barrier recovery occurs at normal rates. Furthermore, addition of TMB-8 (to inhibit translocation of Ca^{2+} from membrane bound vesicles into the cytosol) results in normal recovery rates; addition of calmodulin inhibitor (trifluoperazine) generates the same effect [67].

4.7.1.3 Arachidonic acid pathway: General skin wound healing follows 3 distinct phases, the first phase involving inflammation at the site of injury [78]. This pathway involves the conversion of arachidonic acid into downstream prostaglandins (belonging to the family of eicosanoids), many of which are pro-inflammatory. The eicosanoids are a class of lipid mediators that are oxygenated, hydrophobic derivatives of C20 fatty acids [79]. This family is integrally involved in the body's natural inflammation response, for which arachidonic acid (20:4ω6) serves as the premier precursor [79]. The chemistry involved in the biosynthetic pathway(s) of arachidonic acid metabolism is well known [80]. Arachidonic acid can undergo oxygenation in a process regulated by the cyclooxygenase (COX) enzymes [80, 81]. This leads to the formation of PGH_2, a central intermediate that is further metabolized to other downstream products, including both pro- and anti-inflammatory prostaglandins (PGs) [80, 81]. There are currently 3 recognized isoforms of the COX enzymes [82]. COX-1 is a constitutively expressed form that is considered to be a "housekeeping" enzyme, and under basal conditions is found in almost all tissues. COX-1 is generally thought to be involved more in homeostatic regulation at sites such as the platelets, kidney, and gastric mucosa [80, 83]. Conversely, COX-2 is considered an inducible form and an immediate early response gene product involved primarily with the inflammatory response [80, 83]. COX-3 is a splice variant of COX-1, and its function is currently not well defined [82]. The conversion of arachidonic acid to downstream PGs via the action of the COX pathway has been extensively researched since the 1970s when it was discovered that the nonsteroidal anti-inflammatory drugs (NSAIDs) exhibit their anti-inflammatory effects

through inhibition of this step in the cascade [80, 84]. The most widely accepted mechanism of action of the NSAIDs is their ability to inhibit the conversion of arachidonic acid into downstream PGs, many of which are pro-inflammatory. Figure 4.8 depicts the arachidonic acid cascade.

$$Arachidonic\ Acid$$

$$\underset{\text{Cyclooxygenase-2}}{\text{Cyclooxygenase-1}} \quad\longrightarrow\quad NSAIDs$$

$$PGG_2$$

$$PGH_2$$

$$PGF_{2\alpha} \quad PGD_2 \quad PGE_2 \quad PGI_2 \quad TXA_2$$
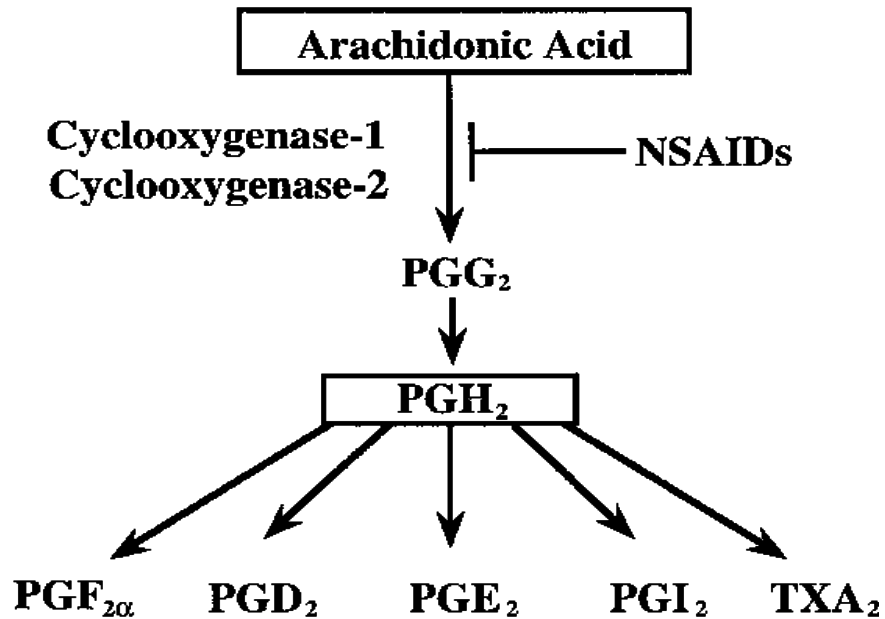
Figure 4.8 Diagram of the conversion of arachidonic acid into downstream prostaglandins and eicosanoids via the cyclooxygenase enzymes. Dubois *et al*, 1998. The NSAIDs exhibit their anti-inflammatory effects by inhibiting COX-1 and COX-2 to varying degrees, resulting in decreased biosynthesis of prostaglandins. Reprinted from *FASEB* with permission from the Federation of American Societies for Experimental Biology.

The skin demonstrates very active metabolism of arachidonic acid, primarily in the epidermal layer. More specifically, COX-1 is found throughout the epidermis, whereas COX-2 is more localized in suprabasal keratinocytes [85]. The downstream products of the COX pathways are important for several processes involved in wound healing, including inflammation, fibroblast proliferation, and angiogenesis [86]. The main

PG products formed via the COX pathway in the skin of many species (including humans) are PGD_2 and PGE_2, both of which are pro-inflammatory [81]. PGE_2 has also been shown to regulate cytokine secretions and epidermal cell proliferation, and is important for the pathophysiology of the skin [85, 87].

4.8 Naltrexone as an ideal model compound for exploring the kinetics of micropore closure

In examining micropore closure kinetics specifically from a pharmacokinetic/drug delivery standpoint, it is necessary to have a model compound that can be easily detected in the plasma and has appropriate physicochemical characteristics for MN-enhanced delivery. Naltrexone (NTX) is a mu opioid receptor antagonist that is FDA approved for the treatment of opioid and alcohol abuse. As a receptor antagonist, the therapeutic effects of NTX relate directly to its ability to block alcohol-induced "highs" and intoxication, ultimately resulting in decreased craving and eventual relapse [88]. Multiple studies have demonstrated the efficacy of NTX in the treatment of alcohol abuse, and it is significantly improved over placebo conditions with or without behavioral therapies [89].

4.8.1 Challenges with current naltrexone formulations

NTX is currently available in oral tablet forms (Revia®, as naltrexone HCl) and an injectable depot form (Vivitrol®, as naltrexone base, 380 mg extended release form delivered as an intramuscular injection every 4 weeks). Despite the proven efficacy of NTX in the treatment of alcohol and opioid abuse, there are multiple downfalls of both of these dosage forms that create problems for chronic dosing scenarios. The oral formulation exhibits unpredictable bioavailability (5 – 40%), due to its extensive first-pass metabolism through the liver [90]. This creates challenges when trying to predict plasma concentrations and response to therapy, and presents a therapeutic safety concern when administered to alcoholics with pre-existing liver complications. The depot injection, on the other hand, possesses a different array of adverse events and therapeutic concerns. The FDA has received reports of injection site reactions with NTX with this formulation, including hematomas, cellulitis, and necrosis. In a report issued in August 2008, there had been 196 reports of injection site reactions, many of which required serious medical attention (in 16 cases, surgery was required). Another serious concern with the use of a depot formulation would arise in emergency situations when a

patient would have an acute requirement for pain control. High (and potentially unsafe) doses of opioids would be required to overcome the narcotic blockade from the NTX, resulting in the need for surgical removal of the depot.

In light of the downfalls of current NTX formulations, transdermal delivery would provide several key advantages, specifically: 1) decreased potential for hepatotoxicity, via avoidance of the first-pass effect; 2) simplicity of application and likely enhanced patient compliance; and 3) ease of removal in the event of an acute need for emergency pain relief.

4.8.2 Physicochemical properties of naltrexone favoring microneedle-enhanced delivery

Despite the clear benefits of transdermal delivery, NTX does not possess ideal physicochemical characteristics to allow it to passive deliver through the SC. Most specifically, it is not hydrophobic enough to passively transverse through the lipophilic milieu of the SC (logP 1.8). Conversely, it does possess sufficient hydrophilicity to partition into the interstitial fluid and aqueous environment in the deeper layers of the skin. For these reasons, NTX is a poor candidate for traditional transdermal delivery, but it is an ideal candidate for MN-enhanced delivery. The creation of aqueous channels from MN insertion would provide a pathway for NTX to diffuse through the SC and into the underlying circulation. Multiple studies in animals and humans have demonstrated the feasibility of this technique for delivering NTX (and its metabolite, 6-β-NTXol) to animals and humans [9, 11, 12, 91, 92]. Furthermore, validated methods exist for its detection in plasma [93]. For these reasons, NTX is an excellent model compound for studying MN-enhanced drug delivery and micropore closure kinetics.

Chapter 5

Development of *in vivo* impedance spectroscopy techniques for measurement of micropore formation

5.1 Introduction

Microneedle (MN) – assisted transdermal delivery represents a minimally invasive physical enhancement technique that increases the permeability of the stratum corneum (SC), the outermost layer of the skin [2, 5]. This allows for various types of molecules to cross the otherwise impermeable outer layers of skin, including macromolecules, proteins, and hydrophilic compounds. Several types of MN delivery systems have been described, including hollow, coated, and dissolving MN systems [5]. In one of the simplest MN techniques, a solid MN array is applied to the skin to create micron-scale pores (also called micropores) in the SC; application of a drug solution or patch to the MN-treated area allows a drug to cross the skin into the systemic circulation (a treatment paradigm known as the "poke (press) and patch" method) [5].

The "poke/press and patch" approach for MN insertion is particularly appealing for a variety of reasons. The creation of micropores in the SC is a very simple process, achieved by placing a MN array on the skin and applying gentle pressure for 10 – 15 seconds, followed by immediate removal of the MNs. This creates a grid of micropores in the SC that can be utilized for drug delivery. The number of micropores can be tailored for the requirements of the condition being treated, the amount of drug needed, and the properties of the drug to be delivered. Second, a drug moiety can be delivered from a variety of sources, including a patch, gel, or solution, providing flexibility in application sites, drug volumes, and patch types. Lastly, the lifetime of the micropores in the skin can be manipulated to allow for a variety of dosing schedules. When unoccluded, the micropores reseal rapidly (approximately 15 minutes to 2 hours), but this can be extended to 48 – 72 hours when the microporated skin is covered by an occlusive patch [9, 10, 13, 14]. The micropore lifetime can be further extended via topical application of a non-specific anti-inflammatory compound, diclofenac sodium, allowing for drug delivery for up to 7 days [11].

The primary factors that influence drug delivery with the "poke/press and patch" MN technique are 1) adequate formation of micropores in the skin, and 2) the lifetime of the micropores in the SC. In order to continue expanding the utilization of this novel drug delivery technique, it is important to develop appropriate *in vivo* models for

evaluating micropore formation and lifetime following MN treatment in animal models and human subjects. Two commonly utilized methods to investigate the barrier function of the skin include transepidermal water loss (TEWL) and impedance spectroscopy. The SC is the skin's primary means of preventing water loss from the body into the external environment, and it also serves as the skin's barrier to movement of ions (i.e. flow of electrical current) [14, 94-97]. TEWL estimates water loss through the skin, derived from the difference in vapor pressure between the skin and the area 4 mm above the skin (REF). TEWL increases when the skin is damaged, while impedance decreases, thus rendering these as complementary techniques for assessing the integrity of the skin's barrier; both have been demonstrated to be reliable techniques for such evaluations [94-96]. The nature of transdermal patches is such that the skin remains occluded underneath the patch for a timeframe of hours to days, resulting in a local increase in skin hydration. This can create a substantial problem with TEWL readings when the micropores in the SC begin to heal and subtle changes are difficult to discern from the effects of the hydration alone. While impedance measurements are also somewhat affected by hydration status, the technique is sensitive enough to detect changes in the micropores under both hydrated and non-hydrated conditions, as the technique is less sensitive overall to hydration effects [14].   Additionally, an impedance setup can be devised that is cost effective, portable, and does not require any software to make measurements – making this an ideal measurement technique for clinical settings.

Impedance measurements of the SC using various methods and techniques have been described previously [94, 98], but there are limited publications describing the use of this technique to evaluate micropore formation following MN treatment in animal models or human subjects. Two animal models commonly used in percutaneous and topical drug delivery studies include Yucatan miniature pigs (large animal model) and hairless guinea pigs (small animal model). Porcine skin is the most similar to human skin with regard to histological and biochemical properties including hair density, epidermal thickness, and composition of intercellular SC lipids [99-101]. Hairless guinea pigs are an excellent small model for permeability studies due to the ease of handling, smooth skin devoid of hair, and histological characteristics similar to human skin [99, 102]. While these are well accepted models for studying permeation properties of xenobiotics *in vitro,* these also serve as excellent *in vivo* models for method development studies.

The aim of this work was to develop sensitive and reproducible impedance measurement techniques in two animal models (Yucatan miniature pig and hairless

guinea pigs) and human subjects, in order to monitor micropore formation in the SC. The studies herein satisfy Research Plan 3.1.

5.2 Methods and materials

5.2.1 Microneedle arrays

Briefly, fixed MN geometries were cut into 50 µm thick stainless steel sheets using chemical etching and were then manually bent perpendicular to the plane of their metal substrate. MNs arrays contained 50 MNs arranged in a 5 x 10 array configuration; each MN measured 800 µm in length and 200 µm in width at the base; the geometry and configuration of the MN arrays were designed and provided by the Prausnitz lab at the Georgia Institute of Technology. For better insertion and adhesion of patches to the skin, microneedle arrays were assembled into adhesive patches with Arclad (Adhesives Research, Inc., Glen Rock, PA). The adhesive serves to hold the MNs firmly against the skin by compensating for the mechanical mismatch between the flexible skin tissue and the rigid MN array. The MN patches were ethylene oxide sterilized before use.

5.2.2 Microneedle application

The same MN application technique was used for animal and human studies. MN insertion is a simple procedure, achieved by placing the 50 MN array on the skin and pressing gently for approximately 10 – 15 seconds and then immediately removed. The array was rotated 45 degrees for a second insertion, in order to create 100 non-overlapping micropores. The same investigator performed all MN insertions in order to eliminate any inter-investigator variability.

5.2.3 Impedance spectroscopy techniques

Impedance measurements were made using Ag/AgCl measurement electrodes and a large electrode with a conductive gel surface, which serves as the reference electrode (Superior Silver Electrode with PermaGel, 70 mm total and active electrode diameter [human and Yucatan pig studies] and 30 mm [hairless guinea pig studies]; Tyco Healthcare Uni-Patch, Wabasha, MN). Two different types of Ag/AgCl measurement electrodes were evaluated: one has a dry active electrode measurement surface (10 mm active electrode diameter; 25 mm x 25 mm total area; Thought Technology T-3404; Stens Corporation, San Rafael, CA), while the other has foam, wet-gel active electrode measurement surface (50 mm diameter, S&W Healthcare Corp,

Brooksville, FA). These types of measurement electrodes are often used for ECG monitoring in a clinical setting, applied to clean dry skin. The reference electrode was placed in the middle of the treatment area, equidistant from all treatment sites. Measurements were made by connecting lead wires to the measurement and reference electrodes, the opposite ends of the wires being connected to an impedance meter. This applies a low frequency alternating current modified with a 200 kΩ resistor in parallel. Figure 5.1 displays the impedance setup.

5.2.4 Animal study procedures

These studies were carried out in two animal models (Yucatan miniature pig and hairless guinea pigs); all studies were approved by the University of Kentucky IACUC. Six sites (Yucatan pig) or 4 sites (guinea pigs) on the dorsal surface were treated with MN arrays. Half of the sites were evaluated with Ag/AgCl dry electrodes, while gel Ag/AgCl electrodes were used at the remaining sites. Repeated baseline (pre-MN) measurements were made at each site: 3 measurements using very light pressure to hold the electrode to the skin, and 3 measurements using more direct pressure, applied by the thumb of the investigator. The same procedure was followed immediately post-MN treatment.

Two different treatment paradigms were investigated, to evaluate impedance measurements made on normal (non-hydrated) vs. hydrated skin. For the hydrated condition, the treatment sites were covered overnight with blank occlusive patches with 3M double-sided medical tape on one side to allow for the patches to adhere closely to the skin; the patches were further secured in place with Bioclusive® waterproof tape. The blank patches thus allowed the skin to locally hydrate under the overnight. Under these conditions, the patches were removed one at a time and all measurements were made at one site before moving to the next.

5.2.5 Clinical (human) study procedures

Healthy human volunteers between 18 – 45 years of age were interviewed and examined to determine appropriateness for the study. Subjects were in general good health (determined by the study physician) with no history of dermatologic disease. All study procedures were approved by the University of Kentucky Institutional Review Board and were completed according to the principles defined in the World Medical

Association Declaration of Helsinki. All subjects provided written, informed consent prior to beginning any study procedures.

All measurements in human subjects were made on hydrated skin (pre-hydration process was the same as that described above for the animals). Six sites on the upper arms of the subjects were treated with MN arrays; 3 sites were evaluated with Ag/AgCl dry electrodes; the other 3 with gel electrodes. Similar to the animal studies, the sites were unoccluded one at a time, and 6 measurements were made at each site: 3 measurements using light pressure and 3 measurements using more direct pressure (similar to the pressure used for a typical doorbell). Following baseline measurements the skin was re-occluded and allowed to re-hydrate for one hour, after being un-occluded for several minutes. Following the re-hydration period, MN arrays were applied to all sites, followed by 6 additional repeated measurements (3 with light pressure, 3 with direct pressure). All measurements took 30 seconds to obtain. Table 5.1 demonstrates the distribution of electrode types and pressure applications amongst the treatment sites.

5.2.6 Calculation of micropore impedance

In the presence of the microporated skin, 3 parallel and independent pathways for electrical current can be distinguished: resistor box (Z_{box}), intact skin (Z_{skin}, pre-MN baseline), and micropores (Z_{pores}). Therefore the measurements yield a total impedance value (Z_{total}) that is a function of the 3 pathways. The Z_{total}, Z_{box} and Z_{skin} are known; therefore, micropore impedance can be calculated according to the following equation (employing the assumption that the micropores occupy approximately 2% of the total measurement area):

$$Z_{total} = \frac{1}{\frac{1}{Z_{box}} + \frac{1}{Z_{skin}} + \frac{0.02}{Z_{pores}}}$$

Equation 5.1

According to this equation, the Z_{pores} can be calculated, and the "upper limit" of impedance at the 2% area occupied by the micropores can also be estimated, allowing for comparison of the impedance difference pre- and post-MN treatment at the same small skin area affected by the MN treatment. This method of calculation completely removes the effect of the relatively large area of intact skin surrounding the micropores that is also measured under the electrode surface.

5.2.7 Transepidermal water loss (TEWL) measurements

In the hairless guinea pigs, TEWL was measured as a complementary technique to impedance. TEWL measurements were made at baseline and post-MN treatment, using an evaporimeter (cyberDERM, INC., Broomall, PA). Measurements were made by simply placing the probe on the surface of the skin until the reading stabilized (the TEWL is calculated by the device in units of $g \cdot m^{-2} \cdot h^{-1}$); each measurement took approximately 30 – 60 seconds to obtain.

5.2.8 Staining techniques

Skin staining was utilized in both animal models to visually confirm the presence of micropores in the SC. Gentian violet stains microporated skin sites, making this a quick and effective means of visualizing the sites where microneedles were inserted into the skin [103]; in the presence of micropores, a grid can be clearly visualized. Following MN treatment the dye was applied to the skin for approximately one minute, followed by removal of excess dye with isopropanol alcohol wipes. A non-treated site was also stained as a control.

5.2.9 Data analysis

Student's t tests were used to compare the calculated impedance of the micropores (Z_{pores}, calculations described above) to pre-MN baseline impedance values at that same site; the same statistical tests were used to compare pre and post-MN TEWL values. $p < 0.05$ was considered statistically significant (GraphPad Prism® software, version 5.04).

5.3 Results
5.3.1 Animal studies

5.3.1.1 Hairless guinea pigs: Male and female hairless guinea pigs (n = 3, mean (± SD) weight of 785 ± 51 g) were treated with MNs at 4 independent sites on the dorsal surface. Due to the smaller surface area of the animals, only 4 sites were treated rather than 6 sites as in humans and the Yucatan pig. All studies were performed on both non pre-hydrated and pre-hydrated skin, to confirm that similar trends would be observed irrespective of skin hydration status. Impedance measurements were made at each site pre- and post-MN, and a TEWL measurement was taken immediately following the impedance measurement at all sites. Impedance measurements dropped significantly

baseline to post-MN (p < 0.05, Student's t-test) at all sites, irrespective of skin hydration status, electrode type, or pressure applied. The conditions that resulted in the lowest amount of variability in the guinea pigs were dry electrodes, applied with direct pressure. On non pre-hydrated skin, mean (± SD) %RSD on pre-MN and post-MN skin were 22.4 ± 11.1% (range 3.2 – 35.4%) and 5.9 ± 2.5% (3.9 – 9.8%), respectively, compared to pre-MN values of 10.8 ± 7.1% (3.4 – 23.5%) and post-MN 19.9 ± 10.0% (6.0 – 29.5%) for gel electrodes under the same conditions. All %RSD values for hydrated and non pre-hydrated skin made with dry electrodes, direct pressure can be seen in Table 5.3, and representative impedance measurements can be seen in Figure 5.1.

TEWL values were low at baseline regardless of skin hydration, confirming an intact barrier function. Mean (± SD) baseline TEWL values were 2.0 ± 0.69 $g•m^{-2}•h^{-1}$ (non pre-hydrated) and 20.2 ± 2.3 $g•m^{-2}•h^{-1}$ (pre-hydrated). A significant rise in TEWL was observed after MN treatment at all sites (p < 0.05, Student's t-test), with post-MN measurements on non pre-hydrated and pre-hydrated skin of 27.4 ± 7.6 $g•m^{-2}•h^{-1}$ and 47.4 ± 17.7 $g•m^{-2}•h^{-1}$, respectively. Representative TEWL measurements are displayed in Figure 5.2.

In order to visualize the micropores using a third independent means of evaluating MN insertion, one guinea pig was treated on non pre-hydrated skin at an additional site with one application of a 50 MN array, followed by staining with gentian violet. As seen in Figure 5.2, a grid in the SC can clearly be visualized, demonstrating the presence of 50 non-overlapping micropores. No staining was observed at the control site when gentian violet was applied to intact skin.

5.3.1.2 Yucatan miniature pig: One male Yucatan miniature pig (weighing approximately 60 kg) was treated with MN arrays at 6 independent sites on the dorsal surface and repeated impedance measurements were made pre- and post-MN treatment on pre-hydrated vs. non pre-hydrated skin. A total of 72 measurements were made on pre-hydrated skin; the same number of measurements were made on non pre-hydrated skin; one measurement was thrown out as an outlier from the pre-MN measurements under pre-hydrated conditions. Similar to the guinea pigs, a significant drop in impedance was seen following MN treatment at all sites (p < 0.05, Student's t-test), irrespective of skin hydration status, electrode type, or pressure applied In the pig, the lowest overall variability under both hydration conditions was observed with gel electrode measurements applied with direct pressure, as demonstrated by lower %RSD values. For non pre-hydrated skin, mean (± SD) %RSD on pre-MN and post-MN skin

were 13.9 ± 2.6 (range 10.8 – 15.3%) and 4.1 ± 1.8% (2.3 – 5.5%), respectively, compared to pre-MN values of 15.1 ± 9.0% (7.0 – 24.8%) and post-MN 4.7 ± 5.3% (1.0 – 10.8%) for dry electrodes under the same conditions. Table 5.3 displays all %RSD values from measurements made with gel electrodes applied with direct pressure.

In the same manner as applied to the guinea pig, one additional (non pre-hydrated) site was treated with a MN array to create 50 micropores (rather than the 100 micropores used for the impedance measurements) and stained with gentian violet dye. All 50 micropores could be clearly seen in the skin, confirming the breach in the SC and the formation of 50 independent micropores (image not shown). Additionally, the non-MN treated control site did not display any staining patterns following removal of the dye.

5.3.2 Human studies

Four males and six females completed the protocol; mean (± SD) age was 27 ± 4.1 years. General demographics are described in Table 5.2. Six sites were treated on the upper arm of each subject; impedance measurements were made pre- and post-MN treatment with dry Ag/AgCl electrodes (3 sites) and gel Ag/AgCl electrodes (3 sites) applied with light or direct pressure (applied by the thumb of the investigator (the applied pressure was similar to the force used to ring a doorbell). Based on this study design, a total of 360 measurements were made for each electrode type, further divided into 180 baseline pre-MN measurements (90 measurements with light pressure; 90 measurements with direct pressure) and 180 post-MN measurements, also divided equally between light and direct pressure techniques. A total of 331 measurements were analyzed across the 10 subjects. All MN applications were well tolerated and no infection or irritation was seen at any MN treatment sites. Some subjects experience mild irritation from the Bioclusive® tape that was used to secure the occlusive patches to the skin for the overnight hydration period. The irritation resolved completely following a short course of topical steroid treatment.

Mean impedance values dropped significantly from baseline to post-MN for all treatment sites, irrespective of pressure or electrode type (p <0.05, Student's t test). The overall variability was lowest with gel electrodes, particularly for the calculated impedance of the micropores. In several subjects there was no variation at all between the 3 measurements made post-MN. The mean ± SD pre-MN and post-MN %RSD was 9.7 ± 6.1% (0.8 – 24.1%) and 2.4 ± 3.0% (0.00 – 11.8%) respectively, across all 10 subjects. A representative profile from one subject is shown in Figure 5.3.

5.4 Discussion

MN technologies offer a wide range of flexibility as a drug delivery technique in that several parameters can be modified to meet specific therapeutic needs; such parameters include the delivery method, geometry of the needles, drug formulation, re-sealing kinetics of the micropores, and type of drug moiety. In the realm of a "poke/press and patch" MN technique, adequate formation of micropores is critical to the success of the delivery approach. A variety of methods are available for evaluating micropore formation in the SC, including optical coherence tomography, confocal microscopy, infrared spectroscopy, impedance spectroscopy, and TEWL. Most of these techniques, while effective for visualizing and evaluating micropore formation, require equipment and software that are less convenient and user-friendly than what is desired in a clinical research environment. The impedance setup described in these studies is portable, requires very little training to use, and has no need for software to obtain measurements, making it ideal for a range of clinical environments as well as animal studies.

5.4.1 Differences between skin conditions and measurement techniques

In both animal models and in human subjects, measurements were noisy and somewhat erratic on pre-MN, intact skin (regardless of hydration status). This is not unexpected, as it represents the skin's effective barrier in preventing the movement of current between the internal and external environments; similar results have been observed previously when impedance methods were used to monitor micropore closure kinetics in human subjects [14]. The post-MN measurements were less variable and noisy, likely due to creation of an un-impeded and consistent pathway for movement of the current. An overall trend was observed that the measurements were generally lower when more direct pressure was applied to the electrode during the measurement, regardless of dry vs. gel electrode, or pre- vs. post-MN. This is likely due to enhanced contact between the electrode surface and the skin, providing a more consistent (and hence less tortuous) pathway for the current to travel. Additionally, the measurements using gel electrodes were generally more stable and did not fluctuate during the measurements, as compared to the dry electrodes (both light and direct pressure). This was observed for intact and post-MN treated skin, but was most notable on MN-treated skin. This could be the case for a variety of reasons. First, the gel provides a pathway of lesser resistance compared to the dry electrodes, as the gel provides an aqueous

pathway for the current to move across. Second, the gel surface likely creates enhanced contact between the electrode and the micropores, which would result in a lower impedance measurement due to the higher number of micropores present in a small measurement area. This would also help explain why measurements are consistently lower with direct pressure measurements when compared to light pressure techniques with the same electrode type. The direct pressure would allow for better contact with the whole grid of 100 micropores, whereas lighter pressure might not provide complete contact between all of the micropores under the small electrode surface. Thus, the optimal situation would be to make measurements with the gel electrodes while applying direct pressure to maintain close contact between the electrode and the skin. In fact, this is consistent with our observation that the lowest variability was observed in human subjects and the Yucatan pig when this technique was used.

Due to typical inter-subject variation, some subjects have naturally lower baseline impedance measurements in general (regardless of electrode type). In these situations it can make the difference between baseline and post-MN treatment somewhat more difficult to interpret from the raw impedance values (Z_{total}). Despite this potential challenge it is not likely be clinically significant, as 1) it is not a uniform concern across all subjects, and 2) the calculation of Z_{pores} clearly distinguishes that the SC has been sufficiently breached, despite a seemingly small difference in the raw values pre-and post-MN.

5.4.2 Skin hydration

In half of the animal experiments and all of the human studies, measurements were made on skin that had been pre-hydrated during an overnight occlusion period. The hydration status represents the truest clinical scenario for transdermal delivery systems, in which the skin remains occluded for hour to days under a patch, resulting in an increase in local skin hydration. Anytime the skin is occluded after MN treatment (the typical situation for the "poke/press and patch method"), impedance measurements for the resulting treatment period would be made on hydrated skin. While MNs would not likely be applied to pre-hydrated skin in clinical practice, in a controlled research setting the pre-hydration removes an additional variable in the impedance setup (dry vs. hydrated skin, a discrepancy that would arise if the baseline measurements were made on dry skin but all other measurements were made on skin that had been occluded). For

these reasons, we explored the impedance techniques on non pre-hydrated AND pre-hydrated skin in the animal models. As demonstrated by the results (in both animal models), the skin's hydration status does not affect the efficiency of MN insertion into the skin, nor does it affect the ability of the impedance setup to determine that the barrier has been breached. The primary difference observed between the hydration states was that the baseline measurements were somewhat more erratic on non pre-hydrated skin, as demonstrated by greater %RSD values. However, the absolute values of the baseline measurements are not as critical because the MN treatment produces such a clear effect on the impedance measurements. Furthermore, in a situation when micropore impedance would be followed over time (during which time the skin would hydrate under a patch), a non-MN treated control site under the same conditions would be used in the equation for calculating Z_{pores}, thus removing the need for the initial baseline value after the first measurement. For these reasons, it would be suitable to use impedance methods for measuring micropore formation in a typical clinical scenario, when human subjects would be treated on dry baseline skin.

5.4.3 Impedance measurements for assessing micropore closure kinetics

One novel application that impedance measurements are well suited for is monitoring micropore lifetime under various conditions after one application of a MN array, by following the Z_{pores} value over time. To be used in this setting, however, it was necessary to develop a measurement setup that minimizes variability between measurements, in order to accurately characterize the kinetics of micropore closure. As the micropores begin to heal the measurements would be expected to become more erratic as the biological processes in the skin begin to restore the intact barrier baseline. In fact, this trend is consistent with previous reports in human subjects treated with MNs of varying geometries, using an identical setup with dry Ag/AgCl electrodes [14]. Investigators in this study found that a significant amount of experimental noise was present when measurements were made on intact skin, but this was not the case on microporated skin, irrespective of the geometry of the MN array applied (varied number or length of the MNs). For this reason it is imperative to have a measurement technique that introduces the least amount of variability, such that the variations observed are directly reflective of the skin re-sealing, rather than the measurement technique itself.

In the current study, the Z_{pores} value was calculated apart from the total impedance measurement that was comprised of 3 parallel pathways. By calculating the

upper limit of the impedance values expected at the 2% area occupied by the micropores, the Z_{pores} can be followed over time until it reaches the upper limit, at which times the micropores would be considered "closed" or "re-sealed". While this method has the advantage of providing a clear numerical target for evaluating when the micropores have completely healed, it could be perceived to falsely exaggerate the difference between pre- and post-MN impedance values. Thus, it is important to evaluate the formation of the micropores with an alternative method to ensure the applicability of the current methods. An additional method that would be suitable for monitoring micropore formation and closure kinetics over time would be to calculate the permeable area ($A_{permeable}$) of all micropores created by the application of a MN array, according to the following equation, as described by Gupta et al [14]:

$$A_{permeable} = \frac{\rho L}{Z}$$

Equation 5.2

where ρ represents the electrical resistivity of interstitial fluid present in the skin (~78 Ω-cm), L is an estimate of the thickness of the SC (approximately 15 µm over most parts of the body), and Z is the absolute impedance measured. Under the technique that generated the least amount of variability in human subjects (gel electrodes applied with direct pressure), this equation results in a range of total permeable area spanning from 4.65×10^{-4} mm^2 to 2.81×10^{-3} mm^2; these values are less than the cross-section of a human hair. Furthermore, the radii of each individual micropore can be calculated (assuming a circular cross section and that each micropore contributes 1/100 of the total $A_{permeable}$). According to these assumptions, the mean (± SD) radii of the individual micropores was 1.97 ± 0.51 µm, which is remarkably consistent with previous estimates of an effective radius of ~2 µm [14, 42]. In a similar manner, a limit of the $A_{permeable}$ can be estimated based on pre-MN measurements, which would also provide a numerical target for reaching the conclusion that the micropores have been re-sealed. Thus, our method demonstrated adequate formation of micropores in the SC based on the $Z_{pores,}$ and the suitability of this method is confirmed by the similarity of our data with previous reports, based on the alternative calculation of the $A_{permeable}$.

The use of impedance spectroscopy is particularly appealing in that it can be used to evaluate MN treatment parameters and micropore closure kinetics, but that it could also be expanded to evaluate other physical enhancement techniques that also create pores in the skin (i.e. thermal ablation, electroporation, etc.). For that reason, this

method of measurement is well suited for a variety of scenarios in clinical and research environments .

5.5 Conclusions

In summary, this is the first methods development study to explore various impedance spectroscopy conditions to minimize experimental variability when monitoring micropore formation in animal models and human subjects. The impedance setup allows for great flexibility that can be tailored to the conditions of MN treatment (varying hydration status, different animal models, different electrode types and pressure applications) and is highly appropriate for clinical research setting. Additionally, the impedance of the micropores can be specifically calculated, or the permeable area of the microporated skin can be determined, allowing for various means for comparing the effectiveness of treatment and monitoring the closure of the micropores over time.

Table 5.1

	Dry Ag/AgCl electrodes		Gel Ag/AgCl electrodes	
	Light pressure (n = 3 sites)	Direct pressure (n = 3 sites)	Light pressure (n = 3 sites)	Direct pressure (n = 3 sites)
Pre-MN	9 measurements	9 measurements	9 measurements	9 measurements
	One-time MN treatment (50 MN array applied twice)		One-time MN treatment (50 MN array applied twice)	
Post-MN	9 measurements	9 measurements	9 measurements	9 measurements
Total	36 total measurements per subject (18 measurements of intact skin baseline; 18 measurements of MN-treated skin)		36 total measurements per subject (18 measurements of intact skin baseline; 18 measurements of MN-treated skin)	

Table 5.1 Description of repeated measurements made at a total of 6 treatment sites on the upper arms of healthy human volunteers. All measurements were made on skin sites that had been pre-hydrated under blank occlusive patches overnight. The same measurement techniques were used in the Yucatan pig and the hairless guinea pigs, with additional measurements made on non pre-hydrated skin in the animal models.

Table 5.2

Sex	4 male
	6 female
Mean age, years (SD)	27.4 (4.1)
	(range 23 – 37)
Mean body mass index, kg/m^2 (SD)	27.2 (5.7)
	(range 20.4 – 40.6)
Race	7 Caucasian
	3 Asian

Table 5.2 Subject demographics across 10 healthy human volunteers.

Table 5.3

		Non pre-hydrated	Pre-hydrated
Yucatan pig **(gel electrodes,** **direct pressure)**	Pre-MN	13.9 ± 2.63 (10.8 – 15.3)	8.01 ± 2.99 (5.09 – 11.06)
	Post-MN	4.14 ± 1.68 (2.27 – 5.52)	8.77 ± 2.87 (6.74 – 10.80)
Guinea pigs **(dry electrodes,** **direct pressure)**	Pre-MN	22.4 ± 11.1 (3.2 – 35.4)	5.99 ± 1.61 (3.11 – 7.41)
	Post-MN	5.9 ± 2.5 (3.9 – 9.8)	16.29 ± 9.92 (5.95 – 33.23)
Human subjects **(gel electrodes,** **direct pressure)**	Pre-MN	NA	9.69 ± 6.13 (0.84 – 24.07)
	Post-MN	NA	2.36 ± 3.01 (0 – 11.80)

Table 5.3 All %RSD values for the conditions that generated the least variability in 2 animal models and 10 human subjects. In the animal models, measurements were taken on dry, non pre-hydrated skin and also on skin that had been pre-hydrated with blank occlusive patches overnight. Human measurements were only taken on skin that had been hydrated overnight. In the Yucatan pig, values were calculated from measurements made at 3 sites; for the guinea pigs the %RSD values were calculated from measurements made at 9 sites in 3 guinea pigs. For the human subjects, the %RSD was calculated across 30 treatment sites in 10 subjects.
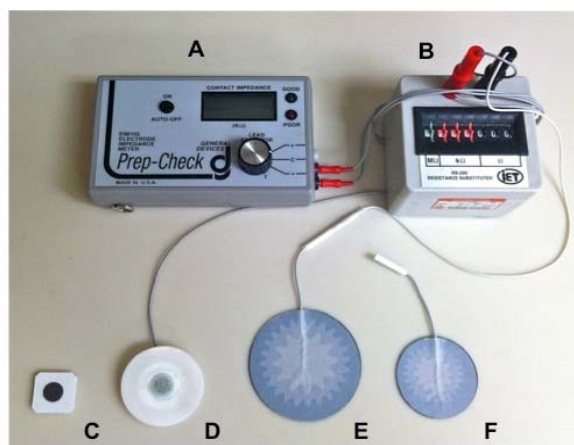
Figure 5.1 Impedance setup used for all human and animal studies.
A: Prep-Check impedance meter; B: 200 kΩ resistor in parallel; C: dry Ag/AgCl measurement electrodes; D: gel Ag/AgCl measurement electrodes; E: Reference electrode for Yucatan miniature pig and human studies; F: reference electrode used for hairless guinea pig studies.
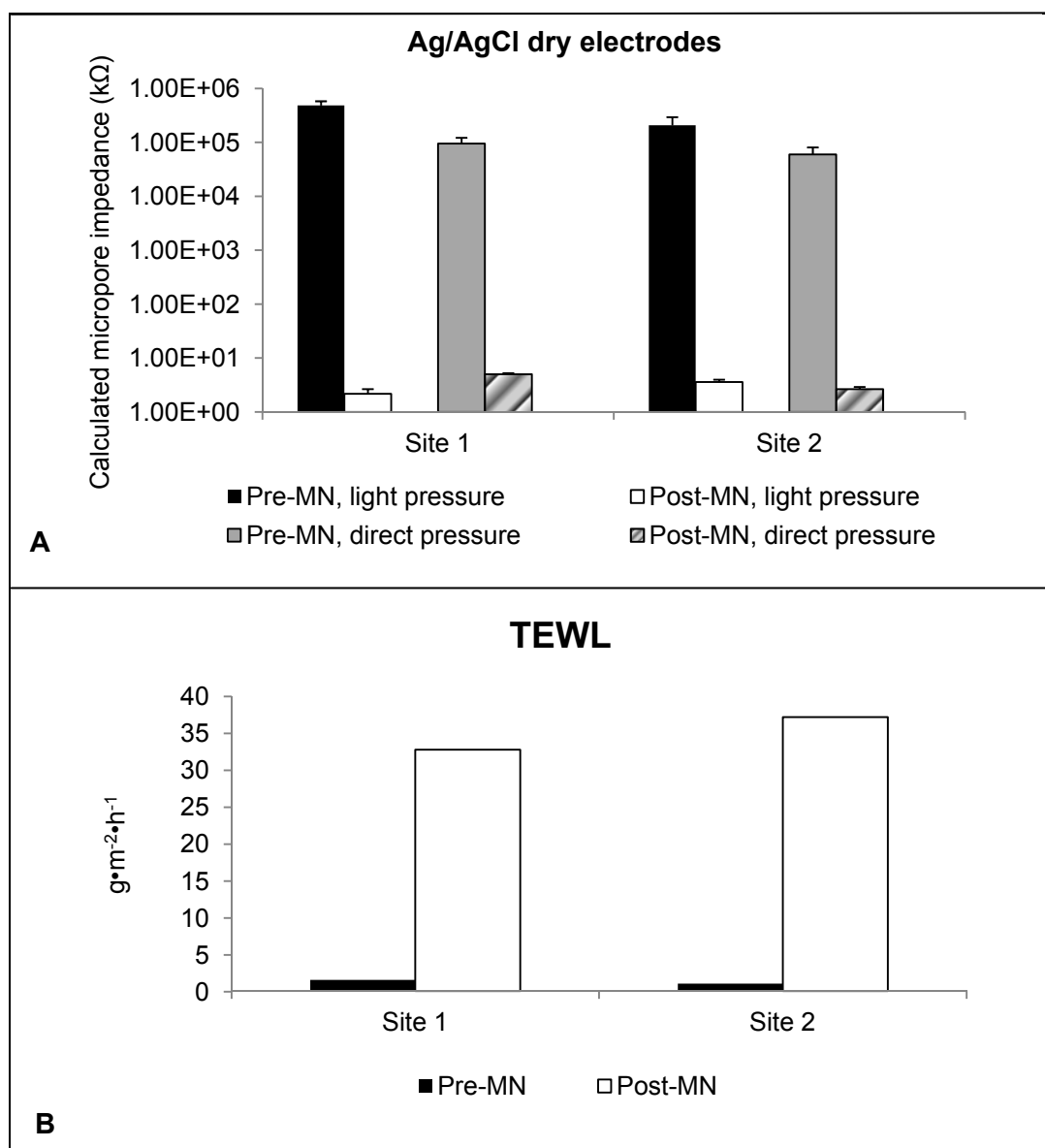
Figure 5.2 Representative impedance and TEWL measurements made pre- and post-MN on non pre-hydrated skin in one hairless guinea pig. A: Representative impedance measurements made pre- and post-MN using dry electrodes. Across all guinea pigs, the dry electrodes applied with direct pressure resulted in the least amount of variability, demonstrated by lower %RSD. For this animal, mean ± SD %RSD pre- and post-MN were 31.0 ± 15.3% and 17.1 ± 8.3% (respectively) when dry electrodes were applied with light pressure, compared to 31.8 ± 5.2% and 7.3 ± 3.6% for the same electrodes applied with direct pressure. B: Representative TEWL measurements made pre- and post-MN, demonstrating an alternative approach for monitoring micropore

formation in the SC (TEWL measurements were not made in triplicate like the impedance measurements; this figure represents single measurements). Baseline TEWL measurements were 1.6 and 1.1 $g \cdot m^{-2} \cdot h^{-1}$ at Sites 1 and 2, respectively, compared to post-MN measurements of 32.8 and 37.2 $g \cdot m^{-2} \cdot h^{-1}$ at the same sites.
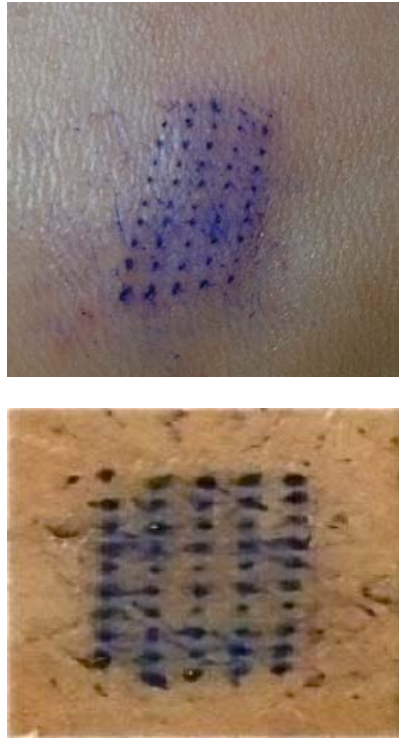
Figure 5.3 A micropore grid on the dorsal surface of a hairless guinea pig (top) and a Yucatan miniature pig (bottom) treated once with a 50 MN array. The 50 individual micropores can be clearly visualized in the skin in both animals, demonstrating adequate penetration of the SC with the MN array.
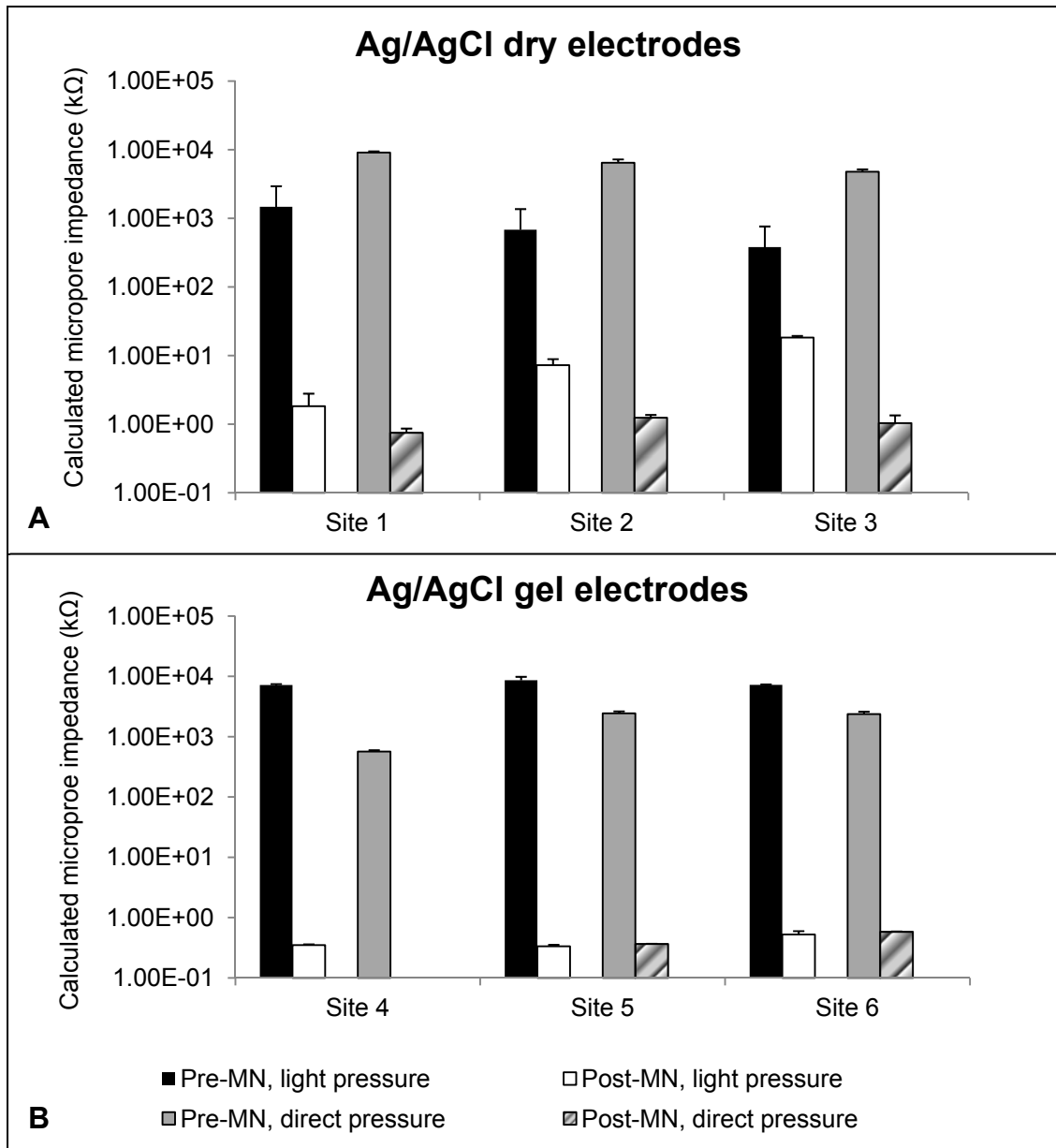
Figure 5.4 Representative impedance profiles in six treatment sites on one human subject; all measurements were made on the hairless upper arm following an overnight pre-hydration period. Each bar represents the mean ± SD (error bars) of 3 measurements. **A:** measurements made at 3 independent with dry Ag/AgCl electrodes. **B:** measurements made at 3 independent with gel Ag/AgCl electrodes.

Under all conditions, irrespective of electrode type or pressure applied during the measurements, the variability between measurements was lowest with gel electrodes

applied with direct pressure. For this subject, mean (± SD) %RSD with gel electrodes under direct application for pre-MN was 7.86 ± 2.09% (range 5.59 – 9.70%), and 0.58 ± 0.54% (range 0.00 – 1.07%) for post-MN. Under the same conditions (direct pressure) for the dry electrodes, the mean %RSD pre-MN was 8.59 ± 3.82% (range 4.71 – 12.35%) and 18.0 ± 10.1% (range 9.68 – 29.29%) for post-MN.

Chapter 6

Prolonging micropore lifetime *in vivo* via application of topical diclofenac in healthy human subjects

6.1 Introduction

Transdermal drug delivery provides significant advantages over other traditional delivery routes by decreasing systemic side effects, avoiding first-pass hepatic metabolism, and increasing ease of application for patients. Despite these advantages, very specific physicochemical properties are required for a drug molecule to passively cross the stratum corneum (SC, the outermost layer of skin), thus limiting this delivery method to a very small number of molecules [1]. Much work has been done towards developing physical methods of disrupting the barrier function of the skin in order to expand the transdermal field to a wider variety of drugs; such methods include iontophoresis, microdermabrasion, and microneedles [2].

Microneedles (MNs) are a minimally invasive means of increasing the permeability of the skin by piercing the SC and creating transient micropores through which a drug can passively diffuse [5]. This novel delivery method allows for a wider variety of molecules to pass the skin's barrier, thus allowing the advantages of transdermal delivery to be applied to a large range of clinical applications including diabetes, severe osteoporosis, and influenza vaccination [5]. MN application generally removes the limitations on the molecular size of the drug moiety, which provides an avenue for the delivery of much larger molecules than what has been previously feasible, including peptides and macromolecules. Perhaps most importantly however, is that treatment with MN arrays is relatively painless and generally well tolerated by most patients, making this a very realistic technique for clinical implementation [5, 7, 43, 59, 104]. In fact, the first commercial MN product in the United States was approved in 2011 for influenza vaccination in adults aged 18 – 64 (Fluzone® Intradermal, Sanofi Pasteur) [8].

New advances using MNs have shown promising results towards achievement of therapeutic clinical outcomes, including systemic delivery of naltrexone (an opioid antagonist approved for treatment of alcohol and opioid addiction). A recent study described transdermal delivery of naltrexone in healthy human subjects following pretreatment with solid MNs (a treatment process known as the "poke (press) and patch" method) [9]. In subjects pretreated with MNs, application of a naltrexone patch yielded

therapeutic blood levels, while application of the naltrexone patch without MN pretreatment failed to achieve therapeutic levels of naltrexone. This is the only human pharmacokinetic study in the literature describing MN-assisted delivery in humans, and it supports the feasibility of this novel transdermal technique. Other human studies have been completed using MNs to deliver recombinant human parathyroid hormone 1-34, teriparatide (PTH), and positive gains in bone mineral density were seen at the hip and lumbar spine, confirming use of MN delivery techniques for achieving clinical benefit [105].

Several factors affect the efficiency of drug transport following MN treatment, including physical parameters of the MNs, properties of the drug compounds to be delivered, and the lifetime of the micropores created in the skin [106]. There has been a great deal of work examining the MN parameters and properties of drug compounds, but very little is known about the kinetics of micropore closure following MN treatment. This factor is critical to the success of MN-assisted delivery for the "poke (press) and patch" MN technique in which MNs are applied to the skin to create micropores followed by application of a drug patch over the top of the treated area [5, 107], and therefore the rates of micropore closure must be optimized for continued forward progress towards clinical implementation. Bal *et al* demonstrated that micropores may close as quickly as 15 minutes following MN treatment in healthy human subjects when the treatment sites remain exposed to air, while another study concluded that the micropores may close in a timeframe of hours [10, 13]. The pharmacokinetic study previously described suggests that the micropores may close by 48 – 72 hours following MN treatment under occluded conditions, preventing any further transdermal delivery [9]. This severely limits the clinical utility of MN application, and thus it is imperative to develop effective means of extending micropore lifetime to achieve a once weekly dosing schedule (the ideal for transdermal delivery).

The physiological processes underlying micropore closure in humans are not known. One possibility is that there may be mild subclinical local inflammation (at a microscopic level), which would serve as a potential therapeutic target for extending the lifetime of the micropores via topical application of anti-inflammatory agents. Non-steroidal anti-inflammatory drugs (NSAIDs) exert their effects by inhibiting the cyclooxygenase (COX) enzymes that are integral to the body's inflammatory response via the arachidonic acid pathway and prostaglandin production, and several topical NSAID formulations are commercially available. A recent study demonstrated that daily

application of 3% diclofenac sodium (a non-specific inhibitor of COX-1 and COX-2) extends micropore lifetime in hairless guinea pigs, allowing transdermal delivery of naltrexone for up to 7 days [11]. This was the first study to demonstrate the feasibility and applicability of extending micropore lifetime with topical NSAIDs.

There are many techniques that can be employed to monitor micropore formation in the skin, both qualitatively and quantitatively. The SC serves as the primary barrier to movement of water and ions, and these properties can be used as a means to evaluate the state of the skin's barrier [16]. Transepidermal water loss (TEWL) measures the movement of water between the skin and the external environment, and an increase in TEWL reflects that the skin's barrier has been compromised [108]. Despite being a widely used technique, however, TEWL measurements are exquisitely sensitive to the hydration status of the skin, presenting a significant challenge for evaluating small changes in SC that has been occluded for hours to days (the typical scenario for a transdermal patch). Impedance spectroscopy is another useful technique that reflects disruption of the SC by measuring the movement of ions. It is well known that human skin presents a large impedance to the movement of electrical current, thus displaying a high electrical resistance that is primarily due to the SC [97, 109, 110]. Accordingly, the electrical impedance of the SC provides important information regarding the state of the skin's barrier function (notably, the impedance of intact, healthy skin is quite high, but decreases in response to injury or insult) [95, 97, 109, 111, 112], and this has been shown to be a reliable method of evaluating barrier function [94-96, 113]. Impedance measurements can detect small changes in skin that has been hydrated, and this technique has very recently been described for specifically studying the kinetics of micropore closure under the effects of occlusion, making this an excellent technique for clinical applications and evaluating "real world" transdermal scenarios with microneedle application [14, 110]. The inverse of the electrical impedance (admittance) can also be used as a measure of the skin barrier integrity as high admittance values signify compromised barrier integrity, while low baseline values are typical under normal physiological conditions (similar trends to those observed with TEWL).

The objective of the present study was to extend the lifetime of the micropores created from MN insertion in healthy human subjects by targeting the COX enzymes via topical application of diclofenac. Impedance spectroscopy was utilized to monitor micropore closure following one-time MN treatment, and tristimulus colorimetry was employed to assess local erythema and skin irritation. These are the first data to

demonstrate that application of small bioactive drugs can effectively delay micropore closure in human subjects. These studies fulfill Research Goal 3.2, and have been submitted for publication to the Journal of Controlled Release.

6.2 Methods and materials

6.2.1 Preparation of drug formulations

Solaraze® gel (3% diclofenac sodium, 2.5% hyaluronic acid, PharmaDerm, Melville, NY) and 0.2% sodium hyaluronate gel (Cypress Pharmaceutical, Inc., Madison, MS) were purchased through the University of Kentucky. Sodium hyaluronate powder (Macronan-P) was a gift from American International Chemical, Inc. (Framingham, MA). A 2.5% hyaluronic acid gel served as the placebo vehicle control, and was prepared from the 0.2% sodium hyaluronate gel and the Macronan-P powder.

6.2.2 Preparation of microneedle arrays and occlusive patches

Briefly, fixed MN geometries are cut into 50 µm thick stainless steel sheets and are manually bent perpendicular to the plane of their metal substrate. The arrays contain 50 MNs arranged in a 5 x 10 configuration. The arrays are further assembled into adhesive patches with Arclad (Adhesives Research, Inc., Glen Rock, PA), which allows for close contact between the MNs and the skin during treatment (methods described previously) [9]. This close contact compensates for the mismatch between the flexible skin tissue and the rigid MN substrate. Each MN measures 800 µm in length and 200 µm in width at the base. The MN patches were ethylene oxide sterilized before use. Figure 6.1 displays one of the MN arrays.

Blank occlusive patches were made by fabricating a rubber-ringed barrier with a drug-impermeable backing membrane on one side (Scotchpak 1109 SPAK 1.34 MIL heat-sealable polyester film; 3M, St. Paul, MN) that was secured to the rubber ring with 3M double-sided medical tape. The patches were held closely to the skin with Bioclusive dressing (Systagenix Wound Management, Quincy, MA). The patches on a subject's arm can be seen in Figure 6.2.

6.2.3 Electrodes and impedance measurements

Ag/AgCl measurement electrodes (Thought Technology T-3404; 25 mm x 25 mm total area; 10 mm active electrode diameter; Stens Corporation, San Rafael, CA) were used to measure the impedance at treatment sites. A large electrode with a conductive

gel was placed in the middle of the treatment sites and served as the reference electrode (Superior Silver Electrode with PermaGel, 70 mm total and active electrode diameter; Tyco Healthcare Unit-Patch, Wabasha, MN). Lead wires were connected to the measurement and reference electrodes, and the opposite ends of the wires were connected to an impedance meter (EIM-105 Prep-Check Electrode Impedance Meter; General Devices, Ridgefield, NJ). The meter applied a low frequency (30 Hz) alternating current that was modified with a 200 kΩ resistor in parallel (IET labs, Inc., Westbury, NY).

6.2.4 Clinical study procedures

All study procedures were approved by the University of Kentucky Institutional Review Board and were carried out in accordance with the principles governing clinical research as defined in the World Medical Association Declaration of Helsinki; all subjects provided informed consent prior to beginning any study procedures. Healthy volunteers were examined and interviewed to determine appropriateness for the study. Volunteers were between 18 – 45 years of age and in general good health with no history of dermatological disease. Subjects were excluded if they had any of the following conditions: severe general allergies (indoor, outdoor, or seasonal); allergy to diclofenac sodium, Solaraze® gel, or hyaluronic acid; previous adverse reaction to MN insertion; known allergy or adverse reaction to medical tape or adhesive. Subjects were also excluded if they were pregnant/nursing or had HIV/AIDS. Immediately prior to and during the study, subjects were asked to refrain from taking any oral anti-inflammatory drugs. At each visit, the subjects sat in the clinic room for 30 minutes prior to any study activities in order to acclimate to normal room temperature of ~25°C. At the first visit, 6 sites were marked on the arm of each subject; each site received a different treatment (Table 6.1).

The treatments were applied to either the volar forearm or upper arm, and three different treatment schedules were examined (Table 6.2). Sites were randomly numbered for the subjects treated on the volar forearm. The observed trends in closure kinetics were similar irrespective of the site; thus for the remaining subjects the sites were not randomized, but were kept consistent. Site 1 was marked at the 12 o'clock position (nearest to the shoulder) and Sites 2 – 6 were number consecutively in a clockwise fashion. After the first three subjects, the treatment sites were moved to the upper arm in order to more accurately represent a possible site of patch placement in clinical practice, and the sites were kept consistent to further eliminate any source of

inter-subject variability. All gel treatments consisted of 200 µl of total gel, rubbed gently into the skin. Fresh gels and new occlusive patches were re-applied at each study visit.

6.2.5 Microneedle treatments

At each MN-treated site, subjects were treated with 100 MN insertions (50 MN array applied twice). MN insertion was achieved by placing the MN array on the skin and pressing gently for approximately 10 – 15 seconds; the array was rotated 45 degrees for the second insertion so as not to overlap the same micropores created by the first insertion. All MN applications were performed by the same investigator to eliminate inter-investigator variability.

6.2.6 Micropore closure kinetics

Micropore closure was assessed via impedance spectroscopy. Prior to any measurements, all excess gel or moisture was gently blotted from the skin with sterile gauze. Each measurement took 30 seconds to obtain. Baseline measurements were obtained, repeated immediately following MN treatment, and then obtained at each clinic visit. Assuming three parallel and independent pathways for electrical current (resistor box (Z_{box}), intact skin (Z_{skin}) and micropores (Z_{pores})), the impedance measurements yield a total impedance value (Z_{total}) that is a function of the three pathways:

$$Z_{total} = \frac{1}{\frac{1}{Z_{box}} + \frac{1}{Z_{skin}} + \frac{0.02}{Z_{pores}}}$$

Equation 6.1

The Z_{skin} was independently estimated from the control sites, and thus the impedance of the micropores could be calculated (employing the assumption that the micropores occupy approximately 2% of the total measurement area) [114]. This approach allows for elimination of confounding variables (influence of the resistor box and hydration state of the skin). The hydration state was further controlled for in schedules 2 and 3 by the fact that MN treatments were applied to pre-hydrated skin.

The inverse of the impedance (admittance, Y) was calculated from the Z_{pores}. Admittance is also a measure of skin barrier integrity and behaves similarly to transepidermal water loss measurements (e.g. high admittance values signify compromised barrier integrity, while low baseline values are typical under normal physiological conditions). Admittance was normalized to the highest post-MN admittance, and any contribution from the control site was subtracted out (i.e. any effect

attributed to the gels or hydration status). For diclofenac and placebo sites, the area under the admittance-time curve (AUC) was calculated (GraphPad Prism® software, version 5.04) to allow for comparison between treatments. At placebo sites it was assumed that the change in admittance values follows approximately first-order kinetics, thus providing an additional means of estimating the kinetics of micropore closure without any active treatment. Micropore closure rate constants (k's) were determined according to the simple model:

$$Y_{pores} = Y_{pores,0} * e^{-kt}$$

Equation 6.2

Admittance values were logarithmically transformed to fit a log-linear form of the model and obtain apparent first-order rate constants. Each subject served as their own control, and a paired t-test was performed to compare the effects of diclofenac vs. placebo treatment. $p < 0.05$ was considered statistically significant.

6.2.7 Skin irritation assessments

Tristimulus colorimetry readings were made on the upper arms of six subjects in order to assess the skin irritation potential of the treatments. Erythema was quantified with a Konica Minolta meter (ChromaMeter CR-400, Konica Minolta, Japan) according to previously published guidelines [115]. This technique is non-invasive, measurements are very quick (less than 5 seconds each), and the device is handheld and portable, making it suitable for a clinical environment. The colorimeter was calibrated daily against a white plate provided by Konica Minolta. Measurements were made by placing the head of the instrument gently on the skin area to record the color reflectance. Readings were taken in triplicate at every site at each study visit and the mean a* value was calculated. The change in erythema was reported as a change from the baseline, Δa*, calculated as Δa* = a^*_t (at time t days after starting the study) $-a^*_0$ (at time 0, prior to application of treatment). Statistical analysis was performed using a one-way ANOVA with post-hoc Tukey's analysis (GraphPad Prism®, version 5.04).

6.3 Results
6.3.1 Subjects

Thirteen healthy volunteers completed this study: 7 males and 6 females (general demographics described in Table 3); treatment paradigms and schedules are

described in Table 4. The various paradigms and schedules allowed for the investigation of different scenarios, including: 1) the effects of pre-hydration on micropore closure; 2) evaluation of micropore closure kinetics under different frequencies of diclofenac application; and 3) comparison of admittance profiles following identical treatment at two independent sites. MN treatments were well tolerated by all of the subjects and no irritation or infection was noted at any of the treatment sites. Some subjects had mild to moderate irritation/allergic reactions to the Bioclusive adhesive tape that was used to secure the blank occlusive patches to the skin (to cover the treatment sites). These local reactions were isolated to the areas of skin covered by the Bioclusive and were determined by the study physicians to be unrelated to the MN or gel treatments themselves. All reactions were treated with brief courses of topical steroids, and all resolved quickly.

6.3.2 Formation of micropores in the stratum corneum

A total of 50 MN treatments were applied in 13 subjects at diclofenac and placebo treated sites (one MN treatment consists of two applications of a 50 MN array, in order to create 100 micropores). Z_{pores} (impedance of the micropores) was calculated as described above in the Methods section. Impedance dropped significantly from baseline immediately following MN treatment in all subjects (p = 0.002, paired t-test) indicating formation of micropores in the SC and significant disruption of the skin's barrier function (one subject's measurements were excluded as outliers, n = 2).

The most relevant clinical scenario for transdermal patches is such that the skin remains occluded beneath a patch for a timeframe of hours to days. Impedance measurements can be made on skin with varied levels of hydration [112], but this does impose an additional factor that could create variability in the measurements. In some subjects the skin was pre-hydrated before MN treatment in order to completely remove any possible effects of hydration on the impedance measurements (n = 20 MN treatments). However, the employed basic research method of calculating the Z_{pores} described in the Methods section (using the measurements at corresponding control sites to estimate the value of hydrated intact skin) also allows for removal of hydration effects. Therefore, to more accurately depict the truest clinical scenario, the pre-hydration period was removed from the treatment schedule (n = 28 MN treatments). Two subjects completed the study in a crossover design, once with pre-hydration and once without pre-hydration. There was no significant difference (p > 0.5, Student's t-test) in

the post-MN impedance measurements at diclofenac vs. placebo sites, regardless of hydration status at the time of treatment (Figure 6.3); therefore, the hydration of the skin did not appear to introduce additional variability in the measurements. As expected, in all subjects the baseline impedance of intact skin was quite high (always greater than 1500 kΩ, data not shown), which is required for the skin to maintain its effective barrier function. MN treatment breaches this barrier, leading to a substantial decrease in impedance. At pre-hydrated sites (n = 20 total; 10 diclofenac sites and 10 placebo sites), micropore impedance (average ± SD) immediately post-MN treatment was 0.87 ± 0.42 kΩ at diclofenac sites vs. 0.90 ± 0.47 kΩ at placebo sites (p = 0.9, Student's t-test). At non pre-hydrated sites (n = 28 total; 14 diclofenac sites and 14 placebo sites), micropore impedance immediately following MN treatment at diclofenac and placebo sites was 0.45 ± 0.49 kΩ vs. 0.43 ± 0.52 kΩ, respectively (p = 0.9, Student's t-test). All initial post-MN measurements can be seen in Figure 3. Thus, while there is some variation between subjects in the impedance measurements immediately following MN treatment, in each individual subject the formation of micropores can be easily detected when compared to that subject's high intact skin baseline.

6.3.3 Micropore closure kinetics

Micropore closure was assessed via impedance spectroscopy, a method well described for monitoring skin integrity and barrier function under various conditions [110-112, 116, 117]. Admittance values (inverse of the impedance measurements) were calculated and %-normalized to the highest post-MN admittance value (in some subjects the admittance increased slightly at 24 hours following MN treatment) and plotted vs. time such that the area under the admittance-time curve (AUC, %·days) was calculated. In the first five subjects, additional control sites were applied including occlusion of intact skin, MN-treated skin under occluded conditions (no gels applied), and MN-treated skin exposed to air. In all subjects, measurements at unoccluded MN-treated sites had returned to baseline by the time of the next clinic visit, and the AUC at MN-treated sites under occlusion were not significantly different from placebo (p = 0.6, paired t-test). Therefore, the remaining subjects were not treated with these controls, but rather had replicates of MN + diclofenac and MN + placebo treatment sites.

As expected with a biological system, a wide range in the AUC values was observed at both diclofenac and placebo treatment sites (87.3 – 426.0 %·days vs. 53.5 – 309.6 %·days, respectively); the overall difference between treatments was significant (p

< 0.0001, paired t-test). Figure 6.4 displays the AUC at diclofenac and placebo sites for each subject. Two subjects had notably higher AUC for both diclofenac and placebo sites, while two subjects did not display any difference between active and placebo AUC. The subjects who received the fewest applications of diclofenac had the highest AUC compared to the other subjects (AUC of 309.6 %·days and 380.2 %·days, vs. values of <300 %·days for all other subjects); the AUC for these subjects was also calculated over a total of 7 days post-MN treatment, which could contribute to the higher values. However, the difference between active and placebo AUC is still significant if these values are removed from the analysis (p < 0.0005, paired t-test). Despite these variations, the results are neither surprising nor discouraging, as differences in therapeutic response, outliers, and non-responders are all typical with human clinical data. Representative admittance profiles are seen in Figure 6.5. For the subjects who completed the crossover design (Subjects 6 and 9), the overall effect of the pre-hydration period was somewhat inconsistent between the two subjects, although the shapes of the profiles within each subject were consistent (irrespective of the skin's hydration status at the time of MN treatment). The average ± SD AUC values at the pre-hydrated diclofenac treatment sites were 240.5 ± 88.5 %·days and 145.8 ± 17.0 %·days (Subjects 6 and 9, respectively), vs. the AUC at non-prehydrated diclofenac sites of 271.4 ± 55.6 %·days and 131.9 ± 25.4 %·days. Pre-hydrated placebo site AUC values were 74.6 ± 6.2 %·days (Subject 6) vs. 59.8 ± 8.9 %·days (Subject 9), compared to the non pre-hydrated values of 170.1 ± 3.8 %·days and 81.1 ± 3.4 %·days. Therefore, a positive treatment effect (i.e. higher AUC at diclofenac sites) was seen in both subjects under both treatment schedules (Figure 6).

For the majority of subjects, admittance of the micropores exhibited approximately exponential decay at the MN + placebo treatment sites, and logarithmically transforming this data allowed for determination of apparent first-order rate constants (k's). The average ± SD rate constant was 0.92 ± 0.32 days^{-1} (range 0.41 – 1.60 days^{-1}). Based on the rate constants, the average first-order $t_{1/2}$ of micropore closure (without any active drug moiety to prolong micropore lifetime) was approximately 0.76 ± 0.35 days (range 0.43 – 1.67 days). In contrast, the kinetics at sites treated with MN + diclofenac did not generally follow an exponential decay process, and there was more inter-subject variability in the shape of the profiles. In subjects who had duplicate treatments (i.e. the same treatment applied to two independent sites), the shapes of the profiles were markedly similar, for both diclofenac and placebo treated sites,

71

demonstrating the reproducibility of this surrogate marker technique for monitoring micropore closure (Figure 6.5).

To more consistently compare treatment effects between subjects, the ratio of diclofenac to placebo AUC was calculated (Figure 7). By comparing the active to placebo treatment sites within the same subject, a better comparison of the magnitude of treatment effect can be made between subjects. All ratios were >1.0 (range 1.01 – 3.23), demonstrating a positive treatment effect (slower micropore closure) attributed to diclofenac. The hydration status of the skin did not appear to have any consistent effect on the magnitude of the treatment effect, which was especially notable in subjects 6 and 9, who completed the crossover design (Figure 6.6).

6.3.4 Effects of diclofenac on human skin

Colorimetry measurements in six subjects (treatment paradigm 2, schedule 1) were taken to confirm that the observed differences between diclofenac and placebo sites were in fact a result of the diclofenac sodium and were not due to nonspecific irritation. In all subjects, a* and Δa* values over the entire treatment course were lower than values expected for positive controls following treatment with mild skin irritants in humans or guinea pigs [118, 119] (Figure 6.8). There was no significant difference in erythema between any of the treatment sites ($p = 0.2$, one-way ANOVA) and no redness or irritation was observable by the naked eye. These combined factors indicate that no clinically significant skin irritation contributed to the enhanced admittance observed at the diclofenac treatment sites, and also confirms other findings that microneedle treatment in humans is not irritating [7, 9, 59, 104].

6.3.5 Benefits of examining multiple treatment schedules

Examining the effects of diclofenac under the 3 different treatment schedules provides some unique insight about the measurement techniques and treatment effects. In the crossover subjects, completing Schedules 1 and 2 helped confirm that the impedance measurements were reproducible regardless of the skin's hydration status, demonstrating the consistency of this measurement technique under various clinical conditions. Second, a positive treatment effect from the diclofenac was seen in both subjects for both schedules, confirming that the skin's restoration response after MN treatment (and attenuation of that response with an anti-inflammatory) is not altered based on the skin's hydration status. For all subjects who completed either Schedule 1

or 2, it was valuable from a safety perspective for the investigators to remove the gels and patches daily to visually inspect the skin to ensure that no infection or irritation was present. This also provided an opportunity to measure subclinical erythema with the colorimetry methods. Finally, Schedule 3 demonstrated that daily application of the diclofenac gel was not necessary in order to observe a positive effect from the diclofenac. This suggests that the unique gel base (containing hyaluronate sodium) created a depot in the skin providing a local anti-inflammatory effect, rather than a systemic effect. Lastly, this schedule further confirmed that the skin follows the same restoration response with or without anti-inflammatory treatment under short (24 hour) vs. longer (72 hour) pre-hydration periods, suggesting that the hydration under a transdermal patch applied for a full week would not negatively affect the treatment response from diclofenac.

6.4 Discussion

The benefits of transdermal drug delivery are well established, but the strict physicochemical parameters required for a drug to cross the skin barrier limits the number of molecules that can be passively delivered. Physical enhancement methods have greatly expanded the potential number of drug molecules that can be transdermally delivered, but despite these advances none of the methods are yet suitable for delivering a drug over a week-long time frame, (the ideal for transdermal patches). This is the first human study to demonstrate that the lifetime of micropores following one-time application of MN arrays can be enhanced via simple topical application of a nonspecific COX inhibitor. The commercial development of this technology would allow for transdermal treatment of a variety of indications with less frequent patch application, which would likely increase patient compliance and satisfaction with therapy.

Previous studies have demonstrated that daily application of diclofenac prolongs micropore lifetime in hairless guinea pigs [11], and the present work demonstrates that micropore closure kinetics are also prolonged in human subjects via evaluation of the AUC over several days following MN treatment. The AUC is typically reported for drug concentration-time data to demonstrate total drug exposure, allowing for a comparison of exposure between different treatments. In this case, we used AUC to compare the change in the admittance values between diclofenac and placebo treatment sites. While this does not explicitly describe the kinetics of micropore closure, per se, it can be extrapolated that a higher AUC would correlate with slower rates of closure, as a higher

AUC would be a result of higher admittance values over the entire treatment period. Therefore, this model incorporates the general assumption that slower kinetics of micropore closure are described by higher AUC values.

The diclofenac formulation used in these studies is unique in that the vehicle contains 2.5% hyaluronic acid, a naturally occurring polysaccharide found in the skin. Studies have demonstrated that hyaluronic acid aids the partitioning of diclofenac into the skin and promotes its retention within the epidermis, ultimately creating a local depot of drug [120]. For the purposes of enhancing micropore lifetime this property is particularly appealing, as it ensures that the effects of the diclofenac are a result of local concentrations at the micropores, rather than any effects from systemic delivery. The subjects with the highest AUC were those that completed the treatment schedule with the fewest applications of diclofenac, suggesting that daily application of the diclofenac is not necessary (which is likely partly attributable to the depot of diclofenac formed in the skin). The AUC values for the subjects in Schedule 3 were calculated over a total of 7 days post-MN treatment, which could also contribute to the higher values. It was not feasible to accurately determine the AUC over a 4 day post-MN period in these subjects because this would have generated an AUC from a much smaller number of data points, which is likely to greatly overestimate the values and produce the appearance of a more pronounced treatment effect. It is also possible that the increased exposure to air (created by daily impedance measurements) at the MN-treated sites in the other subjects may have contributed to faster micropore closure, as MN-treated skin heals markedly faster when unoccluded. Any systemic absorption of diclofenac from the topical dose (200 µl of a 3% w/w gel, 6 mg total) would be considered negligible, as this is far below the lowest oral dose of diclofenac given for systemic indications (100 mg/day with 50% oral bioavailability equating to a 50 mg systemic dose) [121].

6.4.1 Effect of formulation pH on micropore closure kinetics

The experimentally measured pH values of the diclofenac and placebo gels were 7.3 and 4.7, respectively. The effect of pH on skin wound healing has been investigated in the literature and it has been shown that pH does not play a role in wound healing for lesser insults [122]. However, in the case of acetone disruption when the "acid mantle" of the skin is disturbed, the rate of healing is slower at pH 7.4 compared to pH 5.5. This can be attributed to the acidic pH optimum of β-glucocerebrosidase, an enzyme responsible for the post-secretion modifications of polar to non-polar ceramides [122].

Since the pH of the diclofenac gel was higher compared to the placebo in this study, we examined the role of formulation pH in the re-sealing of the micropores. Micropore closure kinetics were evaluated *in vivo* under 3 different pH conditions in a Yucatan miniature pig: pH 5.5, 6.5 and 7.4 (gels made in 100 mM citrate buffer and gelled with 3% hydroxyethylcellulose). Three MN treated sites and 1 untreated control site were used for each pH condition; all sites were under occlusion after one time MN application. There was no significant difference in admittance values among the 3 conditions after the first 24 hours (p>0.05). The difference in admittance up to 24 hours is consistent with previous reports demonstrating significant differences in TEWL (following acetone treatment) between pH 5.5 and pH 7.4 at 2h and 4h (p<0.01) and 24h (p<0.05) [122]. After the early time points, however, the rates of recovery normalize in spite of the pH difference. Thus, as the skin begins to heal itself over time, the effect of formulation pH becomes less evident in the repair mechanism. Hence it can be concluded that the effect of diclofenac seen in this study is independent of the formulation pH of the gels, beyond the 24h time point. Based on the pH data and all of the above mentioned factors it can be concluded that the differences in micropore closure (between diclofenac and placebo) that were observed in this study are related to the local concentration of diclofenac, not from a systemic anti-inflammatory effect, or from the effects of the gel vehicles.

6.4.2 Potential factors contributing to inter-subject variability

The ability of drugs to permeate intact human skin is related both to the individual characteristics of the subject's skin as well as the structural and physicochemical properties of the drug compound (molecular weight, octanol/water partition coefficient, and hydrogen bonding) [123]. For *in vitro* human skin experimental permeability data alone, it is not unusual to observe as much as 30% variation [24, 124]. Responses to topical treatments can sometimes be quite unpredictable, and there are currently no methods to accurately predict whether or not a subject will be an outlier in the typical response to a topically applied drug. In the present study there are various reasons why some subjects had higher or lower levels of response. First, previous work has demonstrated that drug-metabolizing enzymes (DMEs) are expressed in human skin [125], and inter-subject differences in the expression of these enzymes could be related to the magnitude of treatment effect observed from a variety of topical treatments. Diclofenac metabolism in the skin is thought to be similar to the metabolism seen following oral administration (conversion to glucuronide conjugates) [126], and varied

expression of the enzymes involved in this metabolism could impact the treatment effect observed following topical diclofenac application. It is noteworthy here, however, that the amount of drug applied per unit area for typical topical drug applications would likely saturate the enzyme systems, and therefore differences in metabolism of diclofenac in the skin would likely have a minimal effect in this regard. Second, expression of the COX enzymes in normal skin can vary [127], and it is possible that a subject with lower COX enzyme expression may not display as pronounced an effect to the diclofenac treatment (the opposite would be true for subjects with greater COX expression in the skin). Third, expression of DMEs in the skin can be increased or decreased to varying degrees in response to topical treatments used in clinical practice, which could further contribute to the observed variation [125]. Despite these possible inter-subject variations, the overall trend demonstrated a significant difference between active and placebo treatments in a relatively small sample size.

6.4.3 Drug delivery window in relation to micropore lifetime and transdermal systems

It is important to note that extending micropore lifetime is not the only factor that will contribute to enhanced delivery of a drug molecule to therapeutically relevant systemic concentrations. The nature of transdermal patches dictates that a treatment site is occluded for the duration of patch application, which leads to a local increase in skin hydration. This natural byproduct of the treatment system can lead to enhanced drug delivery for many compounds [128] and helps the micropores to remain open for days (as seen by the drug delivery window observed in the human pharmacokinetic study) vs. approximately 15 minutes (observed when the micropores remain unoccluded) [9, 10]. The enhanced micropore lifetime seen in this study combined with the increased drug delivery related to the local hydration represents the truest clinical scenario and would be expected to produce an additive effect on drug delivery.

In MN-assisted drug delivery, the concept of micropore lifetime is only useful in the context of a window during which a drug can be transdermally delivered to a therapeutic plasma concentration. The first MN-assisted pharmacokinetic study demonstrated that naltrexone can be transdermally delivered through micropores for 2-3 days under occluded conditions in the absence of any active drug moiety to prolong micropore lifetime [9]. An average micropore closure half-life of 0.76 days was observed in the current study, corresponding with the pharmacokinetic drug delivery window of approximately 2-3 days (or 3-5 half-lives) when ~87.5 - 97% of the micropores would be

closed (according to the impedance measurements). While the notion of first-order rate constants cannot be extrapolated directly to the diclofenac sites because of the non-exponential decay of the admittance profiles, it does illustrate that the true drug delivery window is significantly longer than what is predicted based on the kinetics of micropore closure alone. It is probable that the impedance measurements overestimate the micropore closure rate, and this method is not as sensitive as evaluating drug diffusion in a pharmacokinetic study. A proof-of-concept pharmacokinetic study will be necessary, but impedance is a useful surrogate marker to conduct micropore closure formulation study screening.

In addition to providing a better understanding of the drug delivery window, the consistency of rate constants at the placebo treatment sites also provides a novel method of evaluating other treatments for enhancing the lifetime of micropores. The ratio of active treatment to placebo treatment effects (in this case, AUC) offers a means to understand the magnitude of a treatment effect, allowing for more direct comparison between subjects. Without drug plasma concentrations to measure the amount of drug delivery through the micropores, this ratio solely describes the difference between AUC values; thus, a ratio of 2.0 would correlate to 2-fold slower rates of micropore closure at diclofenac sites vs. placebo sites (based on the assumption that higher AUC indirectly describes slower kinetics of micropore closure). This ratio of 2.0 would then also loosely predict that the maximum amount of drug that could be delivered through the micropores at diclofenac treatment sites would be approximately twice that seen at placebo sites. This analysis was not only useful in the current work, but will likely also prove to be beneficial for screening additional compounds for similar effects. This ratio allows for a direct comparison of the utility of various treatments within the same subject by allowing the subject to serve as their own control, while also allowing for comparison between subjects. Furthermore, these techniques could be expanded to measure pore closure in other physical enhancement techniques that create pores in the skin (e.g. microdermabrasion or electroporation).

6.4.4 Tolerability of microneedles and topical treatments

Skin erythema after MN treatment and topical gel applications was quantified using a tristimulus colorimeter. This technique allows for analysis of blue, red, and green light reflected from the skin, providing a quantitative means of assessing skin color that mimics the perception of the human eye. The a* measurement represents the red-green

axis, and this value becomes more positive as erythema appears on the skin (i.e. less green light is reflected) [115]. The a* values obtained with a colorimeter correlate well with erythema and can be used to quantify skin irritation; the Δa* demonstrates change in local erythema from a pre-treatment baseline at that site [115]. It has been reported that Δa* values can reach up to 4.73 in humans following treatment with sodium lauryl sulfate (a known skin irritant) and as high as 8.9 in hairless guinea pigs [119, 129]. Hairless guinea pigs are a well accepted model for studying skin irritation as they are more sensitive than humans to mild irritation, allowing for a more conservative estimation of skin irritation potential [130]. In this study, Δa* values were well below those of typical positive controls, confirming the lack of erythema and providing additional support that the observed changes in micropore lifetime are not related to nonspecific local irritation.

The concern often arises that prolonging micropore lifetime may increase the risk of local infection at MN treated sites. From a practical point of view, however, this is not a prominent concern. Prior to application of MN arrays, the skin is treated with 70% isopropyl alcohol and the arrays are sterile and only used once (similar precautions to those used in routine clinical care for inserting a hypodermic needle into the skin). All topical treatments applied to the MN treated skin would be in a preparation suitable for human use, i.e. the formulation would contain bacteriostatic/cidal preservatives designed to prevent local bacterial infection [9]. Finally, despite all of the research performed on MN-assisted delivery, no reports have described any kind of infection (local or systemic), and *in vitro* work has demonstrated that microbial penetration is significantly less following treatment with a MN array vs. a 21G hypodermic needle [62].

6.4.5 Limitations

There are some limitations to this work. Due to the rapid closure of the micropores in unoccluded conditions, repeated impedance measurements could not be made at each time point because of the prolonged exposure to air that this would allow. Despite this limitation, the profiles were similar in shape in those subjects who had multiple sites for identical treatments, and placebo rate constants were similar between subjects, demonstrating the reliability and reproducibility of the results. Secondly, MN insertion is a somewhat imprecise process and there are currently no non-proprietary standardized means of applying MN arrays to the skin. This was controlled for as much as possible by having the same investigator apply all of the MN treatments, to avoid

inter-investigator variability. There was no significant difference in the post-MN measurements between diclofenac and placebo treatment sites, and therefore the imprecise nature of MN application would not be expected to substantially affect the results. Finally, in this study diclofenac was applied daily to the skin for the majority of subjects. This does not represent the ideal clinical situation, as it would be cumbersome for a patient to apply the gel daily. Additionally, in a regulatory sense the concept of using diclofenac to enhance micropore lifetime might seem impractical because of the frequent applications and off-label use of a commercial product. However, the application schedule was a necessary component of this work given the proof-of-concept nature of the study and the need to remove the gels in order to make impedance measurements; furthermore, the diclofenac gel represented the safest formulation due to the lack of systemic delivery from the gel vehicle. Current work in our lab is focused on developing codrugs for integrating diclofenac into a patch system that would allow for continued local delivery of the diclofenac. A codrug consists of two drug moieties joined by a chemical linker (in this case diclofenac sodium linked to another drug), in order to improve the delivery of one or both drugs. Our efforts are aimed at developing a codrug system with diclofenac that will dissociate within the skin, thus separating the two independent drugs and allowing for local delivery of diclofenac sodium while allowing the other drug moiety to passively diffuse through the micropores into the systemic circulation. This would thereby eliminate the need for daily application of the diclofenac moiety and would be a product designed specifically for enhancing micropore lifetime to allow for a longer drug delivery window [131].

6.5 Conclusions

In summary, this is the first study in human volunteers to demonstrate that topical application of a nonspecific COX inhibitor can prolong micropore lifetime. Future directions of this work will include a pharmacokinetic proof-of-concept study to demonstrate the clinical utility of extending micropore lifetime, as well as continued development of diclofenac codrugs. This work indicates that MN-assisted transdermal delivery has immense potential to continue expanding to allow for delivery of a vast array of drug compounds for a variety of clinical uses.

Table 6.1

Site	Treatment paradigm 1 (n = 5 subjects)
1	MN array + occlusion
2	MN array + diclofenac gel + occlusion
3	Diclofenac gel + occlusion
4	Occlusion of non-treated skin
5	MN array, unoccluded
6	MN array + placebo gel + occlusion

Site(s)	Treatment paradigm 2 (n = 8 subjects)
1 and 2	MN array + diclofenac gel + occlusion
3 and 4	MN array + placebo gel + occlusion
5	Diclofenac gel + occlusion
6	Placebo gel + occlusion

Table 6.1 Description of the treatments applied to each subject to examine the effect of diclofenac and placebo gels on micropore closure kinetics. All treatments consisted of 200 µl total volume. Three subjects in paradigm 1 received treatment on the volar forearm; the remaining two subjects in this treatment paradigm and all subjects in paradigm 2 were treated on the upper arm.

Table 6.2

Schedule 1 (n = 9)		Schedule 2 (n = 4)		Schedule 3 (n = 2)	
Day of study	Applied treatments	Day of study	Applied treatments	Day of study	Applied treatments
0	MN treatment, application of gels, occlusion of sites	0	Application of blank occlusive patches to intact skin	0	Application of blank occlusive patches to intact skin
1 - 3	Daily application of fresh gels and occlusive patches	1 (following 72 hours of occlusion)	MN treatment, application of gels, occlusion of sites	1 (following 24 hours of occlusion)	MN treatment, application of gels, occlusion of sites
4 (96 hours post-MN)	Removal of gels/patches	2 – 4	Daily application of fresh gels and occlusive patches	4 (72 hours post-MN)	Re-application of gels and occlusive patches
		5 (96 hours post-MN)	Removal of gels/patches	8 (7 days post-MN)	Removal of gels/patches

Table 6.2 Description of the different treatment schedules to determine the effect of varying timeframes of pre-hydration on micropore closure kinetics. Three different schedules were examined, with varying timeframes of pre-hydration (0, 24 or 72 hours of pre-hydration). Two subjects completed both schedules 1 and 2 in a crossover-type design.

Table 6.3

Subject demographics	Count
Sex	
Male (%)	7 (54)
Female (%)	6 (46)
Mean age, years (SD)	27.5 (5.8)
Minimum age	22
Maximum age	45
Race	
Caucasian (%)	11 (85)
Asian (%)	2 (15)
Mean body mass index (SD)	27.4 (5.6)
Minimum BMI	
Maximum BMI	18.7
	39.7

Table 6.3 Human subject demographics (n = 13).

Table 6.4

Subjects	Treatment paradigm	Schedule	Treatment site
1 – 3	1	1	Volar forearm
4 – 9	2	1	Upper arm
6, 9, 10 – 11	2	2	Upper arm
12, 13	1	3	Upper arm

Table 6.4 Description of the combinations of treatment paradigms, schedules, and treatment sites for all subjects. Subjects 6 and 9 completed both Schedules 1 and 2.
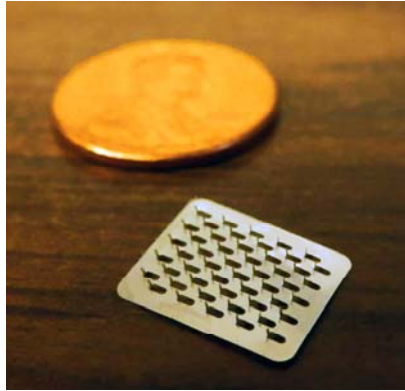
Figure 6.1 Image of a microneedle array. The MN arrays are arranged in a configuration of 5 x 10 needles, with a total of 50 MNs per array. The array is displayed next to a penny in order to demonstrate the relative small size of the whole array.

Figure 6.2 Treatment patches and electrodes on a subject's upper arm. The reference electrode was placed in the middle of all the treatment sites, which were protected during the study by blank occlusive patches. The top treatment site displays one of the Ag/AgCl measurement electrodes, which is moved from site to site to make impedance measurements. Both the reference and measurement electrodes are connected by lead wires to the impedance meter.
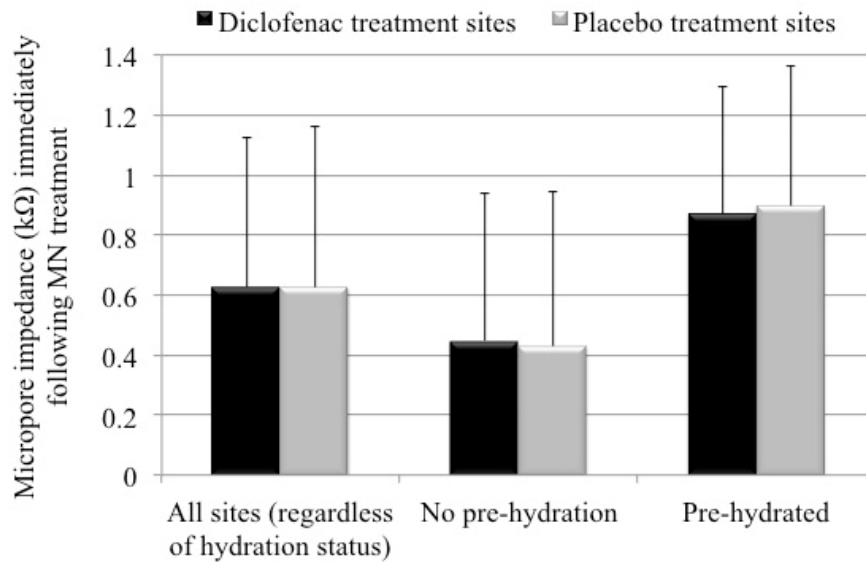
Figure 6.3 Impedance of the micropores immediately following MN treatment. All data are represented as average ± SD. Black bars represent diclofenac treatment sites, and grey bars represent placebo sites. One subject's impedance values were excluded as outliers (n = 2 measurements). Regardless of hydration status, no significant difference was found between the impedance measurements at diclofenac vs. placebo sites. Micropore impedance (irrespective of hydration status, n = 24 in each group) at diclofenac treatment sites was 0.62 ± 0.50 kΩ, compared to 0.62 ± 0.54 kΩ at placebo treatment sites (p = 1.0, Student's t-test). At non pre-hydrated sites (n = 14 in each group), micropore impedance at diclofenac and placebo treatment sites was 0.45 ± 0.49 kΩ and 0.43 ± 0.52 kΩ, respectively (p = 0.9, Student's t-test). Finally, sites that were pre-hydrated (n = 10 in each group) at diclofenac and placebo treated sites had an impedance of 0.87 ± 0.42 kΩ vs. 0.90 ± 0.47 kΩ, respectively (p = 0.9, Student's t-test).
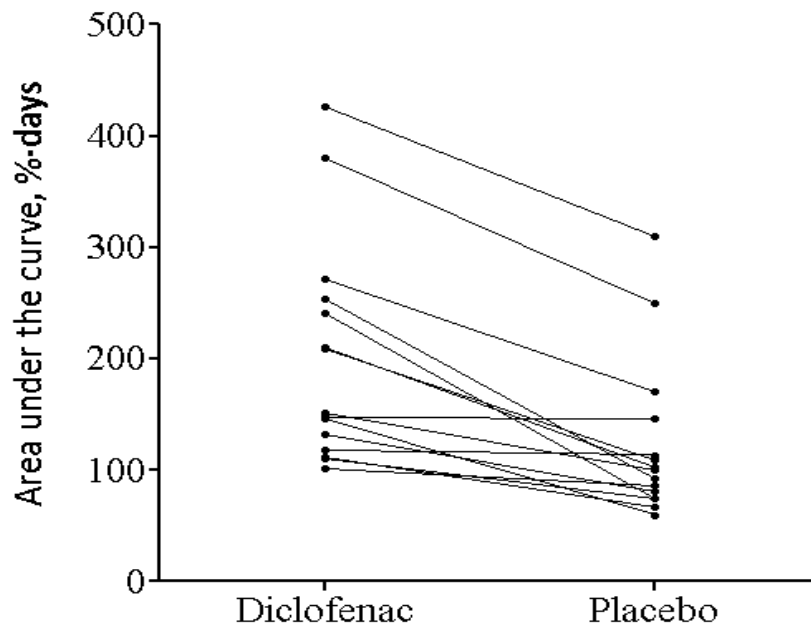
Figure 6.4 Comparison of AUC values at diclofenac vs. placebo treatment sites.
The AUC (%·days) at MN + diclofenac and MN + placebo treated sites were calculated
from %-normalized admittance measurements and compared within each subject over
the entire treatment period (n = 15 treatment periods in 13 subjects, because two
subjects completed a crossover design). For those subjects who had two independent
sites each for diclofenac and placebo treatments, the average was calculated and used
to determine the AUC. The overall difference in AUC was statistically significant (p <
0.0001, paired t-test).
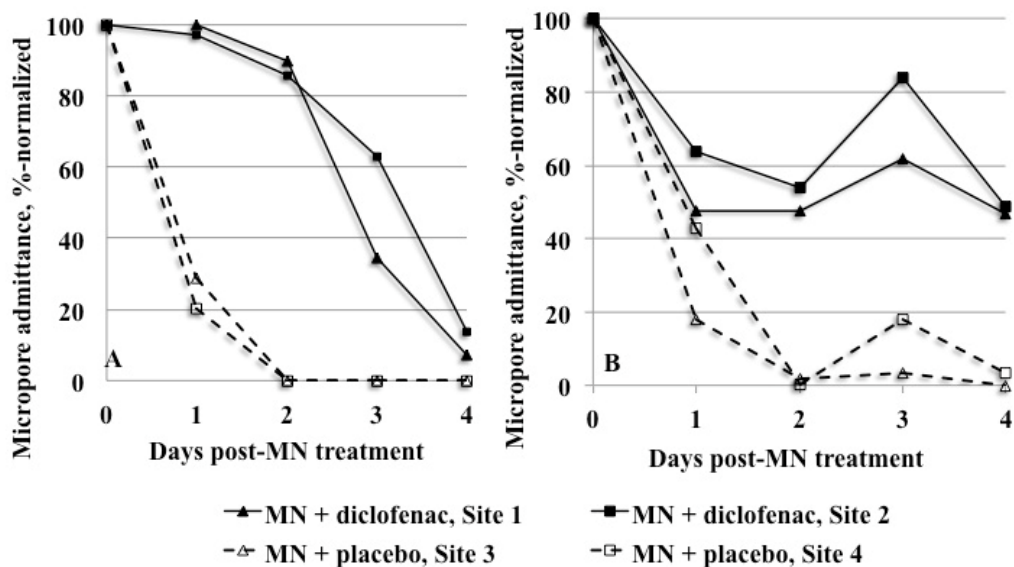
Figure 6.5 Representative profiles of micropore admittance from two subjects.
These profiles demonstrate inter-subject differences in the change in micropore admittance over a 5 day period (MN treatment occurring on Day 0). Values were normalized to the highest post-MN admittance value. Two independent sites were treated with MN + diclofenac (solid lines with solid shapes), and two additional sites were treated with MN + placebo (dashed lines with open shapes), and the area under the admittance-time curve, %·days (AUC) was calculated from the normalized admittance values. Subject A completed treatment schedule 2, and Subject B completed treatment schedule 1. Subject A: AUC for diclofenac and placebo was 240.5 ± 88.5 %·days vs. 74.6 ± 6.2 %·days, respectively. Subject B: Average (± SD) AUC for diclofenac sites was 253.2 ± 32.1 %·days vs. 92.9 ± 28.0 %·days at placebo sites. Despite differences in the shape of the profiles at diclofenac sites, all placebo treatment sites follow an approximately exponential decay. Under this model, the calculated $t_{1/2}$ of the micropores at placebo sites for Subject A is 11.7 ± 2.1 hours and 18.3 ± 4.5 hours for Subject B.
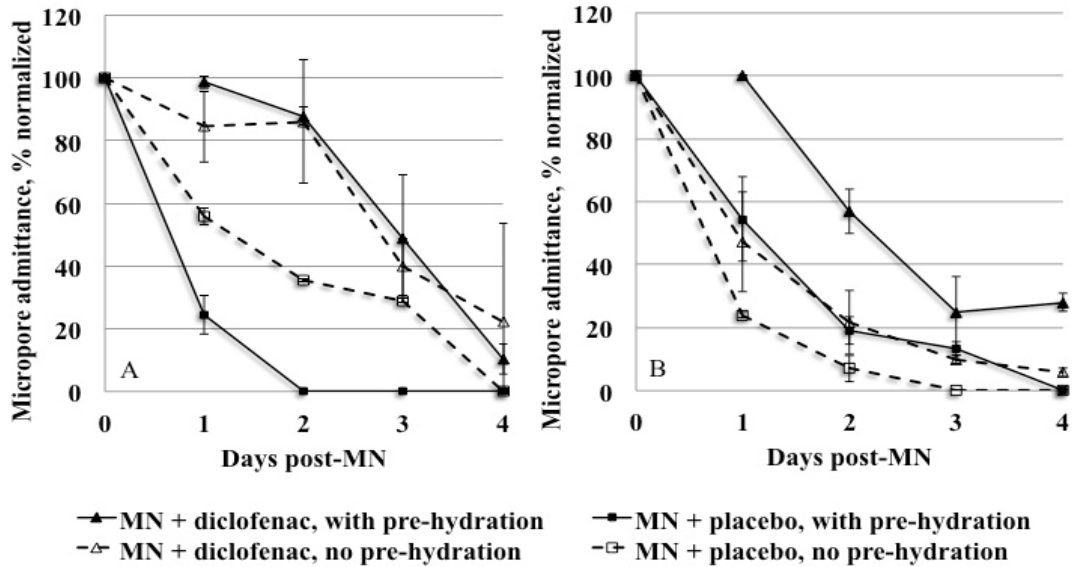
Figure 6.6 Comparison of admittance profiles in two subjects who completed a crossover design. Subject 6 (graph A, left) and Subject 9 (graph B, right) completed both schedules 1 and 2 in order to examine the effect of pre-hydration on the AUC. Triangles represent the diclofenac treatment sites, and squares represent the placebo sites. Solid lines with solid shapes display the sites with pre-hydration, and dashed lines with open shapes represent non pre-hydrated sites. As seen in the profiles, the effect of pre-hydration was not consistent between the two subjects, though the shape of the profiles (regardless of hydration status) was consistent within each individual subject. The average ± SD AUC at the pre-hydrated diclofenac treatment sites for was 240.5 ± 88.5 %·days and 145.8 ± 17.0 %·days (Subject 6 and 9, respectively), vs. the AUC at non-prehydrated diclofenac sites of 271.4 ± 55.6 %·days and 131.9 ± 25.4 %·days. Pre-hydrated placebo site AUC values were 74.6 ± 6.2 %·days (Subject 6) vs. 59.8 ± 8.9 %·days (Subject 9), compared to the non pre-hydrated values of 170.1 ± 3.8 %·days and 81.1 ± 3.4 %·days.
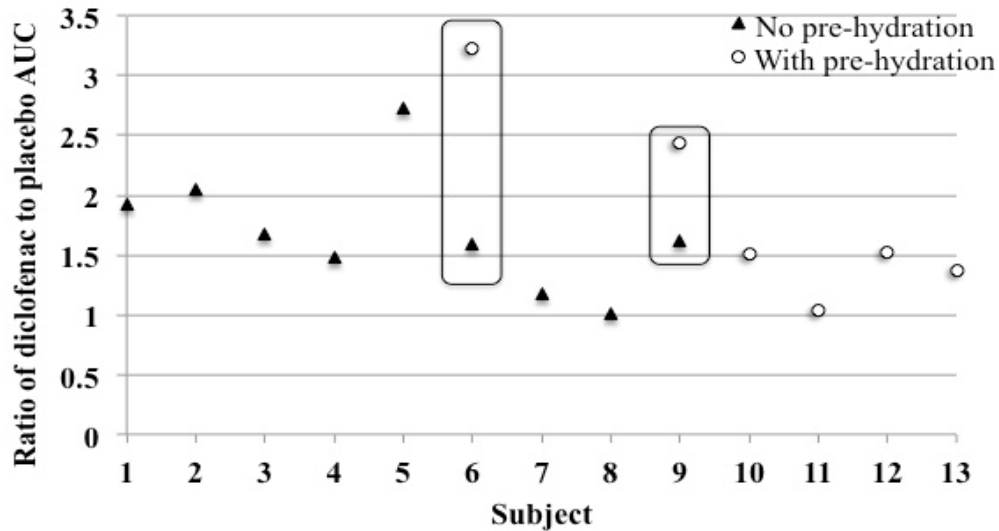
Figure 6.7 Ratios of diclofenac to placebo AUC. A simple ratio of the AUC values of active treatment (diclofenac) to placebo was calculated for each subject in order to demonstrate the magnitude of a treatment effect, thus allowing for a more direct comparison between subjects (n = 13). Solid triangles represent subjects with no pre-hydration, open circles represent subjects with pre-hydration. For subjects who had 2 treatment sites each for diclofenac or placebo, the average AUC for each treatment type was calculated and used to determine the ratio. The 2 subjects who completed the treatments with and without pre-hydration are outlined by the open boxes. Any ratio >1 demonstrates a favorable treatment effect for diclofenac. The average ± SD ratio was 1.76 ± 0.62 (range 1.01 – 3.23). The skin's hydration state at the time of MN treatment did not have a consistent impact on the treatment effect, which is particularly evident for the 2 subjects who completed the crossover schedule.
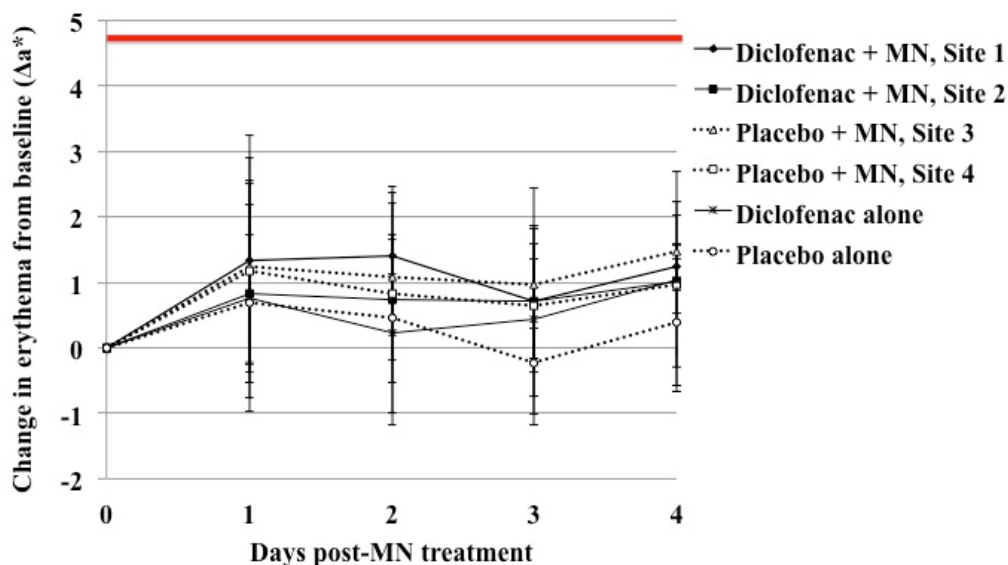
Figure 6.8 Assessment of skin irritation. Erythema was quantified via daily colorimetry readings. Change in erythema from baseline at each site was assessed by calculating the Δa^* value according to the equation: $\Delta a^* = a^*_t$ (at time t days after starting the study) $- a^*_0$ (at time 0, prior to application of treatment); data is displayed as the mean $\pm$ SD at each timepoint (n = 6 subjects). The bold line at 4.7 depicts a typical value expected after treating humans with sodium lauryl sulfate [119]. Sites treated with diclofenac are depicted by solid lines, whereas dashed lines represent placebo treated sites. Overall, no significant skin erythema was noted between diclofenac and placebo treatment sites (p = 0.2, one-way ANOVA).

Chapter 7

In vitro determination of naltrexone flux and quantification of diclofenac in microneedle-treated skin and *in vivo* assessment of skin irritation

7.1 Introduction

In recent years, microneedle-assisted transdermal delivery has proven to be a minimally invasive, patient-friendly technique for delivering drug compounds across the impermeable outer layers of the skin. Application of microneedles (MNs) to the skin creates micropores in the stratum corneum (SC, the outermost layer of the skin) through which a drug can diffuse and bypass the barrier functions of the SC. While only microns in dimension, the micropores allow for percutaneous delivery of macromolecules (insulin, oligonucleotides, human growth hormone) [47, 53, 56, 57, 132] and compounds that cannot otherwise permeate the lipophilic structure of the SC (naltrexone, desmopressin) [9, 11, 48].

This unique physical enhancement method offers immense flexibility for means of application, and previous reports have described successful drug delivery using dissolving MNs, coated MNs, hollow MN systems, and solid metal and polymer MN arrays. In the "poke (press) and patch" technique, a solid MN array is applied to the skin once and removed, creating a grid of micropores in the SC. A drug gel, solution, or patch can be applied over the MN-treated skin, permitting the drug to passively diffuse from the formulation into the micropores, ultimately resulting in systemic delivery. The first drug to be described in a human pharmacokinetic study using this MN technique was naltrexone (NTX), an opioid mu-receptor antagonist approved for the treatment of opioid and alcohol abuse. Therapeutic plasma concentrations of NTX were detectable for 48 – 72 hours following one application of a MN array with topical application of a 16% NTX gel [9].

While the "poke and patch" technique is both simple and effective, the drug delivery window is dependent on the lifetime of the newly created micropores. When the skin remains exposed to air after application of the MNs, the barrier function of the SC is restored within a period of 15 minutes to 2 hours [10, 13, 14]. That timeframe is extended to approximately 48 – 72 hours when the skin is occluded beneath a patch or impermeable membrane, as demonstrated by impedance spectroscopy and pharmacokinetic plasma data from humans and guinea pigs [9, 12, 14].

While the specific physiologic events contributing to micropore re-sealing are not explicitly understood, it is possible that subclinical inflammation is involved in the early phases of barrier restoration, as inflammatory responses are one of the first steps of the skin's wound healing cascade. In fact, previous work from our lab (Banks, *et al*) has demonstrated that application of topical diclofenac sodium (a non-specific anti-inflammatory drug) to MN-treated skin in hairless guinea pigs allows for delivery of NTX through the skin for up to 7 days [11]. Additionally, as described earlier, (Research Plan 3.2) this effect can also be achieved in human subjects, as seen by a significant difference in micropore closure kinetics between diclofenac and placebo gels when applied to MN-treated skin.

A proof-of-concept human study is necessary (Research Plan 3.6) to characterize the pharmacokinetics of NTX after application to MN-treated skin in the presence of diclofenac sodium for extending micropore lifetime. The overall objective of the studies in this chapter was to optimize the dosing scenario for a pharmacokinetic study, based on 3 parameters: 1) local concentration of diclofenac sodium in MN-treated skin *in vitro;* 2) *in vitro* flux of NTX in the presence of diclofenac sodium or placebo gel; 3) the irritation potential of the combination of diclofenac sodium and NTX when applied to the same treatment area. The data presented in this chapter satisfy Research Plans 3.3 and 3.4.

7.2 Methods and materials

7.2.1 Preparation of drug formulations

The following components were purchased through the University of Kentucky: Solaraze® gel (PharmaDerm, Melville, NY), naltrexone HCl (Mallinkrodt, Mansfield, MA), propylene glycol (VWR, Atlanta, GA), benzyl alcohol (Fisher Scientific, Hanover Park, IL), polyethylene glycol methyl ether 350 (Dow Corporation, Louisville, KY), and sterile water for injection. Hyaluronate sodium (Rita Corporation, Crystal Lake, IL) and hydroxyethylcellulose (HEC, Ashland Specialty Ingredients, Wilmington, DE) were gifts from the companies. An 11% NTX•HCl gel was prepared as follows: 110 mg/ml NTX•HCl, 10% propylene glycol, 1% v/v benzyl alcohol, 89% sterile water, and 2.5% HEC. The placebo gel was prepared with all components in the same proportions (minus the diclofenac sodium) as the active Solaraze® gel): 20% polyethylene glycol methyl ether 350, 1% benzyl alcohol, 79% sterile water, and 2.5% hyaluronate sodium.

All of the components were combined, vortexed, and allowed to stir on a stir plate for approximately 5 minutes before the hyaluronate sodium was added as the gelling agent.

7.2.2 *In vitro* diffusion studies

Full-thickness Yucatan miniature pig skin was harvested from the dorsal surface of a euthanized animal (approximately 6 months old). The animal protocol was approved by the University of Kentucky IACUC. A scalpel was used to remove all subcutaneous fat, and all skin samples were approximately 1 – 2 mm thick, as measured by calipers. All skin samples were stored at -20° C until use; a 30 minute thawing period was allowed before using the skin for diffusion studies. The skin was treated with a solid metal, 5 MN "in-plane" array (Mark Prausnitz's lab, Georgia Institute of Technology, Atlanta, GA) with the following MN dimensions: 750 µm long, 200 µm wide, and 75 µm thick. For the MN treatment, a polydimethylsiloxane polymer wafer was placed beneath the skin in order to mimic the natural mechanical support of the tissue underlying the skin *in vivo*. MN insertion was achieved by manually pressing the array gently into the skin and removing it immediately. Twenty applications were applied to create 100 non-overlapping micropores on a 0.95 cm^2 area of skin.

A PermeGear In-Line flow-through diffusion system (Hellertown, PA, USA) was used for skin diffusion studies. The skin was mounted into the diffusion cells and the experiments were initiated by charging the cells with 100 or 200 µl of Solaraze® gel ± 500 µl of NTX gel. The Solaraze® gel was rubbed gently into the skin using a Teflon rod, followed by application of the NTX gel over top. For the studies determining the local skin concentration of diclofenac in the absence of NTX, the receiver solution consisted of nanopure water with 20% EtOH, adjusted to a pH of 7.4; the EtOH generally increases drug solubility in the receiver solution. For the studies containing both diclofenac and NTX, the receiver solution consisted of isotonic pH 7.4 HEPES-buffered Hank's balanced salts with 87 µM gentamicin sulfate (to prevent bacterial growth in the receiver solution). For all studies the receiver solution was kept at a flow rate of 1.5 ml/min and temperature of 37°C and the skin temperature was maintained at 32 - 35° C with a circulating water bath. Samples were collected at 6 hour intervals and stored at 4°C until analysis by HPLC.

7.2.2.1 HPLC conditions: The HPLC system consisted of the following components: Waters 717 plus autosampler, Waters 600 quaternary pump, and a Waters 2487 dual wavelength absorbance detector with Waters Empower™ software. The UV

detector was set to wavelengths of 215 or 278 nm and used with a Brownlee (Wellesley, MA, USA) C-18 reversed phase Spheri-5 μm column (220x4.6 mm) with a C-18 reversed phase guard column (15x3.2mm, Perkin Elmer®, Waltham, MA, USA). For analyzing NTX flux, the mobile phase was 70:30 v/v ACN:buffer (0.1% TFA with 0.065% 1-octane sulfonic acid sodium salt, adjusted to pH 3 with TEA). A flow rate of 1.5 ml/min and run time of 4 minutes (5 minutes for samples containing only diclofenac sodium) were used, with an injection volume of 100 μl. Standard curves of diclofenac sodium and NTX in the linear range of 100 – 10,000 ng/ml were analyzed and displayed excellent linearity under the above conditions (R^2 always ≥ 0.97). NTX had a retention time of 2.55 ± 0.1 min, while diclofenac sodium had a retention time of 3.78 ± 0.3 minutes.

7.2.3 Quantification of diclofenac in the skin

At the end of each diffusion experiment, the skin was removed from the diffusion apparatus, rinsed twice with water and blotted gently with Kimwipes® to remove excess drug from the skin surface. The skin sample was tape stripped twice and the skin weight was recorded. The skin was suspended in acetonitrile and shaken in a 32°C water bath overnight. Diclofenac concentration was analyzed by HPLC. Skin concentrations were expressed as μm/gram of skin.

7.2.4 Determination of naltrexone flux

The cumulative quantity of NTX collected in the receiver solution was plotted as a function of time and the flux was determined from the slope of the line at steady state. Fick's First Law of diffusion was used according to the equation:

$$\frac{1}{A}\left(\frac{dM}{dt}\right) = J_{ss} = P\Delta C$$ Equation 7.1

where A is the area of the skin (0.95 cm^2), M is the cumulative amount of NTX permeating through the skin (nmol) during time (t), J_{ss} is the flux at steady state (nmol/cm^2·hr), P is the effective permeability coefficient (cm/h), and ΔC represents the difference in NTX concentration between the donor and receiver compartments. Sink conditions were maintained in the receiver solution throughout the experiment, allowing ΔC to be approximated by the initial drug concentration applied to the donor compartment.

<u>7.2.5 *In vivo* assessment of skin irritation</u>

      7.2.5.1 Microneedle treatment and gel application: Male and female hairless guinea pigs weighing approximately 800 - 1000 g each were treated on the dorsal surface with 50 MN arrays of the following MN dimensions: 750 μm long, 200 μm wide, and 75 μm thick. The arrays were sterilized before treatment by autoclaving under high pressure saturated steam at 121° C for 15 minutes. Immediately prior to treatment, the arrays were assembled into adhesive patches with sterile Arclad adhesive backing (Adhesives Research, Inc., Glen Rock, PA), allowing for very close contact between the MNs and the flexible skin during treatment. The treatment sites were cleaned with isopropyl alcohol wipes and allowed to dry before applying the MN arrays. Each treatment site received two applications of a MN array, with the 2nd application rotated 45 degrees so as not to overlap the first, to create 100 non-overlapping micropores. MN application is achieved by gently pressing the array onto the skin for approximately 15 – 20 seconds followed by immediate removal of the array. All MN applications were performed by the same investigator in order to avoid inter-investigator variability. Diclofenac sodium (delivered via application of 100 or 200 μl of Solaraze® gel) and 11% NTX gel (500 μl) were applied to the skin immediately post-MN and then at various intervals for the remaining days in the study (treatment paradigms described in Table 7.1).

      7.2.5.2 Assessment of local erythema: Tristimulus colorimetry was used to evaluate the skin irritation potential of the gel combination when applied *in* vivo to MN-treated hairless guinea pigs. Erythema was quantified with a Konica Minolta meter (ChromaMeter CR-400, Konica Minolta, Japan) according to previously published guidelines [115]. Tristimulus colorimetry measures a three-dimensional scale of color (L*a*b*). The L* value (luminance) represents the black/white axis and the relative brightness, which is expressed as a range of total black (L* = 0) to pure white (L* = 100). The red/green axis is represented by the a* value, as increasing redness (i.e. erythema) results in higher a* values (+100 represents full red); b* describes the yellow/blue axis. The colorimeter was calibrated daily against a white plate provided by Konica Minolta. Measurements were made by placing the head of the instrument gently on the skin area to record the color reflectance. Readings were taken in triplicate at every site at each time point and the mean a* value was calculated. The change in erythema was reported as a change from the baseline, Δa^*, calculated as $\Delta a^* = a^*_t$ (at time t days after starting the study) $- a^*_0$ (at time 0, prior to application of treatment).

<u>7.2.6 Data analysis</u>

Statistical analysis was performed using Student's t-tests and one-way ANOVA with Tukey's post-hoc analysis (GraphPad Prism®, version 5.04); p<0.05 was considered statistically significant.

7.3 Results

<u>7.3.1 Diclofenac skin concentration, in the absence of naltrexone</u>

Diclofenac in the skin was quantified following the same treatment schedule as the proof-of-concept human micropore lifetime study (Research Plan 3.2). Two hundred µl of Solaraze® (equivalent to 6 mg of diclofenac sodium) was applied to MN-treated skin daily for 5 days, resulting in local skin concentrations ranging from 0.38 to 0.84 µmol/g of skin, from 48 to 96 hours. A second study was also conducted to examine diclofenac skin concentrations following one-time application of 200 µl of Solaraze® immediately post-MN treatment. Resulting skin concentrations spanned a range of 0.32 to 0.96 µmol/g of skin, and the concentration steadily increased daily. There was no significant difference between skin concentrations following daily application vs. one application of diclofenac immediately post-MN (p > 0.05, one-way ANOVA). All skin concentrations can be seen in Table 7.1.

<u>7.3.2 Diclofenac skin concentration, in the presence of naltrexone</u>

To determine the local concentration of diclofenac in the skin in the presence of an 11% NTX gel (to mimic the conditions that will be used in an upcoming pharmacokinetic study), 100 µl of Solaraze® gel and 500 µl of NTX gel were applied to MN-treated skin at baseline and then re-applied every 48 hours or just once at 96 hours post-MN. When applied every 48 hours (a total of 3 re-applications over 7 days), the skin concentration of diclofenac ranged from 0.96 to 3.14 µmol/g of skin, which was not significantly different from the concentrations of 0.59 to 2.3 µmol/g of skin observed when the treatment schedule was prolonged to one re-application at 96 hours post-MN treatment (p > 0.05, one- way ANOVA).

<u>7.3.3 *In vitro* flux of naltrexone through microporated skin</u>

The flux of NTX in the presence of diclofenac sodium or placebo was evaluated to calculate an appropriate number of patches for a human pharmacokinetic study. Table 7.1 and Figure 7.1 display the mean (± SD) flux values under the various

conditions. The flux of NTX alone through microporated skin was 195.66 ± 47.35 nmol/cm^2·hr, which was not significantly different from the flux of 170.84 ± 32.12 nmol/cm^2·hr, obtained when NTX was applied in the presence of a 2.5% hyaluronate sodium placebo gel (p = 0.49, Student's t-test). In contrast, when co-applied with diclofenac sodium, the resulting NTX flux of 42.58 ± 7.88 nmol/cm^2·hr was significantly lower compared to NTX alone (p = 0.005) or in the presence of a placebo gel (p = 0.003).

7.3.4 Tolerability of microneedle treatments and gels

Three hairless guinea pigs were treated with 100 μl of diclofenac sodium and 500 μl of 11% NTX gel for a total of 6 treatment courses (2 independent courses per guinea pig). Four sites were evaluated: 2 MN-treated sites, one intact skin site treated with gels alone, and one non-treated control site that was occluded with a blank patch. The treatments were well tolerated. An initial increase in erythema was noted across all animals from baseline to the 48 hour post-MN measurement, as evidenced by a mean (± SD) Δa* of 2.85 ± 2.97 (range -2.24 to 6.89) at one MN-treated site, and 2.22 ± 2.83 (range -0.01 to 5.04) at the second MN-treated site. Despite the initial increase, the Δa* quickly subsided and decreased to a mean of 0.63 ± 1.14 (96 hours) and -0.8 ± 0.97 (144 hours) at Site 1 (MN treated) and 0.34 ± 0.62 (96 hours) and 0.41 ± 0.68 (144 hours) at Site 2 (MN treated). There was no significant difference between any of the applied treatments (p = 0.11, one-way ANOVA). All Δa* values can be seen in Table 7.3, and the trend of Δa* can be seen in Figure 7.2.

7.4 Discussion

Previous animal and human studies have demonstrated that micropore lifetime (following one-time application of a MN array) can be extended via topical application of diclofenac sodium [11]. This novel drug delivery principle is only relevant in a clinical scenario, however, if 2 conditions can be simultaneously achieved: 1) a drug compound can be delivered to therapeutic plasma concentrations for the duration of the micropore lifetime (in this case, NTX serving as the model compound for systemic delivery); and 2) the skin is not irritated by the diclofenac, NTX gel, or the combination of both compounds. An upcoming pharmacokinetic study is planned to assess these parameters in human volunteers (Research Plan 3.6) via application of a NTX gel to skin treated with MNs and diclofenac. The objective of the current studies was to determine

the flux of NTX through microporated Yucatan pig skin *in vitro*, local concentrations of diclofenac in the skin, and irritation potential of the combination of diclofenac and NTX gels. The information gained from this work will allow for calculation of an appropriate patch number, gel volume, and treatment schedule for the human pharmacokinetic study.

7.4.1 Local diclofenac concentrations under various treatment paradigms

The proof-of-concept human studies described earlier (Research Plan 3.2) established that daily application of Solaraze® gel significantly extends micropore lifetime compared to placebo conditions. An additional treatment schedule in that study also demonstrated that daily application may not be necessary to exhibit effects on micropore lifetime, as similar results were observed in subjects only treated with diclofenac once at baseline and again at 96 hours post-MN. Thus, the current studies determined local concentrations of diclofenac in MN-treated skin under various schedules of diclofenac application (daily, every 48 hours, or just one re-application at 96 hours post-MN). The concentration of diclofenac in the skin was determined under similar conditions to the proof-of-concept study, in which 200 μl of Solaraze® gel was applied to MN-treated skin. The concentration was notably consistent at 48 and 72 hours post-MN, and increased slightly at the 96 hour time point, likely as a result of increased drug on the skin surface and/or accumulation of the diclofenac within the viable epidermis. The Solaraze® formulation used to deliver the diclofenac to the micropores is unique in that the vehicle contains 2.5% hyaluronate sodium, a large polyanionic polysaccharide that is naturally present in almost all human organs, but is particularly abundant in human skin. It is present in the SC, epidermis (~0.5 mg/g wet tissue) and dermis (~0.1 mg/g wet tissue). [120]. This polysaccharide has been used extensively in cosmetic formulations, and is particularly notable for its ability to promote formation of a local depot of drug in the skin, allowing for a localized effect of the active drug moiety. This property is particularly appealing for the purposes of extending micropore lifetime, as the anti-inflammatory effects of diclofenac are only necessary in the local micropore environment. Interestingly, there was no significant difference in the local diclofenac concentrations when daily application of Solaraze® was compared to one application of 200 μl immediately post-MN treatment, confirming that local drug concentrations are sufficiently maintained without the need for daily re-application. This

is especially encouraging as fewer treatment applications would improve patient satisfaction and compliance with therapy.

For the purposes of extending micropore lifetime, the diclofenac in these studies is intended for a local effect at the micropores, and thus the minimum amount of gel that can be applied to the skin but still achieve similar skin concentrations is desired. The patch size that can be applied *in vivo* for irritation studies is somewhat restricted based on the small size of the hairless guinea pigs, and a smaller patch area is also desirable for human studies in order to increase patient satisfaction with therapy. As the only treatment applied, 200 µl of diclofenac gel can be easily contained underneath a small occlusive patch. However, in combination with the additional NTX gel for a pharmacokinetic study, the volume of diclofenac gel needs to be reduced to allow for a sufficient amount of NTX to also be contained under the patches. From a practical standpoint, 100 µl of gel is sufficient to completely cover the micropore treatment area and be rubbed into the skin, while allowing enough space under the patch to allow for up to 500 µl of the NTX gel. The local skin concentrations of diclofenac in microporated skin were determined following application of 100 µl of Solaraze® at baseline, with re-application every 48 hours or just once at 96 hours. This was in combination with 500 µl of an 11% NTX gel, to determine that the presence of another drug moiety would not affect local diclofenac concentrations. There was no significant difference in diclofenac concentrations between the treatment schedules, or compared to the application of 200 µl daily. This confirms that application of 100 µl of Solaraze® in the presence of NTX provides local concentrations of diclofenac sufficient to maintain micropore lifetime, under a variety of application schedules.

7.4.2 *In vitro* naltrexone flux in the presence of diclofenac

In order to calculate the appropriate number of NTX patches for safe and effective delivery in human subjects, it was necessary to determine the flux of NTX in the presence or absence of diclofenac. In the current study, the local concentrations of diclofenac were adequately maintained in the presence of the NTX gel, though the interaction of the 2 active moieties created a hindrance to the flux of NTX through the micropores, demonstrated by the significant decrease in flux from 195.66 ± 47.35 nmol/cm^2•hr (NTX alone) to 42.58 ± 7.88 nmol/cm^2•hr (NTX + diclofenac). This decrease in the flux was not observed in the placebo conditions, in which a 2.5% hyaluronate sodium placebo was applied to the MN-treated skin in lieu of the diclofenac

formulation. The resulting NTX flux under placebo conditions was 170.84 ± 32.12 nmol/cm^2•hr, which was not significantly different from the NTX gel alone. All flux values can be seen in Table 7.2 and Figure 7.1.

The basis for the decrease in flux observed between when Solaraze® and NTX gels are applied together is likely due to the differing physicochemical characteristics of the active moieties, diclofenac sodium and NTX•HCl. When co-applied to a small treatment area, a mild precipitate forms at the interface of the gels, and there are a few possible explanations for how this might decrease the flux of NTX. First, the precipitate may initially be physically blocking the micropores, which would impede this drug pathway to the underlying circulation. Second, the NTX that precipitates out of the gel formulation would decrease the diffusional gradient, thus reducing the driving force for the passive diffusion of the NTX. Despite these limitations, the flux of NTX in the presence of diclofenac is still adequate to allow for therapeutic systemic delivery in humans; in fact, the flux is similar to that observed in the *in vitro* studies used for patch calculations in the first human pharmacokinetic study with NTX (39.0 ± 13.1 nmol/cm^2•hr) [9]. The formation of a precipitate between the 2 independent gel formulations also provides justification for the development of a codrug of diclofenac and NTX, in which the 2 molecules are joined by a chemical linker. Upon entry into the skin the linker is enzymatically cleaved by skin enzymes, releasing the active moieties and allowing for delivery of NTX while providing a local diclofenac concentration from the same formulation [133]. Thus, the application of 2 separate gels creates some logistical challenges, but in spite of these limitations the treatments are still appropriate for a proof-of-concept human study.

7.4.3 Local erythema and tolerability of the treatments

One of the most important components of a successful transdermal delivery system is negligible skin irritation from the patch and/or drugs applied to the skin. In the current study we investigated the tolerability of diclofenac and NTX when co-applied to MN-treated skin. Hairless guinea pigs are often used for studying irritation and sensitization potential for topical and transdermal therapies, as their skin is more sensitive to topical xenobiotics, as compared to humans [130]. This allows for a more conservative estimation of irritation that might be expected in humans under the same treatment conditions. In the previous diclofenac proof-of-concept human study (Research Plan 3.2), there was no significant difference in irritation between diclofenac

and placebo treatments in human subjects. In the current study, the same result was observed when diclofenac was co-applied with the NTX gel, as there was no significant difference in Δa^* values between any treatments. This is very encouraging, as humans are unlikely to experience irritation to the gels if they are well tolerated by the guinea pigs. A mild increase in erythema was observed initially (at 48 hours post-MN), though this was still lower than typical reactions observed in guinea pigs topically treated with a known skin irritant [134]. The erythema also subsided for the remainder of the study. Some mild irritation has been noted in previous studies of NTX applied to MN-treated skin, so the initial increase in erythema is not necessarily surprising [9]. However, a mild increase in the Δa^* value does not necessarily correlate with erythema that would be clinically significant for human subjects. To demonstrate this point, no subjects withdrew from the NTX pharmacokinetic study based on local skin irritation, and the irritation quickly subsided upon completion of the study.

Based on the diclofenac skin concentrations described above, re-application of the gels every 48 hours is not necessary from a drug delivery standpoint. From a clinical safety perspective, however, this dosing schedule would be appropriate for a first-in-human study, as it allows for visual inspection of the skin every 2 days. This adds an additional conservative safety component to the study, as the gels could be quickly removed if any significant irritation was observed.

7.5 Conclusions

The studies described in this chapter have demonstrated that co-application of diclofenac sodium and NTX to MN-treated skin achieves local diclofenac concentrations suitable for prolonging micropore lifetime and sufficient NTX flux for achieving therapeutic plasma concentrations in healthy human subjects. A variety of treatment schedules would be appropriate for a pharmacokinetic study, allowing for a great deal of flexibility in designing study parameters. These data also allow for calculation of an appropriate patch number and treatment schedules suitable for human subjects, without concern for clinically significant skin damage or irritation.

Table 7.1

Donor	Frequency of donor re-application	Concentration of diclofenac in MN-treated skin (µmol/g)		Average skin thickness (mm)
3% diclofenac sodium, 200 µl	Once at baseline	24 hours	0.32 ± 0.06	2.17 ± 0.06
		48 hours	0.45 ± 0.23	2.3 ± 0.1
		72 hours	0.62 ± 0.37	2.27 ± 0.06
		96 hours	0.96 ± 0.57	2.33 ± 0.06
3% diclofenac sodium, 200 µl	Every 24 hours	48 hours	0.38 ± 0.08	1.67 ± 0.2
		72 hours	0.38 ± 0.11	1.80 ± 0.09
		96 hours	0.84 ± 0.51	1.6 ± 0.0
3% diclofenac sodium, 100 µl 11% NTX•HCl, 500 µl	Every 48 hours	48 hours	0.96 ± 0.11	1.53 ± 0.06
		96 hours	2.90 ± 0.73	1.50 ± 0.10
		7 days**	3.14 ± 1.10	1.55 ± 0.07
3% diclofenac sodium, 100 µl 11% NTX•HCl, 500 µl	Once at 96 hours post-MN	96 hours	0.59 ± 0.34	1.96 ± 0.04
		7 days	2.3 ± 0.33	1.8 ± 0.04

Table 7.1 Quantification of diclofenac sodium in MN-treated Yucatan miniature pig skin under various schedules of application, in the presence or absence of 11% NTX gel (10% propylene glycol formulation, described by Milewski and Stinchcomb [135]). All conditions represent n = 3 cells. Diclofenac sodium was delivered from Solaraze® gel (3% diclofenac sodium in a 2.5% hyaluronate sodium vehicle).

* n = 2 cells

Table 7.2

Type of skin	Donor	Frequency of donor re-application	NTX flux (nmol/cm^2·hr)
Human [9]	16% NTX	NA	39.0 ± 13.1
Yucatan pig	11% NTX		195.66 ± 47.35 (n = 3)
	11% NTX 3% diclofenac sodium	Every 48 hours post-MN	42.58 ± 7.88 (n = 3)
	11% NTX 2.5% HA placebo		170.84 ± 32.12 (n = 3)

Table 7.2 Comparison of *in vitro* flux from 2 formulations of NTX through 100 micropores in the presence of diclofenac sodium. The placebo gel was a 2.5% hyaluronate sodium gel, similar to the commercial Solaraze® formulation. The 16% NTX gel formulation contained 30.75% propylene glycol (as described by Wermeling, Banks and Stinchcomb [9]), while the 11% NTX gel was formulated in 10% propylene glycol [135].

Table 7.3

Treatment	Δa*		
	48 hours	96 hours	144 hours
MN + diclofenac + NTX, Site 1	2.85 ± 2.97 (2.23 – 6.89)	0.63 ± 1.14‡ (-1.03 – 1.70)	-0.80 ± 0.97‡ (-1.78 – 0.38)
MN + diclofenac + NTX, Site 2	2.22 ± 2.83 (-2.18 – 5.04)	0.34 ± 0.62‡ (-0.53 – 1.15)	0.41 ± 0.68† (-0.59 – 0.90)
Intact skin + diclofenac + NTX	-1.63 ± 1.06 (-2.48 – 0.39)	-1.13 ± 0.99 (-2.14 – 0.46)	-1.27 ± 1.40 (-2.59 – 0.96)
Occluded, non-treated skin	1.13 ± 2.05 (-0.07 – 5.28)	0.13 ± 1.36 (-2.05 – 1.85)	-0.04 ± 1.19 (-1.61 – 1.49)

Table 7.3 Assessment of skin irritation. Erythema was quantified via colorimetry measurements at 48 hour intervals. Δa* values were calculated over a 6 day period to determine tolerability of the combination of diclofenac sodium and NTX following MN treatment. MNs were applied once at baseline and gels were replenished every 48 hours. Data is displayed as the mean ± SD (range) at each time point (n = 6). An initial increase in erythema was seen at 48 hours at the MN treated sites, but subsided by the later time points. There was no significant skin erythema between any treatment sites, irrespective of treatment applied (p = 0.11,one-way ANOVA).
†n = 4, ‡n = 5
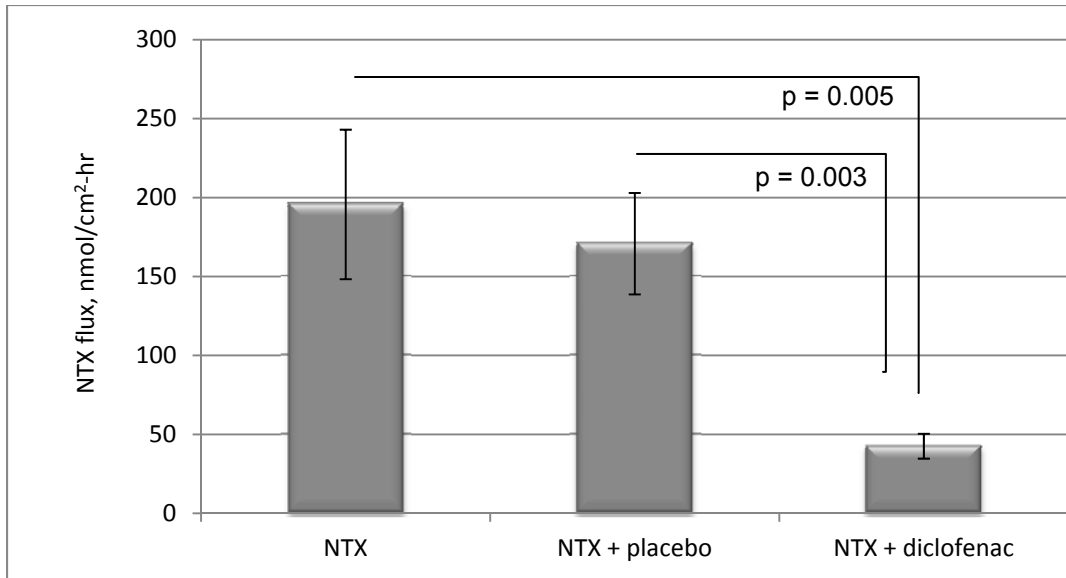
Figure 7.1 *In vitro* **flux of NTX through microporated skin in the presence of diclofenac sodium or 2.5% HA placebo gel.** Yucatan pig skin was treated with a MN array to create 100 micropores; 100 μl of Solaraze® gel or placebo gel was applied with 500 μl of an 11% NTX gel; gels were replenished every 48 hours. The flux of NTX was significantly lower when applied with diclofenac sodium ($p = 0.005$, Student's t-test).
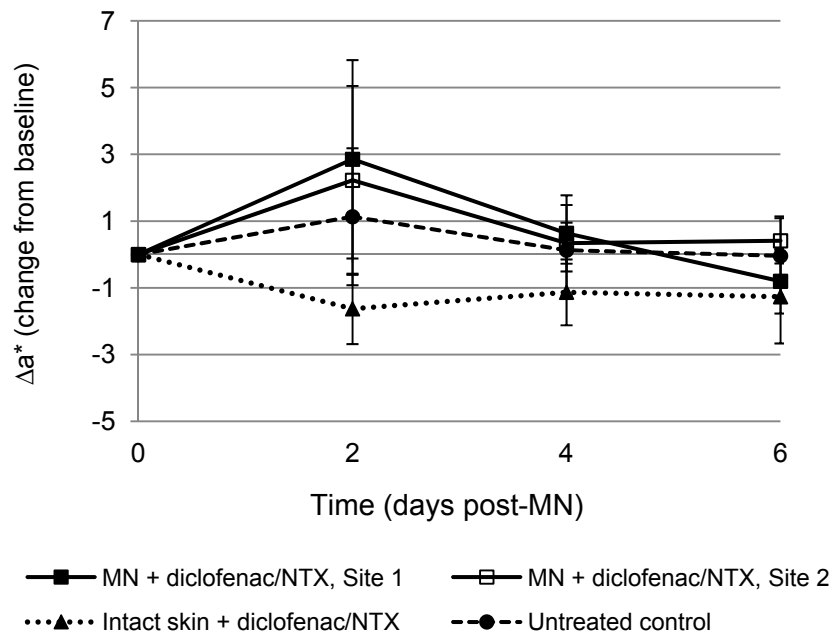
Figure 7.2 Trends of erythema in hairless guinea pigs following application of NTX and diclofenac gels to MN-treated skin every 48 hours. An initial rise in the Δa^* value was seen at 48 hours (confirming increased erythema over baseline), but quickly subsided for the remaining treatment period. There was no significant difference in erythema between any treatment sites (p = 0.11, one-way ANOVA).

Chapter 8

Pharmacokinetic evaluation of microneedle/diclofenac sodium enhanced 7-day transdermal delivery of naltrexone HCl in healthy human volunteers

8.1 Introduction

Transdermal drug delivery avoids several major downfalls of other common drug delivery paradigms (i.e. oral, injectable). Through application of patches that adhere to the skin and passively deliver drugs into the underlying circulation, transdermal delivery systems are able to avoid first-pass metabolism through the liver, enzymatic degradation in the gastrointestinal tract, and the pain of an injection. One substantial challenge with transdermal systems, however, is the strict physicochemical properties required for a drug to effectively permeate through the skin (primarily the stratum corneum (SC), the outermost skin layer). As such, a very limited number of drug moieties can be successfully delivered via this route (as of 2008, the U.S. market has less than 20 drugs approved for passive transdermal delivery systems) [2].

In order to expand the transdermal drug delivery field to a larger number of active drug molecules, a number of physical enhancement techniques have been explored to temporarily breach the SC, including iontophoresis, electroporation, sonophoresis, and microneedles. Of these methods, microneedles (MNs) are arguably the most "clinically-friendly" technique, as there is no requirement for software, equipment, or extensive training in order to apply the MNs. While there are various application methods, the simplest MN technique is known as the "poke (press) and patch" method, in which a MN array is pressed gently into the skin and immediately removed, leaving behind a grid of micropores in the SC. A drug solution, patch, or gel can be applied over the treatment area, allowing for passive delivery of the drug through the micropores and into the underlying circulation.

Two critical factors directly relate to the effectiveness of this method of MN-enhanced permeation: 1) sufficient breaching of the SC via creation of micropores; and 2) the lifetime of the micropores. The topic of micropore lifetime has recently become of great interest, as it is now known that the micropores will heal quickly (ranging from 15 minutes to 2 hours) when exposed to air, and this window can be extended to approximately 48 – 72 hours under occluded conditions [9-12, 14]. The first pharmacokinetic study using this MN technique (Wermeling, Banks *et al*) confirmed that one-time application of MNs allows for transdermal delivery of naltrexone HCl (NTX•HCl)

for 48 – 72 hours in healthy human subjects, as determined by plasma concentrations of both NTX and its active metabolite, 6-β-NTXol [9]. Previous work from this same research group has demonstrated that topical application of diclofenac sodium, a non-specific cyclooxygenase (COX) inhibitor, can prolong the lifetime of the micropores in hairless guinea pigs, allowing for transdermal delivery of NTX•HCl for up to 7 days [11], and proof-of-concept human studies have demonstrated a similar trend, using impedance spectroscopy as a surrogate marker (described previously in Research Plan 3.1). The underlying hypothesis of these studies was that subclinical local inflammation at the micropores contributes to the re-sealing process; as such, inhibition of this inflammation via a topical COX inhibitor (i.e. diclofenac) blunts the re-sealing process. Prolonging micropore lifetime alone is not beneficial, however, unless an active drug moiety can be delivered through the micropores for a clinically relevant timeframe in humans (7 days of delivery would be ideal for a transdermal system). The objective of the present studies was to collect pilot pharmacokinetic human data in healthy subjects to demonstrate delivery of NTX•HCl over a 7 day time period following one-time MN treatment and application of a transdermal NTX•HCl gel, with co-application of diclofenac or a placebo gel. These studies satisfy Research Plan 3.6.

8.2 Methods and materials

8.2.1 Preparation of drug formulations

The following gels and components were purchased through the University of Kentucky: Solaraze® gel (PharmaDerm, Melville, NY), naltrexone HCl (Covidian/Mallinckrodt, Hazelwood, MO), benzyl alcohol (Fisher Scientific, Hanover Park, IL), polyethylene glycol monomethyl ether (Dow Chemicals, Louisville, KY), propylene glycol (VWR, Atlanta, GA), and sterile water for injection. Hyaluronate sodium powder (Rita Corporation, Crystal Lake, IL) and hydroxyethylcellulose (Ashland Specialty Ingredients, Wilmington, DE) were gifts from the companies.

An 11% NTX gel was compounded as follows: 110 mg/ml NTX•HCl, propylene glycol (10% v/v), benzyl alcohol (1% v/v), sterile water (89% v/v), and hydroxyethylcellulose (2% w/v). A 2.5% hyaluronate sodium placebo gel (containing no diclofenac sodium) was compounded with polyethylene glycol monomethyl ether (20% v/v), benzyl alcohol (1% v/v), water (79% v/v), and hyaluronate sodium (2.5% w/v). To compound the NTX•HCl gel, NTX•HCl was weighed out and allowed to dissolve in the mixture of propylene glycol, benzyl alcohol, and water. The solution was vortexed and

allowed to mix on a stir plate for approximately 5 minutes before addition of the gelling agent (HEC). The same procedure was followed for the components of the placebo gel (no diclofenac or NTX•HCl present), with addition of the hyaluronate sodium serving as the final gelling step. The gels were allowed to sit at room temperature overnight before being used; no particulates were observed. All gels were compounded in the University of Kentucky Investigational Drug Services Pharmacy. The commercially available Solaraze® gel (3% diclofenac sodium, 2.5% hyaluronate sodium) was used to deliver the diclofenac sodium topically.

8.2.2 Preparation of microneedle arrays and occlusive patches

The design and geometry of the MN arrays was provided by the Prausnitz lab at the Georgia Institute of Technology. Microneedle arrays were cut into stainless steel sheets (50 µm thick) in a 5 x 10 array, to provide 50 MNs per array; the MNs were manually bent perpendicular to the plane of the metal substrate. In order to enhance contact between the MNs and the skin during treatment (to overcome the mismatch between the rigid metal of the array and the flexibility of the skin tissue), the arrays were further assembled into adhesive patches with Arclad (Adhesives Research, Inc., Glen Rock, PA). Each MN was 800 µm in length and 200 µm in width at the base; all arrays were ethylene oxide sterilized at University of Kentucky Medical Center prior to use.

Blank occlusive patches were made to allow for full occlusion of the treatment sites and containment of the drug gels over the microporated skin for the duration of the study. A rubber ring was fabricated with a drug-impermeable membrane on one side (Scotchpak 1109 SPAK 1.34 MIL heat-sealable polyester film; 3M, St. Paul, MN) that was secured to the ring with 3M double-sided medical tape. The other side of the ring also had a layer of double-sided tape to hold the patches to the skin and prevent leaking of the gels. The patches were further secured to the skin with waterproof Bioclusive dressing (Systagenix Wound Management, Quincy, MA).

8.2.3 Microneedle application technique

The same investigator applied all MN treatments in order to eliminate inter-investigator variability between subjects or treatments. The process of MN insertion is very simple: the array is pressed gently into the skin for approximately 15 – 20 seconds and immediately removed, leaving behind a grid of 50 micropores in the SC. A 2nd

insertion was applied, rotating the array 45° from the first insertion, so as to create a total of 100 non-overlapping micropores.

8.2.4 Clinical study procedures

This was an open-label pharmacokinetic study carried out in healthy human volunteers. All study procedures were approved by the University of Kentucky Institutional Review Board and complied with the principles set forth by the Declaration of Helsinki. Healthy volunteers with no history of dermatologic disease were recruited. Suitability for the study was determined through baseline blood samples (including chemistries and cell counts), urine samples (urinalysis, pregnancy sample if applicable, and drug of abuse screen), and a complete drug/medical history and physical exam. Any subjects with a history of opioid or alcohol abuse or hepatitis were excluded.

Subjects were randomly assigned into 3 groups: MN + diclofenac + NTX (Group 1, n = 6 subjects), MN + placebo + NTX (Group 2, n = 2 subjects), and diclofenac + NTX applied to intact skin (Group 3, n = 2 subjects). On Day 1 of the study, 8 treatment sites were marked for MN treatment on the upper arm for subjects in Groups 1 and 3, and 2 treatment sites were marked for subjects in Group 2. All treatment sites (regardless of treatment group) were wiped with 70% isopropyl alcohol pads and allowed to dry. The subjects assigned to MN-treated groups were treated with MN arrays at each site before gel patch application. As described above, an array of 50 MNs was applied twice to each site, rotating the array by 45 degrees for the second insertion to create a grid of 100 non-overlapping micropores per NTX patch. For Group 1 there were 2x8 MN array insertions per subject, creating 800 total micropores for 8 patch sites; for the subjects in Group 2 there were 2 patch sites, and therefore 2X2 MN array insertions per subject, creating 200 total micropores. Table 8.1 displays all of the patches and treatments applied to the subjects in each group.

Following MN treatment, each site was treated with diclofenac gel (100 µl, rubbed gently into the skin), followed by application of the NTX gel (500 µl) and occlusion with an occlusive patch. The same procedure was followed with Group 2, with placebo gel replacing the diclofenac gel. Group 3 received application of the same gels as Group 1, in the absence of MN treatments. In all groups, 2 non-MN treated control sites on the opposite arm received identical gel applications as the MN sites. Every 48 hours following the initial treatment the patches were removed to allow for visual inspection of the skin for any irritation or erythema; the gels were then replenished and

occluded with clean patches. All gels and patches were completely removed on Day 8 (corresponding to 7 days post-MN), the final day of the study.

8.2.5 Calculation of naltrexone patch number per treatment group

In the first pharmacokinetic study demonstrating delivery of NTX•HCl through MN-treated skin in human subjects, 4 patches were applied to the upper arm of each subject [9]. The calculation of the number of patches for that study was based on the equation: $A = Cl * C_{ss} * J_{ss}$ where Cl is the systemic clearance of NTX (3.5 L/min), C_{ss} is the target minimum therapeutic steady state concentration (2 ng/ml) and J_{ss} is the steady state flux of NTX (39.0 ± 13.1 nmol/cm^2•hr for the previous study). In a sample size of 6 subjects treated with MNs, this yielded a mean (± SD) NTX plasma concentration of 2.5 ± 1.0 ng/ml over a 72 hour period. For the current study, the *in vitro* flux for the Solaraze$^®$ + NTX condition was 42.58 ± 7.88 nmol/cm^2•hr, and 170.84 ± 32.12 nmol/cm^2•hr for placebo gel + NTX. In order to target a higher plasma NTX concentration (approximately 4 ng/ml), 8 treatments sites were necessary for the subjects in Group 1, whereas only 2 sites were necessary to achieve the same plasma concentrations in Group 2, due to the difference in flux between the conditions.

8.2.6 Sampling schedule for pharmacokinetic analysis

On day 1, subjects came to the outpatient research unit in the Center for Clinical and Translational Science. An indwelling catheter was inserted into the antecubital vein and a single blood sample was drawn as a blank baseline. Following MN treatment and NTX patch administration, serial blood samples were obtained at 15, 30, 45, and 60 minutes and at 1.5, 2, 4, 6, and 8 hours. The catheter was removed from the arm and subjects went home for the evening. They returned to the clinic every day for the remainder of the study, and individual venipunctures were performed for all additional time points. For days 2 – 6, one sample was drawn every 24 hours. On days 7 and 8, samples were drawn at 24 and 30 hours following the previous points. All blood samples were approximately 4 ml volume, collected into 4 ml green top plastic collection tubes, spray-coated with 60 USP units of sodium heparin (BD Research, Franklin Lakes, NJ).   Immediately following collection, blood samples were immediately centrifuged at 1308 x g for 10 minutes to separate the plasma from the red blood cells. The plasma was pipetted off and stored at -80°C until analysis.

<u>8.2.7 Plasma extraction procedure and analysis, naltrexone and 6-β-naltrexol</u>

The plasma extraction procedure was similar to that described previously by Valiveti *et al*, with minor modifications [93]. Two hundred μl of plasma was added to 1000 μl of 1:1 ethyl acetate:ACN, resulting in protein precipitation. The mixture was vortexed for 15 seconds and immediately centrifuged for 20 minutes at 12,000 x g. Following centrifugation, the supernatant was pipetted into glass tubes (with care taken to not disturb the pellet) and evaporated under nitrogen. The resulting residue was re-suspended in 200 μl of acetonitrile, vortexed for 15 seconds, and sonicated for 10 minutes. Afterwards the sample was transferred to low volume inserts in glass HPLC vials, and injected onto the HPLC column. Working NTX•HCl and NTXol standards were made in acetonitrile over a range of 10 to 750 ng/ml. In order to make plasma standards, 200 μl of blank human plasma (Innovative Research, http://www.innov-research.com/1-home) was spiked with 20 μl of the ACN working standard and extracted as described above for the experimental plasma samples. The resulting concentrations of the plasma standards were 1 – 75 ng/ml, which displayed excellent linearity over the whole concentration range ($R^2 \geq 0.97$).

All plasma samples were analyzed on a LC-MS/MS system consisting of a HPLC Waters Alliance 2695 Separations Module, Waters Micromass® Quattro MicroTM API Tandem Mass Spectrometer and Masslynx Chromatography software with Waters Quanlynx (V. 4.1) analysis software. Positive mode atmospheric pressure chemical ionization was used for detection of both compounds (APCI+). Multiple reaction monitoring (MRM) was carried out with the following parent to daughter ion transitions for NTX•HCl and NTXol•HCl: m/z 341.8→323.8, m/z 343.8→325.8, respectively. The corona voltage was 3.5 μA, cone voltage 25 V, extractor 2 V, RF lens 0.3 V, source temp 130 °C, APCI probe temperature 575 °C. The collision gas was 20 eV. Nitrogen gas was used as a nebulization and drying gas at flow rates of 50 and 350 l/h, respectively. The chromatographic column was a Waters Atlantis Hilic Silica 5 μm, 2.1x150, with a mobile phase of methanol with 0.1% acetic acid:buffer 95:05 (v/v). Twenty mM ammonium acetate and 5% methanol comprised the aqueous buffer. The injection volume was 40 μl for all samples. Liquid chromatography was carried out in the isocratic mode at the flow rate of 0.5 ml/min with a total run time of 4.5 min.

8.2.8 Impedance spectroscopy and micropore closure kinetics

Adequate formation of micropores in the skin and confirmation of longer micropore lifetime in the diclofenac vs. placebo group was assessed via impedance spectroscopy, which has been shown to be a reliable method of measuring micropore closure kinetics [14]. Impedance measurements were made at 3 time points during the study: baseline (pre-MN), immediately post-MN, and on the final day of the study after all gels and patches were removed. Impedance measurements were made according to previously described procedures (Research Plan 3.1). Gel Ag/AgCl measurement electrodes (Though Technology T-3403; 25 mm x 25 mm total area) were used to measure the impedance at all sites, held to the skin with direct pressure applied by the thumb of the investigator (similar to the pressure required for a typical doorbell); a large electrode with a conductive gel surface served as the reference (Superior Silver Electrode with PermaGel, 70 mm total and active electrode diameter; Tyco Healthcare Unit-Patch, Wabasha, MN). All treatment sites were placed equidistant from the reference electrode. Measurements were made by connecting lead wires to measurement and reference electrodes; the opposite ends were connected to the impedance meter (EIM-105 Prep-Check Electrode Impedance Meter; General Devices, Ridgefield, NJ). A low frequency alternating current was modified with a 200 kΩ resistor in parallel (IET labs, Inc., Westbury, NY). Each measurement took 30 seconds to obtain.

With this impedance setup, three parallel pathways can be distinguished in the presence of MN-treated skin, according to the following equation:

$$Z_{total} = \frac{1}{\frac{1}{Z_{box}} + \frac{1}{Z_{skin}} + \frac{0.02}{Z_{pores}}}$$

Equation 8.1

where Z_{total} is the raw measurement directly from the impedance meter; Z_{box} represents the 200 kΩ resistor in parallel, and Z_{skin} is estimated from the intact skin sites. This setup thus allows for calculation of the impedance specifically at the micropores, assuming that they occupy approximately 2% of the total area under the electrode surface. This also allows for estimation of an "upper limit" at the 2% surface area, providing a reference point for evaluating closure of the micropores (as the micropores begin to close, they will gradually start to approach their own upper limit at that site). On Day 1, each site's own intact skin baseline is used to calculate the upper limit and the difference in pre- vs. post-MN Z_{pores} values; at Day 8 the same process was followed except that the Z_{skin} was estimated from the 2 control sites on the arm opposite from the

MN treatments. This method of calculation allows controls for the mismatch that occurs from the differing skin hydration status from baseline to the end of the study (baseline measurements are made on dry skin, while end of study measurements are made on skin that has been hydrated over an 8 day period under an occlusive patch).

An additional means of monitoring micropore formation in the SC is the calculation of the permeable area ($A_{permeable}$) according to the following equation, described by Gupta *et al* [14]:

$$A_{permeable} = \frac{\rho L}{Z}$$
Equation 8.2

where ρ represents the interstitial fluid electrical resistivity in the skin (~78 Ω-cm), L is the estimated length of the diffusional pathways in the SC (~15 μm, representing the average SC thickness over most of the body), and Z is the absolute impedance. Calculating the $A_{permeable}$ further allows for determination of the radius of each individual micropore, assuming that the micropores have a cylindrical shape and that each micropore occupies 1/100 of the total permeable area (measurements are made on skin that has received 2 applications of a 50 MN array).

8.2.9 Data analysis

The analysis of plasma NTX and NTXol concentration vs. time profiles after MN treatment and NTX patch application was performed by fitting the data to a noncompartmental model with extravascular input (Phoenix™ WinNonlin®, version 6.3, Pharsight Corporation, Mountain View, CA). The data generated was used to determine peak concentration (C_{max}), steady state concentration (C_{ss}), lag time to steady state concentration (T_{lag}), and area under the plasma concentration time curve from 0 to 174 hours ($AUC_{0-174 h}$). Steady state plasma concentration of NTX was calculated according to the equation:

$$C_{ss} = AUC_{0-t}/time$$
Equation 8.3

C_{last} was defined as the plasma concentration at the last time point (t = 174 hours following MN treatment). Statistical analysis was performed with Student's t tests (GraphPad Prism®, version 5.04).

8.3 Results

Nine independent studies were carried out in 10 subjects: 5 males and 4 females, mean (± SD) age of 26.4 ± 3.4 years. Subject demographics and baseline are displayed in Table 8.2. Six subjects enrolled in Group 1 (MN + diclofenac + NTX), while 4 subjects were enrolled in each of the control groups (2 subjects per group). One female subject enrolled as a crossover subject and completed the study twice: once in Group 1 and once in Group 3 (1 week washout period in between).

8.3.1 Micropore impedance and permeable area

In Groups 1 and 2, the $A_{permeable}$ was significantly higher post-MN treatment compared to the intact skin baseline ($p < 0.05$, Student's t test), demonstrating the presence of new pathways for drug diffusion. The calculated micropore radii was within the range of what has been previously reported [14]: 1.8 ± 0.4 μm in Group 1 (n = 46 measurements in 6 subjects), and 1.3 ± 0.04 μm in Group 2 (n = 4 measurements in 2 subjects). Pre- and post-study micropore radii measurements can be seen in Table 8.3.

In all subjects treated with MNs (Groups 1 and 2), the Z_{pores} decreased significantly from baseline to post-MN ($p < 0.05$, Student's t test), confirming an adequate breach of the SC barrier (n = 50 measurements total in 8 subjects; 2 measurements thrown out as outliers). At the end of the study, the Z_{pores} was significantly lower than the intact skin control sites ($p < 0.05$, Student's t test) for all subjects in Group 1 (n = 44 measurements in 6 subjects, 4 measurements thrown out as outliers), suggesting that the lifetime of the micropores had been prolonged for the entire 7 days post-MN. In contrast, by the end of the study, MN-treated sites had reached their Z_{pores} "upper limit" in both subjects in the placebo treatment group (n = 4 measurements in 2 subjects), demonstrating closure of the micropores and re-establishment of an intact skin barrier. Representative impedance profiles can be seen in Figure 8.1.

8.3.2 Pharmacokinetic parameters

All pharmacokinetic data is displayed below in Table 8.4. No NTX (or NTXol) was detected at any timepoints in the subjects from Group 3 (no MN treatment). In contrast, NTX was delivered through the micropores for the duration of the study for all subjects in Group 1 (n = 6), with a mean (± SD) $AUC_{0-174\,hr}$ of 196.5 ± 37.7 ng•h/ml, compared to the $AUC_{0-174\,hr}$ of 188.1 ng•h/ml in one subject in Group 2 (the other subject in Group 2 did not have detectable NTX levels throughout the study, discussed

below). The lag time (T_{lag}) was short, at 0.4 ± 0.8 hours (Group 1) and 0 hours (Group 2). The C_{max} and C_{ss} were quite similar between the groups: C_{max} of 2.6 ± 0.7 ng/ml (Group 1) and 2.8 ng/ml (Group 2); C_{ss} values were 1.2 ± 0.3 ng/ml and 1.1 ng/ml, respectively. A notable difference between the treatment groups, however, was the T_{max}. This parameter was somewhat variable but amongst the subjects in Group 1, with a mean of 112.0 ± 62.7 hours, compared to the T_{max} of 8 hours observed in the subject from Group 2. In all subjects in Group 1, however, NTX was detectable until the end of the study; in contrast, NTX was no longer detectable in the plasma after 72 hours in the subject from Group 2.

The plasma concentration of the active metabolite, 6-β-NTXol, was also quantified in all subjects. NTXol was detectable at one timepoint (48 hours) during the study for the subject in Group 2. However, it was detected from approximately 1 hour onward for the subjects in Group 1, with a mean AUC of 335.8 ± 103.6 ng•h/ml. In contrast to the NTX, a longer delay to max NTXol concentration was observed, with a T_{max} of 126 ± 41.3 hours. The profiles for both NTX and NTXol for all subjects in Group 1 can be seen in Figures 8.1 and 8.2.

8.3.3 Tolerability of treatments

Overall, the MN insertion and gel application process were well tolerated. For most subjects, mild erythema was noted to some degree under the waterproof tape that was used to secure the patches to the skin, but little (if any) redness was observed at the MN and gel treatment sites. The mild irritation from the Bioclusive® waterproof tape resolved over the course of hours to a few days for all subjects. One subject in Group 1 developed a mild contact dermatitis at the MN treatment sites with notable erythema and pruritus over the MN insertion grid; this subject was withdrawn from the study a day early at the decision of the study physician. The irritation and pruritus subsided after a short treatment course with 1% hydrocortisone cream.

The systemic adverse event profile was favorable across all subjects. The most commonly observed side effects included nausea and general gastrointestinal upset, mild dysphoria or anxiety, and sleep disturbances (primarily vivid dreams); the incidence of adverse events can be seen in Table 8.5. No subjects withdrew from the study because of any intolerable adverse events. All of these systemic adverse events were consistent with those observed in the previous NTX pharmacokinetic study in human

volunteers [9], and are consistent expected adverse events following other routes of NTX delivery.

8.4 Discussion

Naltrexone is an FDA approved treatment for opioid and alcohol addiction, is available in an oral and an injectable depot form to help addicts maintain a drug-free state. Unfortunately, currently available forms of NTX have substantial problems that lead to problematic side effects and ultimately decreased patient compliance (which could potentially lead to relapse). Several problems exist with currently available formulations of NTX, including extensive first-pass metabolism and hepatotoxicity associated with the oral formulation (ReVia®), and the high cost and inconvenience of the monthly injectable formulation (Vivitrol®). Transdermal delivery of NTX is desirable for opioid addicts and alcoholics in order to help reduce side effects and improve compliance, though the physiochemical properties of the molecule (specifically its hydrophilicity), do not allow it to pass through the skin barrier and achieve therapeutic concentrations. Conversely, however, the aqueous solubility of NTX is desirable to allow the drug to partition into the interstitial fluid once it has passed through the skin. This creates a significant challenge for delivering NTX via traditional transdermal delivery approaches. However, these properties make NTX an excellent candidate for MN-enhanced delivery, as the micropores create aqueous pathways that allow NTX to pass through the SC, regardless of its hydrophilic nature, allowing it to be readily measured in the plasma. In fact, NTX was the model compound in the first pharmacokinetic study in the literature to describe successful delivery of a drug to therapeutic concentrations with the "poke (press) and patch" method, administered to healthy human volunteers (described above). While therapeutic concentrations were maintained during the study, variability began to increase between 48 – 72 hours post-MN, and not all subjects maintained therapeutic levels beyond 48 hours. These results suggest that the micropores were beginning to re-seal and the skin was restoring its baseline barrier properties. A similar timeframe of delivery has also been observed when the active metabolite of NTX (6-β-NTXol) was administered to hairless guinea pigs with the same MN treatment approach.

The results of the current study demonstrate that topical application of diclofenac (a non-specific COX inhibitor) applied to MN-treated skin can maintain micropore viability and allow for delivery of NTX for 7 days. The shape of the pharmacokinetic profiles (for

both NTX and NTXol) demonstrate sustained delivery over the whole timeframe, which is in stark contrast from the subject who received placebo gel treatment. In that case, the C_{max} was reached at 8 hours, followed by a sharp decline after 72 hours, demonstrating full closure of the micropores under the predicted timeframe of 2 – 3 days.

While the local skin concentrations of diclofenac are sufficient to maintain micropore lifetime following just one application immediately post-MN (described in Chapter 7, Research Plan 3.3), gels were re-applied every 48 hours in the current study to allow for frequent visual inspection of the skin. The MN and gel treatments were well tolerated overall; one subject had some local irritation to the gels and her study was terminated a day early at the decision of the study physician.

8.4.1 Impedance spectroscopy for predicting drug delivery timeframes

The use of impedance spectroscopy has been utilized in previous studies to monitor the formation and lifetime of micropores available for drug delivery [14] (Research Plans 3.1 and 3.2, both submitted for publication). This technique is valuable in that it provides multiple options for monitoring lifetime of the micropores, through calculation of Z_{pores} (impedance specifically at the microporated skin), radii of individual micropores, and $A_{permeable}$ (permeable area of the entire micropore grid). In both groups that received MN treatment in the current study, adequate formation of the micropores was confirmed through a significant difference in both Z_{pores} and $A_{permeable}$ from the intact skin values, and the micropore radii were also similar to previously reported ranges [14].

From the results described in Research Plan 3.2, a drug delivery window of approximately 2 – 3 days was predicted from the Z_{pores} calculations in a placebo treatment setting. This correlates precisely with the data from the placebo subject in the current study, matches the prediction from Gupta *et al* examining micropore re-sealing kinetics under occluded conditions, and is also in agreement with previous pharmacokinetic studies in humans and guinea pigs [9, 11, 12, 14]. Furthermore, our previous impedance data also suggested, based on area under the admittance-time curve, that diclofenac would prolong the drug delivery window approximately 1.76 ± 0.62 times over placebo, resulting in a drug delivery window of 3.4 – 7.1 days (assuming a placebo micropore half life of 0.76 days). The current pharmacokinetic plasma data is in agreement with these values, as the placebo subject did not have detectable NTX in the plasma after 72 hours, whereas the subjects in the diclofenac + NTX group had drug

delivery for up to 7 days post-MN. These data demonstrate the capability of impedance spectroscopy to closely predict a drug delivery window; this valuable technique could be extrapolated to other drug moieties or physical enhancement techniques that create pores in the skin (thermal ablation, electroporation, etc.) to expand the possibilities of prolonging the skin's re-sealing time after a one-time breach.

8.4.2 <u>*In vitro* naltrexone flux and *in vivo* delivery considerations</u>

In the first MN-assisted pharmacokinetic study with NTX, 4 patches were applied to subjects' arms, corresponding to a total of 400 micropores (100 micropores/patch) [9]. The patch calculations were based on an *in vitro* NTX flux of 39.0 ± 13.1 nmol/cm^2•hr, with an estimated systemic clearance of 3.5 L/min and a target plasma NTX concentration of 2 ng/ml. The *in vitro-in vivo* correlation was very good, with a predicted steady state concentration of 1.9 ± 0.7 ng/ml and an observed steady state concentration of 2.5 ± 1.0 ng/ml [9]. This patch calculation was based on a total treatment area of 28 cm^2 for 400 micropores (thus resulting in 4 patches with 100 micropores under each patch). Because the flux of NTX through intact skin is negligible [135], it would be more appropriate for future MN studies to calculate a number of patches based on the number of micropores total.

The *in vitro* NTX flux from the 11% NTX•HCl gel in this study (in the presence of diclofenac sodium) was 42.58 ± 7.88 nmol/cm^2•hr, which is very similar to the flux from the previous study (from a 16% NTX•HCl gel in the absence of diclofenac sodium). In order to achieve higher plasma concentrations, a steady state NTX concentration of approximately 4 ng/ml was targeted, such that NTX and NTXol could still be detected in the plasma if the concentrations decreased towards the end of the study. Assuming similar parameters as those described above to calculate the 4 patch requirement for the first pharmacokinetic study, 8 patches were required for the current study to achieve approximately double the NTX plasma concentration (through twice as many micropores). In contrast, only 2 MN-treated sites with patches were calculated for the placebo condition (200 micropores total), based on the *in vitro* flux of 170.84 ± 32.12 nmol/cm^2•hr.

In both the active and placebo treatment groups (Groups 1 and 2, respectively), the trends of NTX delivery were as predicted: delivery for a full week in the presence of diclofenac, vs. no delivery after 72 hours in the placebo subject. However, in both groups the plasma concentrations were approximately half of what was predicted from

the *in vitro* studies and patch calculations. For the placebo conditions there is a reasonably straightforward possibility to explain this discrepancy. Previous work has described the *in vitro* flux of this NTX formulation through MN-treated skin as ~70 nmol/cm^2•hr, as compared to the value of 170.84 ± 32.12 nmol/cm^2•hr that the calculations were based on for the patch number in the placebo group. Thus, approximately twice as many patches (i.e. 4 patches total) would likely have achieved the target of 4 – 5 ng/ml in the placebo subjects. Large amounts of variability (up to 30%) can be observed with *in vitro* permeation studies, which might have contributed to the error in patch calculation [24, 124], and biological variability for *in vivo* studies can also result in plasma concentrations not achieving the predicted levels. The subject in the placebo group who did not have detectable levels was at the higher end of the BMI range across the subjects, and was also the only African American subject in the study. Both of these factors might have contributed to greater intersubject variability. His blood volume may have been larger as compared to the other subjects, thus requiring higher amounts of drug to reach a detectable concentration. Recovery has been shown to be faster in darker skin following acute barrier perturbation, SC lipid content is higher in African Americans, and increased electrical resistance of the skin in African Americans suggests an increased SC thickness as compared to Caucasians [136]. In combination with too few patches, all of these reasons might have contributed to why this subject did not have detectable NTX or NTXol levels throughout the study. However, despite not having a plasma profile that could be compared to the other subjects, his impedance data followed the expected trend for placebo conditions. The Z_{pores} at the MN-treated sites reached the upper limits at the end of the study, confirming that the micropores had sealed as expected in the absence of diclofenac.

The possible explanations for why NTX concentrations only reached approximately half of the predicted values for the subjects in Group 1 are not quite as straightforward as for the placebo subjects. The impedance data supports that the micropores were viable for the whole treatment period; additionally, despite levels being low, NTX was delivered throughout the full 7 days of the study. Thus, the most logical explanation for the decreased plasma concentrations is that the NTX did not deliver through the micropores as efficiently as expected. During the study, movement of the subjects' arms with day to day activities could have decreased the contact between the gels and the skin, as compared to the constant contact that is present in the *in vitro* studies. Additionally, the diclofenac gel could have been rubbed into the skin differently

on the arms of the subjects as compared to what is achievable for the *in vitro* studies. There is a significant difference in the flux of NTX in the presence of diclofenac when compared to NTX alone ($p < 0.05$, Student's t test), suggesting that the active diclofenac moiety interacts with the NTX•HCl and impedes its flux. This is not entirely unexpected, as diclofenac is an acid and NTX is a base, thus forming a local precipitate when co-applied. There are two possibilities that seem likely with regards to how this precipitate could have affected NTX delivery. While the amount of diclofenac (100 µl) was very small, an equal amount of NTX precipitating with the diclofenac would significantly decrease the diffusional gradient, as 100 µl of NTX would represent 1/5th of the total gel applied at each site. A second possibility is that the precipitate could possibly block some of the permeable area of the micropores, allowing for less NTX to physically pass through the newly created pathways. A combination of both of these scenarios is also possible. Thus, while the diclofenac is effective for inhibiting micropore closure, the greatest challenge from a therapeutic perspective is to develop a system capable of delivering diclofenac locally to the micropores without significantly impeding the NTX flux.

All of the above discussion postulates why the observed concentrations of NTX alone did not reach predicted values. Upon further examination, however, the sum of NTX and NTXol together achieves a plasma concentration that is much closer to the predicted, with a mean C_{ss} of 3.18 ± 0.7 ng/ml (Group 1). NTXol is the primary metabolite of NTX, with a negligible difference in molecular weight from the parent (341.8 and 343.8 for NTX and NTXol, respectively). This allows the sum of NTX and NTXol to be compared directly to the predicted NTX concentration, assuming approximately 1:1 conversion of NTX to NTXol. This also reprsesents the most accurate overall clinical scenario, as near zero-order delivery of NTX will result in the presence of the metabolite over the entire treatment course. Thus, the correlation of *in vitro* predictions to *in vivo* plasma concentrations is 79.5%, which is excellent for human clinical studies.

The flux of NTX from this formulation through intact skin has been described as 8 nmol/cm^2•hr, which would be considered negligible from a systemic delivery perspective [135]. However, due to the increased number of patches in this study compared with previous studies, 10 patches were applied to intact non-MN treated skin in 2 subjects to discern if any of the plasma NTX observed in the subjects in MN groups was partially due to passive diffusion through intact skin. In both control subjects there was no

detectable NTX or NTXol at any timepoints, confirming the lack of flux in the absence of micropores. Thus, the plasma concentrations observed in the MN treatment groups can be attributed to NTX flux through the micropores, rather than passive diffusion from a relatively high number of patches. This was also confirmed by the crossover subject who completed the study twice, once with and once without MN treatment. She had detectable levels throughout the study following MN treatment, but no detectable NTX or NTXol when the treatments were applied to intact skin.

8.5 Conclusions

This is the first study in humans to demonstrate that drug delivery can be achieved for a full week after one application of a MN array, using the "poke (press) and patch" method. Furthermore, the drug delivery windows were accurately predicted by impedance spectroscopy as a surrogate technique, allowing for extrapolation of the technique to other drug moieties and poration techniques. The final challenge for this type of NTX delivery system will be to achieve a formulation NTX and/or diclofenac that will allow for therapeutic plasma concentrations (> 2 ng/ml) to be delivered from a clinically reasonable patch number or size. These data demonstrate the immense potential of MN technologies for drug delivery over longer periods of time than what has been shown previously.

Table 8.1

Group	Total number of micro-pores	Gels applied	*In vitro* flux of NTX•HCl, nmol/cm^2•hr	Predicted [NTX], plasma (ng/ml)	Actual [NTX], plasma (ng/ml)	Actual [NTX] + [NTXol], plasma (ng/ml)
1	800 (8 patches)	Diclofenac + NTX	42.58 ± 7.88 (n = 3)	4	1.2 (0.3)	3.18 (0.7)
2	200 (2 patches)	Placebo + NTX	170.84 ± 32.12 (n = 3)	4	1.1	1.19
3	NA	Diclofenac + NTX	NA	0	0	0

Table 8.1 Description of the number of micropores created for each treatment group and the gels applied to the skin. Patch numbers were calculated based on the previous human pharmacokinetic study demonstrating that NTX plasma concentrations of 2.5 ± 1.0 ng/ml were achieved from 400 micropores (4 patches); the goal of this study was to achieve concentrations closer to ~4 ng/ml.

Table 8.2

Sex	4 male
	5 female
Mean age, years (SD)	26.4 (3.4)
	(range 23 to 32)
Mean body mass index, kg/m^2 (SD)	27.9 (6.9)
	(range 18.5 – 42.2)
Race	8 Caucasian
	1 African American

Table 8.2 Subject demographics across 9 healthy human volunteers.

Table 8.3

Treatment applied	Micropore radii (µm), Day 1	Micropore radii (µm), Day 8
MN + diclofenac + NTX (Group 1)	1.8 ± 0.4 (n = 46)	2.5 ± 0.5 (n = 48)
MN + placebo + NTX (Group 2)	1.3 ± 0.04 (n = 4)	0.9 ± 0.04 (n = 4)

Table 8.3 Radii of the individual micropores in Groups 1 and 2 (subjects in Group 3 did not receive MN treatment). Calculation of the $A_{permeable}$ for the entire microporated skin area allows for estimation of the radii of the individual micropores, assuming a cylindrical shape and that each micropore contributes 1/100th of the total permeable area.

Table 8.4

	NTX			NTXol		
	Group 1	Group 2	Group 3	Group 1	Group 2	Group 3
C_{ss}, ng/ml	1.2 (0.3)	1.1	NA	2.0 (0.6)	NA	NA
T_{lag}, h	0.4 (0.8)	0	NA	2.8 (1.4)	48.0	NA
C_{max}, ng/ml	2.6 (0.7)	2.77	NA	3.5 (1.3)	0.49	NA
T_{max}, h	112.0 (62.7)	8	NA	126.0 (41.3)	48.0	NA
$AUC_{0\text{-}174\ hr}$ ng•h/ml	196.5 (37.7)	188.1	NA	335.8 (103.6)	18.98	NA
C_{last}, ng/ml	1.4 (0.4)	0	NA	1.89 (1.4)	0	NA

Table 8.4 Pharmacokinetic parameters for NTX and its active metabolite, NTXol, in human plasma. Group 1 received treatment with MN + diclofenac + NTX gel (Group 3 received the same treatment but with no MN application), and Group 2 was treated with placebo gel in lieu of the diclofenac gel. The data were fitted to a noncompartmental model with extravascular input (Phoenix WinNonlin® version 6.3).

Table 8.5

Adverse event	Incidence
General GI disturbance	20% (nausea)
Sleep disturbances	10% (vivid dreams)
	20% (hypersomnia)
Mild dysphoria or anxiety	30% (dysphoria)
	10% (anxiety)
Local skin irritation at MN treatment sites	10%

Table 8.5 Incidence of subject-reported adverse events during 7 days of NTX delivery in 9 healthy human subjects.
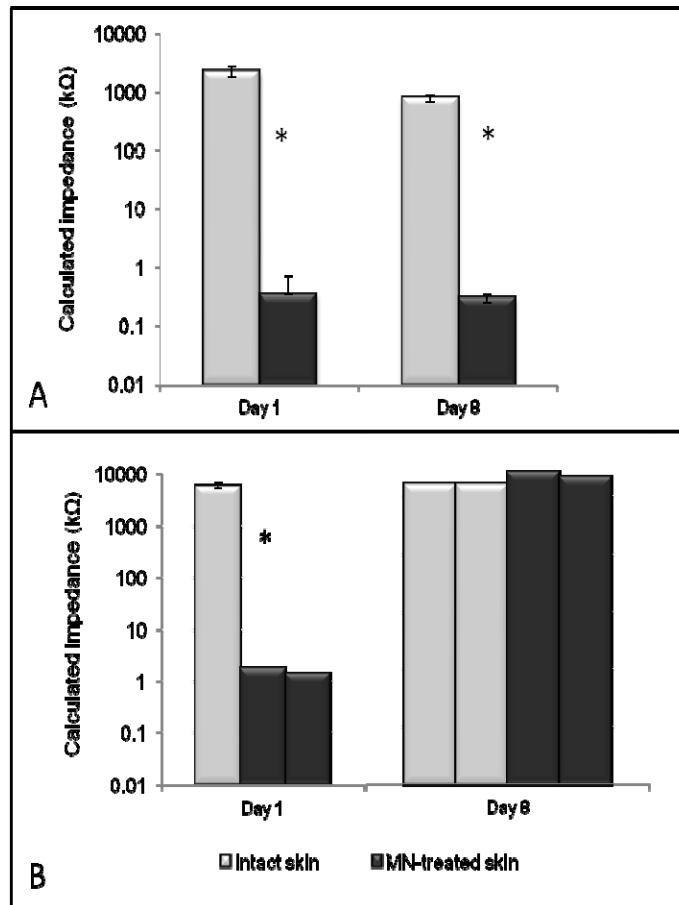
Figure 8.1 Representative impedance profiles from one subject in Group 1 (MN + diclofenac + NTX) and one subject in Group 2 (MN + placebo + NTX). In both subjects, the Z_{pores} decreased significantly from baseline to post-MN, demonstrating a breach of the SC via the creation of micropores. A: At the end of the study (Day 8), a significant difference was still present between intact skin and the MN-treated sites for the subject in Group 1. B: The Z_{pores} had reached its upper limit by Day 8 in the subject from Group 2, confirming that the micropores had healed and would thus prevent any further drug delivery. On Day 1, the grey bar (intact skin) represents the mean impedance of the 4 treatment sites; all other bars represent individual measurements at each site.

129
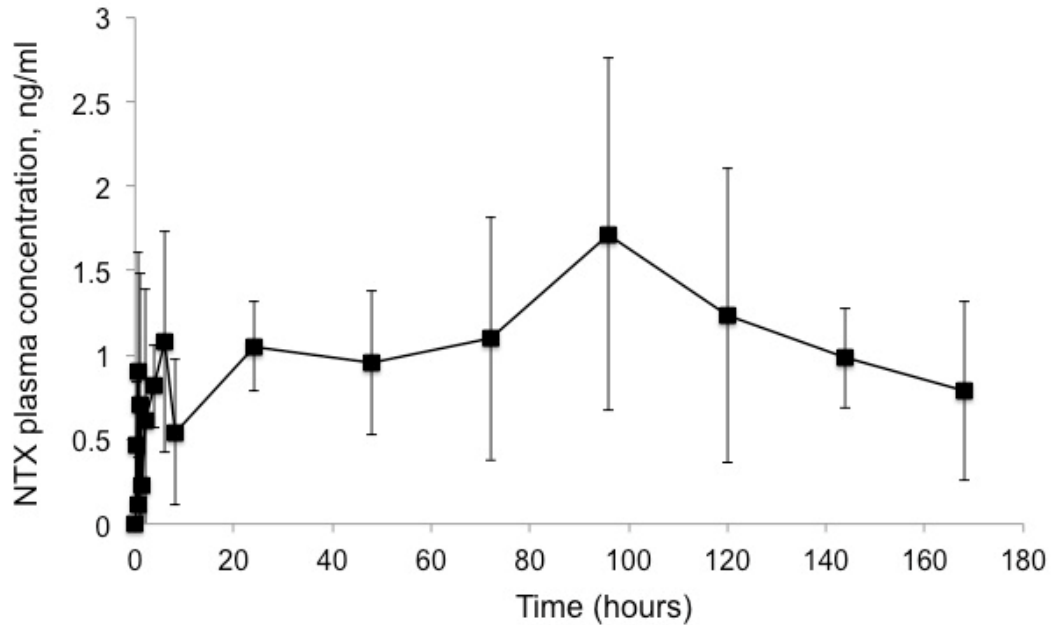
Figure 8.2 NTX plasma profiles following one-time MN treatment and application of diclofenac and NTX gel every 48 hours for 7 days post-MN (n = 6 subjects). NTX was detected to the end of the study for all subjects, with a mean $AUC_{0-174\,hr}$ of 196.5 ± 37.7 ng·h/ml, which correlated with the impedance measurements that predicted micropore lifetime for approximately 3 – 7 days with application of diclofenac.
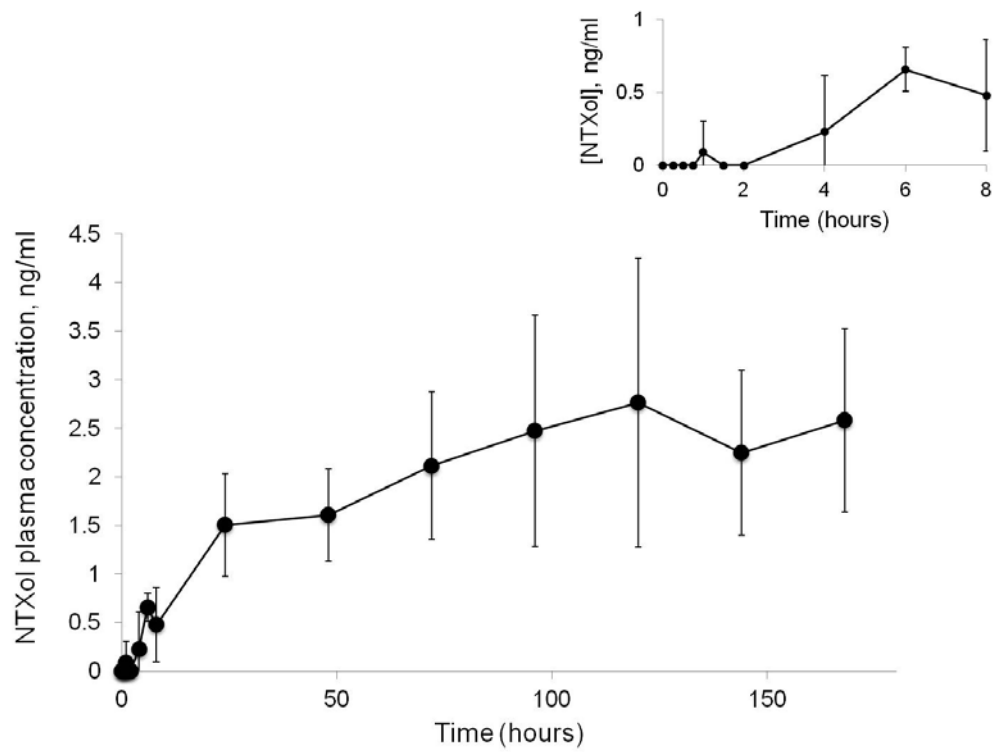
Figure 8.3 NTXol plasma profiles following one time MN treatment and application of diclofenac and NTX gel every 48 hours for 7 days post-MN treatment (n = 6 subjects).

Chapter 9
Pharmacokinetic evaluation of microneedle-enhanced 7-day transdermal delivery of naltrexone via restoration of the epidermal Ca^{2+} gradient in hairless guinea pigs

9.1 Introduction

The stratum corneum (SC) is the outermost layer of the skin, and serves as the primary permeability barrier to most xenobiotics. The structure of the SC is remarkably unique in that it exists in a "brick and mortar" conformation, with keratinocytes (bricks) surrounded by a continuous lipid matrix (mortar). The continuous lipid phase provides most of the permeability barrier, preventing the outward movement of water and the inward flux of xenobiotics and chemicals. Following acute disruption of the SC permeability barrier, a pathway of homeostatic events is initiated to restore the barrier, and the pathways of repair are the same irrespective of the method of disruption (tape stripping, solvent treatment, skin irritants etc.) [66-68, 76]. One of the first changes in the skin that occurs immediately following barrier disruption is increased transepidermal water loss between the skin and the external environment, which dissipates the epidermal calcium gradient. Under normal conditions, a steep epidermal calcium gradient exists such that low concentrations of calcium are found in the basal layer of the epidermis (~180 mg/kg), and high concentrations are found in the outer layers of the stratum granulosum (~460 mg/kg, approximately 10 µm from the skin surface); the gradient drops off sharply and the lowest calcium levels in the skin are found within the SC [76]. When the skin barrier is disrupted, the movement of water between the internal and external environment increases, carrying calcium towards the skin surface and eliminating the steep gradient. Dissipation of this gradient provides a signal for exocytosis of lamellar bodies into the domain between the SC and the stratum granulosum [66-68, 76, 137-139]. This response is initiated quickly after barrier disruption (within 1 hour), and the permeability function of the skin is quickly restored, as displayed in Figure 9.1 [68].

When the change in the calcium gradient after barrier disruption is prevented via application of a vapor-impermeable membrane or submersion in a calcium-containing solution, the secretion of lamellar bodies is not initiated and barrier repair is delayed [66-68]. This suggests that the dissipation of the gradient from the change in water movement provides a signal for the repair response. Based on these properties of the

skin's response to barrier perturbation, we hypothesized that blocking dissipation of the calcium gradient via topical application of calcium gels to microneedle (MN) treated skin would inhibit barrier restoration, allowing for delivery of naltrexone HCl (NTX•HCl) through the micropores for up to 7 days. The intent of this study was to determine the effect of topically applied calcium salts on the kinetics of micropore closure in hairless guinea pigs; these studies satisfy Research Plan 3.7.

9.2 Methods and materials

The following components were purchased through the University of Kentucky: naltrexone HCl (Mallinkrodt, Mansfield, MA), propylene glycol (VWR, Atlanta, GA), benzyl alcohol (Fisher Scientific, Hanover Park, IL), 10% calcium chloride injection, USP (NDC 0409-1631-10, Hospira, Inc., Lake Forest, IL), calcium gluconate 23% solution (NDC 57561-802-50, Agri Laboratories, Ltd. St. Joseph, MO), calcium acetate powder, USP (Spectrum Chemical Mfg. Corporation, ordered through VWR, Atlanta, GA), and sterile water for injection. Hydroxyethylcellulose (HEC, Ashland Specialty Ingredients, Wilmington, DE) was a gift from the company.

9.2.1 Preparation of gel formulations

A gel of 8.4% NTX•HCl was prepared with the following components: 84 mg/ml NTX•HCl, propylene glycol (10%), benzyl alcohol (1%), sterile water (89%), and HEC (2.5%). Gels were prepared with varying concentrations of 3 calcium salts: calcium acetate (8.4%), calcium gluconate (2.5 or 5%), and calcium chloride (1mM or 2mM); each gel only contained one salt form (all gel formulations displayed in Table 9.1). To deliver the calcium to the skin, the salts were added to a NTX•HCl solution to obtain the desired end concentration prior to gelling. The calcium gluconate and chloride were both commercially available as aqueous solutions (23% and 10%, respectively); the solutions were used to add calcium to the gels prior to the final step of gelling the solution via addition of HEC. Calcium acetate was available as a raw powder; a 23% stock solution was made in sterile water and was used to augment the gels to the correct concentration of calcium acetate. For all gels, the solution of NTX•HCl, propylene glycol, benzyl alcohol, and calcium was vortexed and allowed to mix on a stir plate for approximately 5 minute before addition of the HEC. All gels were allowed to sit at room temperature overnight before being used; no particulates or precipitation was observed in any of the gels; the viscosity of the gels was not measured.

9.2.2 Preparation of microneedle arrays and occlusive patches

Microneedle arrays were prepared with methods previously described (NTXol paper); the MN arrays were designed by the Prausnitz lab at the Georgia Institute of Technology. In-plane MN rows were cut into stainless steel sheets with an infrared laser (Resonetics Maestro, Nashua, NH) using a template drafted in AutoCAD® software (Autodesk®, San Rafael, CA). The arrays contained 50 MNs arranged in a 5 x 10 array configuration; each MN measured 750 μm in length and 200 μm in width at the base. While the needles were still in-plane, the arrays were cleaned to de-grease the surface and remove the slag deposited during laser-cutting; this cleaning step was performed with detergent (Alconox, White Plains, NY). Afterwards, the arrays were electropolished in a solution of glycerin, 85% ortho-phosphoric acid, and water (ratio of 6:3:1, all chemicals from Fisher Scientific, Hanover Park, IL). Following the electropolishing procedure, the needles were cleaning by dipping alternatively in 25% nitric oxide (Fisher Scientific) and deionized water (total of 3 times). A final rinse with deionized water performed and the arrays were dried under pressurized air.

For better insertion and adhesion of patches to the skin, microneedle arrays were assembled into adhesive patches with Arclad (Adhesives Research, Inc., Glen Rock, PA). The adhesive serves to hold the MNs firmly against the skin by compensating for the mechanical mismatch between the flexible skin tissue and the rigid MN array. The MN patches were sterilized before use by autoclaving under high pressure saturated steam at 121° C for 15 minutes.

To hold the gels close to the skin and occlude the MN-treated area, blank occlusive patches were made. A rubber ring was secured with 3M double-sided medical tape to an impermeable backing membrane (Scotchpak 1109 SPAK 1.34 MIL heat-sealable polyester film; 3M, St. Paul, MN). The other side of the rubber ring also had a layer of 3M double-sided tape in order to hold the patch closely to the skin and prevent leaking of the gels.

9.2.3 Study procedures

Hairless guinea pigs were treated with MN arrays at 2 sites on the dorsal surface. MN insertion is a simple procedure, achieved by placing the 50 MN array on the skin and pressing gently for approximately 10 – 15 seconds and then immediately removing the array. The array was rotated 45 degrees for a second insertion, in order to create 100 non-overlapping micropores. Immediately following MN application, 200 μl of the

NTX/calcium gel of interest was applied to the microporated skin at each site and immediately covered with an occlusive patch. The patches were secured to the skin with Bioclusive dressing (Systagenix Wound Management, Quincy, MA). The animals were weighed and temperature was recorded daily to monitor for acute illness or intolerance of the treatments. Blood samples were obtained over a period of 5 – 7 days after MN treatment in order to assess NTX plasma concentrations.

9.2.4 Pharmacokinetic sampling

Prior to the studies, all animals underwent surgery to surgically implant indwelling catheters into the jugular vein; all surgeries were performed by Kalpana Paudel, Ph.D. All blood samples were drawn from the indwelling catheter during the studies. Before applying any treatments, a blood sample was drawn as a blank; following MN treatment and NTX gel administration, serial blood samples (approximately 200 µl each) were obtained at 15, 30, 45, and 60 minutes and at 1, 2, 4, 7, and 10 hours. Starting at 24 hours post-treatment, samples were taken at 12 hour intervals for the remainder of the study, collected into tubes coated with a 500 IU/ml heparin solution to prevent blood coagulation. The blood samples were immediately centrifuged at 10,000 x g for 3 minutes; the plasma was separated and stored at -80° C until analysis.

9.2.5 Plasma extraction procedure

The plasma extraction procedure was similar to that described previously by Valiveti *et al*, with minor modifications [93]. One hundred µl of plasma was added to 500 µl of 1:1 ethyl acetate:acetonitrile, resulting in protein precipitation. The mixture was vortexed for 15 seconds and immediately centrifuged for 20 minutes at 12,000 x g. Following centrifugation, the supernatant was pipetted into glass tubes (with care to not disturb the pellet) and evaporated under nitrogen. The resulting residue was re-suspended in 100 µl of acetonitrile, vortexed for 15 seconds, and sonicated for 10 minutes. Afterwards the sample was transferred to low volume inserts in glass HPLC vials, and injected onto the HPLC column. Working NTX standards were made in acetonitrile over a range of 10 to 750 ng/ml. In order to make plasma standards, 100 µl of blank guinea pig plasma was spiked with 10 µl of the ACN working standard and extracted as described above for the experimental plasma samples. The resulting concentrations of the plasma standards were 1 – 75 ng/ml, and displayed excellent linearity (R^2 > 0.98 for all standard curves).

The analysis of plasma NTX concentration vs. time profiles after MN treatment and NTX patch application was performed by fitting the data to a noncompartmental model with extravascular input (Phoenix™ WinNonlin®, version 6.2, Pharsight Corporation, Mountain View, CA). The data generated was used to determine peak concentration (C_{max}), time to peak concentration (T_{max}), lag time (T_{lag}), and area under the plasma concentration time curve from 0 to 96 hours (AUC_{0-96h}).

9.2.7 Data analysis

Student's t tests were used to compare the AUC_{0-96h} and C_{max} between all treatment groups; $p < 0.05$ was considered statistically significant (GraphPad Prism® software, version 5.04).

9.3 Results

The effects of different calcium salts (acetate, chloride, and gluconate) on micropore re-sealing rates were examined in hairless guinea pigs treated once with MN arrays (total of 200 micropores) followed by application of an 8.4% NTX•HCl gel containing different concentrations of the various calcium salts. All pharmacokinetic parameters can be seen in Table 9.2. Three control guinea pigs were treated once with NTX•HCl gel containing no calcium. Mean (± SD) AUC_{0-96h} for these animals was 1,278.3 ± 635.6 ng•hr/ml. NTX was no longer detectable in the plasma after 34, 72, and 96 hours for the 3 control animals.

9.3.1 Calcium acetate

Three guinea pigs (mean ± SD weight of 430 ± 65 g) were treated with MNs + an 8.4% NTX•HCl gel with 8.4% w/v of calcium acetate. AUC was calculated over a period of 96 hours to allow for direct comparison with the control animals. The AUC_{0-96h} was 1204.9 ± 167.5, which was not significantly different from control ($p > 0.05$, Student's t test), and the C_{max} of 58.0 ± 13.2 ng/ml was also not significantly different from control. Despite the AUC_{0-96h} not being significantly higher as a result of the calcium acetate treatment, NTX was detectable in the plasma in all 3 animals up until the end of the study at 178 hours, demonstrating continued delivery of NTX through the micropores (in contrast to the control animals, in which NTX was not detectable after 96 hours).

One guinea pig was treated with an 8.4% NTX•HCl gel containing 1mM $CaCl_2$, while 3 additional animals were treated with a NTX•HCl gel containing 2mM $CaCl_2$. Mean ± SD weight of the animals was 435 ± 73 g. AUC was calculated over a period of 96 hours to allow for direct comparison with the control animals. The AUC_{0-96h} was 1227.9 ng•hr/ml (n = 1 animal, 1 mM $CaCl_2$) and 1213.9 ± 692.6 ng•hr/ml (2 mM $CaCl_2$, n = 3), with a mean C_{max} of 81.4 ± 28.2 ng/ml (n = 4). Both AUC_{0-96h} and C_{max} were not significantly different from control (p > 0.05, Student's t tests). NTX was not detectable in the plasma after 48 hours for one animal treated with a 2mM gel, while the other 2 animals receiving the same treatment still had detectable levels at 96 hours. The animal treated with 1mM $CaCl_2$ had detectable concentrations at 120 hours post-MN.

9.3.3 Calcium gluconate

Three studies were carried out in 3 guinea pigs: 2 studies examining the effect of a 2.5% calcium gluconate gel on micropore closure (applied either once or re-applied every 36 hours), and a 5% calcium gluconate gel; mean (± SD) weight of the animals was 533.3 ± 118.9 g. The AUC_{0-96h} for these treatments were 419.1, 570.0, and 479.4 ng•hr/ml, respectively. NTX was detectable in the plasma for 58, 130, or 96 hours (2.5% gel applied once, 2.5% gel re-applied every 36 hours, and 5% gel applied once, respectively). The AUC_{0-96h} and C_{max} were not significantly different from control (p > 0.05, Student's t test).

9.4 Discussion

The unique structure of the SC provides a barrier to the ingress of noxious chemicals and xenobiotics, and this lack of permeability is primarily dictated by the lipids that form the intercellular domain. The calcium gradient across the epidermal skin layers is a primary signal for stimulating secretion of lamellar bodies, a critical event for restoring normal barrier homeostasis. These studies sought to inhibit the change in the calcium gradient (following MN treatment) through the topical application of a NTX•HCl gel containing various calcium salts. Drug permeability of NTX (measured by plasma concentrations) was used to assess micropore lifetime. In these studies, no-MN treatment controls were not included, as the flux of this NTX formulation through intact skin is negligible [135].

Previous studies examining pharmacokinetic parameters of NTX and its metabolite (6-β-NTXol) following MN-assisted delivery have demonstrated a delivery window of approximately 48 – 72 hours under occluded conditions [9, 11, 12]. The control animals in this study demonstrated similar profiles, as NTX was not detectable after 34 – 96 hours when no calcium was present in the gel formulation. While one animal had a slightly longer delivery window than what is typically observed NTX delivery, some biological variation is expected and this particular animal may have had slightly slower barrier restoration than the other animals.

The AUC was calculated over the timeframe of 0 – 96 hours (rather than the full 0 – 178 hours of the study) because several of the animals loosened their patches or removed them completely around 96 hours in the calcium acetate studies (discussed below). Thus, calculating the AUC over 0 – 96 hours allowed for a more consistent comparison between treatments. None of the calcium salts, regardless of concentration or salt form, displayed significant differences in AUC_{0-96h} or C_{max} compared to the control animals. Furthermore, all of the profiles demonstrated similar shapes, exhibiting an exponential decay and confirming that the treatments did not alter the re-sealing mechanisms of the skin significantly. The shape of all of the profiles can be seen in Figure 11.1. There are various reasons specific to each calcium salt form that may have contributed to the non-significant difference (i.e. lack of treatment effect).

Previous studies have demonstrated prolonged recovery of barrier function following restoration of the calcium gradient via submersion in calcium containing solutions ($CaCl_2$), and a range of calcium concentrations from 0.01 to 10 mM of $CaCl_2$ were effective for delaying repair [67, 139]. The effect of the calcium on barrier repair was most effective at a concentration of 0.1 mM. As a comparison, the concentrations of $CaCl_2$ in the present studies were 1 and 2 mM, which falls in the middle of the range of concentrations studies previously. From the resulting pharmacokinetic profile of NTX delivery, this concentration was not effective for prolonging micropore lifetime as compared to control. This particular salt form is highly water soluble and is typically used in clinical practice as an injectable preparation [90]. It is possible that the high water solubility resulted in diffusion of the $CaCl_2$ from the gel and into the aqueous interstitial fluid within the micropores. Over the duration of the entire study this may have resulted in subtherapeutic concentrations of calcium at the skin surface, therefore not restoring the gradient as needed to delay barrier recovery. In the earlier studies, submersion in calcium containing solutions was only for a period of a few hours, and

barrier recovery (or its delay) was measured for just hours after the treatment. Thus, $CaCl_2$ may not be effective for delaying recovery after MN treatment for such a long period as 7 days. Once the $CaCl_2$ had diffused away from the gel and skin surface, the skin's normal paradigms would likely take over and result in near-normal restoration times.

Calcium gluconate was studied at concentrations of 2.5% w/v and 5% w/v. This salt form was selected as a potential calcium source due to its known tolerability and lack of irritation potential in animals and humans, in which it is used to treat hydrofluoric acid skin burns [140]. In this setting, calcium gluconate is effective for treating hydrofluoric acid burns because of its ability to bind the dissociated fluoride ions and form an insoluble salt. However, it has not been investigated if there are other mechanisms involved in its ability to quickly heal the wounds. While the binding of free fluoride ions seems to be the primary mechanism, if there are other mechanisms involved then those pathways may have affected the micropore re-sealing times in the present studies. Additionally, the elemental calcium component of calcium gluconate is one of the lowest of the available salt forms (9%), and even at the concentrations of 2.5 and 5%, there may not have been sufficient calcium present at the micropores to allow for the gradient to be fully restored.

In these studies, calcium acetate was investigated as a salt form as the source of calcium because of its higher elemental calcium (40%) compared to the other salts. The concentration of the calcium salt in the gel was the highest of all of the studies performed, at 8.4% calcium acetate in an 8.4% NTX•HCl gel. While the $AUC_{0 - 96h}$ was not significantly different from control, NTX was detectable in the plasma for the entire duration of the study (suggesting prolonged delivery of NTX through the micropores as a result of a restored calcium gradient). Upon removal of the patches, however, one notable observation was the odor of vinegar, suggesting the formation of acetic acid from the acetate within the gel. The treatment sites were flaky, peeling, and dry for 2 – 3 days after study termination; on some animals a slightly raised grid of micropores could be clearly observed in the skin. The animals appeared to be bothered by the patches, as many of the guinea pigs chewed or scratched at the patches until they pulled them off the skin. All of these characteristics suggest some level of nonspecific irritation at the treatment sites, which likely contributed to the prolonged barrier perturbation during the treatment period. In fact, 10% acetic acid has been shown to cause skin irritation in humans after just 4 hours of patch exposure [141, 142]. For these reasons, calcium

acetate would not likely be appropriate as a source of calcium for prolonging micropore lifetime due to the high potential to cause irritation at the treatment sites. Other calcium salts with reasonably high elemental calcium such a calcium citrate (21%) or calcium carbonate (40%) might be reasonable targets for future studies, as these formulations would provide high local calcium concentrations with less irritation potential.

Previous studies demonstrating a delay in barrier repair as a result of masking or replacing the epidermal calcium gradient examined a delay in barrier recovery over a period of hours following disruption (2.5 up to 24 hours) [66, 67, 75, 139]. In stark contrast, the studies in this chapter were carried out over 7 days total (although the AUC was calculated over 0 – 96 hours in order to be consistent across all conditions). Ahn *et al* demonstrated that even under occluded conditions, the epidermal calcium gradient is restored by 60 hours, suggesting that occlusion may delay the skin's response to the altered calcium gradient, but that it will ultimately proceed normally [143]. Following tape stripping an immediate disappearance of both intra- and extracellular calcium was observed, demonstrating dissipation of the gradient. By 72 hours after occlusion, re-accumulation of calcium precipitates could be seen, however, confirming that the skin is able to re-establish the gradient even in the presence of occlusion. This suggests that restoring the calcium gradient may not be a suitable method for prolonging micropore lifetime for a period as long as 7 days, as the skin will ultimately restore the gradient on its own.

9.5 Conclusion

These studies attempted to delay micropore closure kinetics via restoration of a dissipated epidermal calcium gradient immediately following disruption. Irrespective of the calcium salt investigated, the treatments were no more effective than control, suggesting that calcium modulation may not be an appropriate mechanism to target for inhibiting micropore re-sealing over a week-long timeframe.

Table 9.1

Salt form	Elemental calcium	[c] of salt form in gel	Gel formulation
Acetate	40%	8.4% v/v	10% propylene glycol
Chloride	27%	1mM	1% benzyl alcohol
		2mM	3% HEC
Gluconate	9%	2.5% v/v	8.4% NTX•HCl
		5% v/v	

Table 9.1 Description of the various calcium salts and concentrations in the NTX gels.

Table 9.2

PK Parameter	No calcium (n = 3)	Acetate (n = 3)	Chloride (n = 4)		Gluconate (n = 3)	
T_{lag}, h	0	0	0		0	
C_{max}, ng/ml	87.8 ± 30.6	58.0 ± 13.2	81.4 ± 28.2		43.8 ± 23.2	
T_{max}, h	1.8 ± 1.9	1.6 ± 0.6	1.7 ± 1.7		2.1 ± 1.9	
AUC_{0-96h}, ng•hr/ml	1278.3 ± 635.6	1204.9 ± 167.5	1227.9 (n = 1)	1 mM	418.1 (n = 1)	2.5%, applied once
			1213.9 ± 692.6 (n = 3)	2 mM	570.0 (n = 1)	2.5%, applied every 36 hrs
					479.4 (n = 1)	5%, applied once

Table 9.2 Pharmacokinetic parameters in hairless guinea pigs treated once with MN arrays (200 micropores total) followed by application of an 8.4% NTX gel containing various calcium salts. There were no significant differences in the AUC_{0-96h} between any of the treatments (p > 0.05, Student's t test) as compared to control, demonstrating no significant barrier delay as a result of the local calcium concentration.
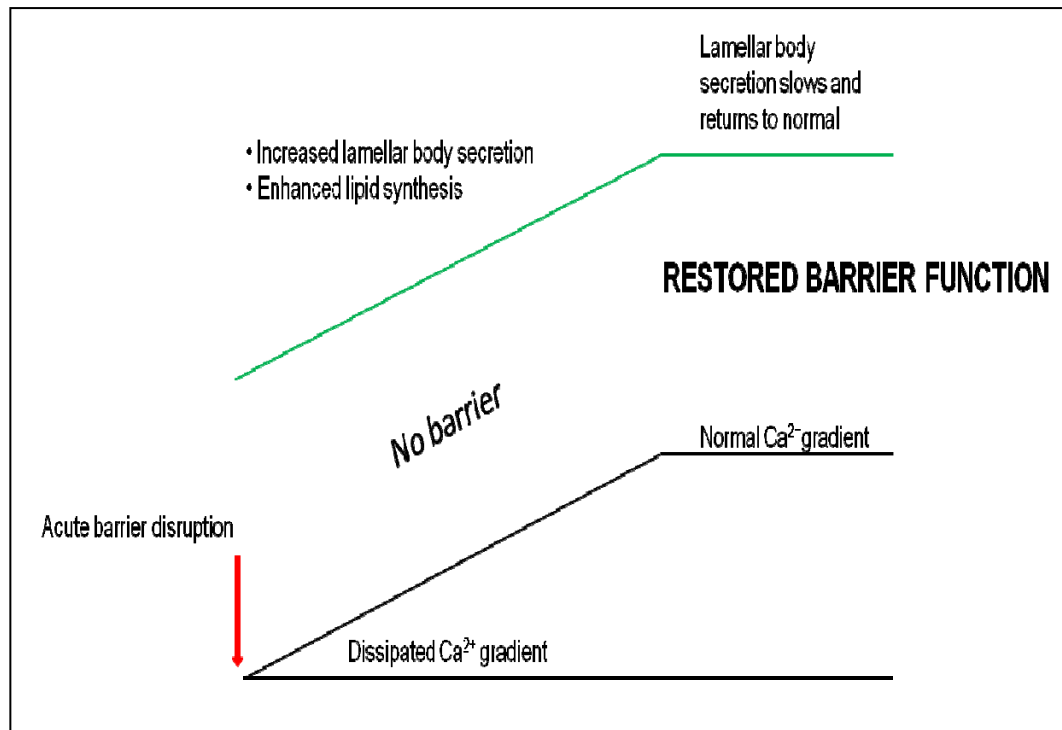
Figure 9.1 Visual depiction of the change in the SC barrier as the calcium gradient is restored after insult.
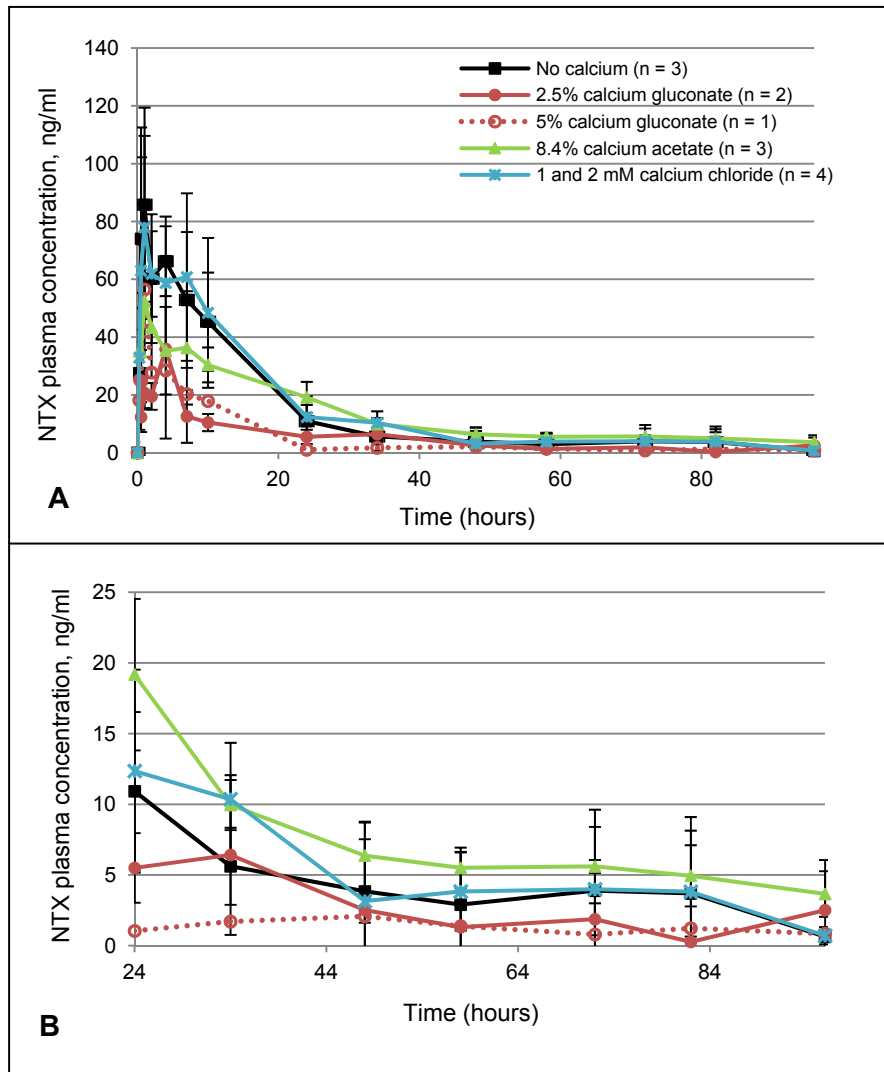
Figure 9.2 Plasma concentrations of NTX following one time treatment with a MN array and application of various calcium-containing NTX•HCl gels. A: plasma profiles over 0 – 96 hours; B: the same plasma profiles, from 24 – 96 hours. All of the profiles demonstrate a similar shape of exponential decay, suggesting that the calcium treatments did not significantly alter the skin's barrier restoration mechanisms following MN treatment.

Chapter 10
Conclusions and future directions

There were two primary objectives that this body of work sought to address: 1) to characterize the lifetime and re-sealing kinetics of the micropores created from MN insertion, and 2) to prolong the lifetime of the micropores via inhibition of the skin's normal wound healing and/or barrier restoration processes.

The first pharmacokinetic study in humans using the "poke (press) and patch" MN approach confirmed that naltrexone, a mu opioid receptor antagonist approved for the treatment of opioid and alcohol abuse, could be delivered to therapeutic concentrations for 2 – 3 days in healthy human subjects treated once with MNs [9]. While this confirmed the feasibility of transdermally delivering an otherwise skin-impermeable drug, the short timeframe of delivery would not be reasonable in clinical practice, as addicts require lifelong therapy. Thus, a 7-day transdermal delivery system of NTX would ideal to enhance patient compliance and satisfaction with therapy.

While pharmacokinetic studies are the most relevant method of evaluating drug diffusion through micropores, these types of studies are very expensive and labor intensive; as such, it would be impractical to use this type of study design for screening new MN designs or therapies intended to prolong micropore lifetime. For these reasons, it was necessary to develop a reliable surrogate technique for predicting micropore lifetime and drug delivery windows under various conditions. While multiple methods exist to monitor micropore closure kinetics, impedance spectroscopy is suitable for both animal and human studies and can be used to evaluate skin in varying hydration states (which is very important in the transdermal field). Furthermore, this technique has been used in other MN studies in human subjects, providing good correlation of micropore closure kinetics with pharmacokinetic data [14]. In the current work various electrodes and pressure application techniques were examined in animals and humans, to develop a reproducible method to monitor micropore formation and closure. Gel Ag/AgCl electrodes applied with direct pressure on microporated skin (human subjects) were able to detect changes in the SC from baseline to post-MN treatment with low levels of variability between measurements (demonstrated by %RSD). This method holds great appeal because it can also be applied to other physical enhancement techniques that also create pores in the SC, such as electroporation or thermal ablation. Through calculation of the Z_{pores} or $A_{permeable}$, closure of the micropores can be followed over time and a drug delivery window can be predicted.

In order to extend micropore lifetime to a more clinically relevant period of time (ideally 7 days of drug delivery following one MN application), a non-specific COX inhibitor (diclofenac sodium) was applied to MN-treated skin in healthy human subjects. Impedance spectroscopy was utilized as a surrogate technique to monitor micropore closure rates over time, comparing diclofenac to placebo conditions. Comparison of area under the curve between treatment groups confirmed that diclofenac prolongs micropore lifetime, with a predicted drug delivery window of approximately 2 – 3 days under placebo conditions. These results were in excellent agreement with the drug delivery window observed from the aforementioned NTX pharmacokinetic study, in addition to results from Gupta *et al* [14], demonstrating that under occluded conditions the micropores will remain viable for approximately 2 days.

Finally, *in vitro* diffusion studies and *in vivo* animal skin irritation studies were completed to design an optimal dosing scheme for a human pharmacokinetic study, with the objective of delivering NTX through MN-treated skin in the presence of diclofenac. As predicted from the previous impedance data, NTX and its metabolite were detected in the plasma for 7 days post-MN in the subjects treated with MN + diclofenac + NTX. In contrast, NTX and NTXol were only detectable for up to 72 hours in the placebo subject, confirming closure of the micropores. These results represent an exciting advance in the MN field, as this is the first study in human subjects to demonstrate such a long drug delivery window following just one application of a MN array.

The MN field has reached an exciting and pivotal stage of development. We now know that a variety of MN delivery techniques can be used to successfully deliver drugs to therapeutic concentrations for a range of timeframes, and the recent introduction of the Fluzone® intradermal vaccine confirms the commercial potential of MN technologies. Additionally, large companies such as 3M have begun developing MN products (both hollow and solid MN systems), suggesting that the commercial market for these devices will continue to grow. The perception of these techniques by patients and healthcare workers has been positive [144], and thus this market has immense potential to expand. One particularly appealing component of MN technologies is the possibility to individualize therapies based on a therapeutic need, timeframe, or drug moiety. MN treatments remove the strict physicochemical restrictions on drug compounds that can be transdermally administered, and it now seems within reach that MN therapy could be tailored to achieve specific delivery windows, which would further broaden the scope of appeal. In particular, prolonging micropore lifetime seems particularly well suited for

delivery of medications for chronic disease states, as once weekly patch application would allow for constant therapeutic delivery of a drug while increasing patient complince. In situations when prolonging micropore lifetime would be desirable for longer periods of drug delivery, the safety profile is also favorable, as the micropores exhibit a "switch-like" behavior, as they close rapidly when occlusion is removed, thus removing the concern of local infection. Additionally, a gel formulation would contain antimicrobial excipients to further prevent the possibility of infection. Further clinical investigation will be necessary to determine the safety profile of extending micropore lifetime in higher risk populations (immunocompromised patients, patients with chronic skin diseases such as atopic dermatitis or psoriasis, or elderly populations).

Delivering NTX for a week-long timeframe is ideal for the treatment of opioid and alcohol abuse, both chronic disorders that require lifelong therapy. Transdermal NTX overcomes some of the most problematic hurdles with the oral and injectable forms of the drug that are commercially available. The next step in developing a MN-assisted transdermal NTX system will be to create a formulation that allows for therapeutic concentrations of NTX to be achieved when delivered in the presence of diclofenac. Despite achieving 7 days of delivery in the current studies, the plasma concentrations of NTX were subtherapeutic (< 2 ng/ml) following treatment with 8 patches. The most likely explanation is the incompatibility of diclofenac and NTX when closely applied, as a precipitate forms that may be impeding flux through the micropores. There are several possibilities for how this could be potentially overcome. First, development of a codrug system (linking diclofenac and NTX together by a chemical moiety that dissociates within the skin) would allow for application of both moieties from a single formulation that would deposit diclofenac in the skin and allow NTX to pass through the micropores. Second, other COX inhibitors with varying specificity for COX-1 and COX-2 could be examined for effects on prolonging micropore lifetime. If the effects of diclofenac are solely related to its ability to reduce local inflammation, then other COX inhibitors might be effective in a similar manner. Finally, it is possible that diclofenac may be exerting its effects through a pathway other than simply inhibiting the COX enzymes, such as cytokine expression or the lipooxygenase pathway. Further investigation of its specific mechanisms of action would allow for better understanding of the micropore re-sealing process, leading to the development of more specific local therapies that might not interact as strongly with the NTX moiety.

The studies presented herein demonstrate great strides in MN delivery techniques, through: 1) the development of a measurement technique that is sensitive enough to monitor micropore lifetime and accurately predict drug delivery windows; and 2) delivery of a model compound through MN-treated skin for 7 days via simple topical application of a non-specific anti-inflammatory. This provides an exciting clinical springboard for the development of MN treatment systems that are suitable for a variety of therapeutics for treating human disorders.

REFERENCES

1.	Naik, A., Y.N. Kalia, and R.H. Guy, *Transdermal drug delivery: overcoming the skin's barrier function.* Pharm Sci Technolo Today, 2000. 3(9): p. 318-326.
2.	Prausnitz, M.R. and R. Langer, *Transdermal drug delivery.* Nat Biotechnol, 2008. 26(11): p. 1261-8.
3.	Prausnitz, M.R., S. Mitragotri, and R. Langer, *Current status and future potential of transdermal drug delivery.* Nat Rev Drug Discov, 2004. 3(2): p. 115-24.
4.	Mitragotri, S., *Synergistic effect of enhancers for transdermal drug delivery.* Pharm Res, 2000. 17(11): p. 1354-9.
5.	Prausnitz, M.R., *Microneedles for transdermal drug delivery.* Adv Drug Deliv Rev, 2004. 56(5): p. 581-7.
6.	Arora, A., M.R. Prausnitz, and S. Mitragotri, *Micro-scale devices for transdermal drug delivery.* Int J Pharm, 2008. 364(2): p. 227-36.
7.	Haq, M.I., et al., *Clinical administration of microneedles: skin puncture, pain and sensation.* Biomed Microdevices, 2009. 11(1): p. 35-47.
8.	*Vaccine Shoppe.* March 7, 2012; Available from: http://www.vaccineshoppe.com/static/FluID2/fluid-video-desktop.html.
9.	Wermeling, D.P., et al., *Microneedles permit transdermal delivery of a skin-impermeant medication to humans.* Proc Natl Acad Sci U S A, 2008. 105(6): p. 2058-63.
10.	Bal, S., et al., *In vivo visualization of microneedle conduits in human skin using laser scanning microscopy.* Laser Physics Letters, 2010. 7(3): p. 242 - 246
11.	Banks, S.L., et al., *Diclofenac enables prolonged delivery of naltrexone through microneedle-treated skin.* Pharm Res, 2011. 28(5): p. 1211-9.
12.	Banks, S.L., et al., *Transdermal delivery of naltrexol and skin permeability lifetime after microneedle treatment in hairless guinea pigs.* J Pharm Sci, 2009. 99(7): p. 3072-80.
13.	Enfield, J., et al., *In-vivo dynamic characterization of microneedle skin penetration using optical coherence tomography.* J Biomed Opt, 2010. 15(4): p. 046001.
14.	Gupta, J., et al., *Kinetics of skin resealing after insertion of microneedles in human subjects.* J Control Release, 2011.
15.	Harding, C.R., *The stratum corneum: structure and function in health and disease.* Dermatol Ther, 2004. 17 Suppl 1: p. 6-15.
16.	Flynn, G.L., *Cutaneous and Transdermal Delivery: Processes and Systems of Delivery*, in *Modern Pharmaceutics*, C.T.R. G.S. Banker, Editor 1990, Marcel Dekker: New York. p. 239 - 298.
17.	Feingold, K.R., *Thematic review series: skin lipids. The role of epidermal lipids in cutaneous permeability barrier homeostasis.* J Lipid Res, 2007. 48(12): p. 2531-46.
18.	Rawlings, A.V. and C.R. Harding, *Moisturization and skin barrier function.* Dermatol Ther, 2004. 17 Suppl 1: p. 43-8.
19.	Bouwstra, J.A., et al., *Structure of the skin barrier and its modulation by vesicular formulations.* Prog Lipid Res, 2003. 42(1): p. 1-36.
20.	Flynn, G.L. and B. Stewart, *Percutaneous drug penetration: Choosing candidates for transdermal development.* Drug Development Research, 1988. 13: p. 169 - 185.

21. Hadgraft, J. and R.H. Guy, *Transdermal Drug Delivery*. 2nd ed2003, New York: Marcel Dekker, Inc.

22. Milewski, M. and A.L. Stinchcomb, *Estimation of Maximum Transdermal Flux of Nonionized Xenobiotics from Basic Physicochemical Determinants.* Mol Pharm, 2012.

23. Barry, B.W., *Novel mechanisms and devices to enable successful transdermal drug delivery.* Eur J Pharm Sci, 2001. 14(2): p. 101-14.

24. Guy, R.H. and J. Hadgraft, *Physicochemical aspects of percutaneous penetration and its enhancement.* Pharm Res, 1988. 5(12): p. 753-8.

25. Scheuplein, R.J. and I.H. Blank, *Permeability of the skin.* Physiol Rev, 1971. 51(4): p. 702-47.

26. Sinha, V.R. and M.P. Kaur, *Permeation enhancers for transdermal drug delivery.* Drug Dev Ind Pharm, 2000. 26(11): p. 1131-40.

27. Sethi, S., et al., *Comparative evaluation of the therapeutic efficacy of dermabrasion, dermabrasion combined with topical 5% 5-fluorouracil cream, and dermabrasion combined with topical placentrex gel in localized stable vitiligo.* Int J Dermatol, 2007. 46(8): p. 875-9.

28. Ogura, M., S. Paliwal, and S. Mitragotri, *Low-frequency sonophoresis: current status and future prospects.* Adv Drug Deliv Rev, 2008. 60(10): p. 1218-23.

29. Smith, N.B., *Perspectives on transdermal ultrasound mediated drug delivery.* Int J Nanomedicine, 2007. 2(4): p. 585-94.

30. Mitragotri, S., *Effect of therapeutic ultrasound on partition and diffusion coefficients in human stratum corneum.* J Control Release, 2001. 71(1): p. 23-9.

31. Kim, D.K., S.W. Choi, and Y.H. Kwak, *The effect of SonoPrep on EMLA cream application for pain relief prior to intravenous cannulation.* Eur J Pediatr, 2012. 171: p. 985 - 988.

32. Galinkin, J.L., et al., *Lidocaine iontophoresis versus eutectic mixture of local anesthetics (EMLA) for IV placement in children.* Anesth Analg, 2002. 94(6): p. 1484-8, table of contents.

33. Runeson, L. and E. Haker, *Iontophoresis with cortisone in the treatment of lateral epicondylalgia (tennis elbow)--a double-blind study.* Scand J Med Sci Sports, 2002. 12(3): p. 136-42.

34. Gupta, S.K., et al., *Fentanyl delivery from an electrotransport system: delivery is a function of total current, not duration of current.* J Clin Pharmacol, 1998. 38(10): p. 951-8.

35. Denet, A.R., R. Vanbever, and V. Preat, *Skin electroporation for transdermal and topical delivery.* Adv Drug Deliv Rev, 2004. 56(5): p. 659-74.

36. Denet, A.R. and V. Preat, *Transdermal delivery of timolol by electroporation through human skin.* J Control Release, 2003. 88(2): p. 253-62.

37. Lombry, C., N. Dujardin, and V. Preat, *Transdermal delivery of macromolecules using skin electroporation.* Pharm Res, 2000. 17(1): p. 32-7.

38. Vanbever, R., E. LeBoulenge, and V. Preat, *Transdermal delivery of fentanyl by electroporation. I. Influence of electrical factors.* Pharm Res, 1996. 13(4): p. 559-65.

39. Vanbever, R., M.A. Leroy, and V. Preat, *Transdermal permeation of neutral molecules by skin electroporation.* J Control Release, 1998. 54(3): p. 243-50.

40. Gill, H.S. and M.R. Prausnitz, *Coated microneedles for transdermal delivery.* J Control Release, 2007. 117(2): p. 227-37.

41. Kim, Y.C., J.H. Park, and M.R. Prausnitz, *Microneedles for drug and vaccine delivery.* Adv Drug Deliv Rev, 2012.

42. McAllister, D.V., et al., *Microfabricated needles for transdermal delivery of macromolecules and nanoparticles: fabrication methods and transport studies.* Proc Natl Acad Sci U S A, 2003. 100(24): p. 13755-60.

43. Mikszta, J.A., et al., *Improved genetic immunization via micromechanical disruption of skin-barrier function and targeted epidermal delivery.* Nat Med, 2002. 8(4): p. 415-9.

44. Henry, S., et al., *Microfabricated microneedles: a novel approach to transdermal drug delivery.* J Pharm Sci, 1998. 87(8): p. 922-5.

45. Qiu, Y., et al., *Enhancement of skin permeation of docetaxel: a novel approach combining microneedle and elastic liposomes.* J Control Release, 2008. 129(2): p. 144-50.

46. Baek, C., et al., *Local transdermal delivery of phenylephrine to the anal sphincter muscle using microneedles.* J Control Release, 2011. 154(2): p. 138-47.

47. Martanto, W., et al., *Transdermal delivery of insulin using microneedles in vivo.* Pharm Res, 2004. 21(6): p. 947-52.

48. Cormier, M., et al., *Transdermal delivery of desmopressin using a coated microneedle array patch system.* J Control Release, 2004. 97(3): p. 503-11.

49. Zhu, Q., et al., *Immunization by vaccine-coated microneedle arrays protects against lethal influenza virus challenge.* Proc Natl Acad Sci U S A, 2009. 106(19): p. 7968-73.

50. Kim, Y.C., et al., *Enhanced memory responses to seasonal H1N1 influenza vaccination of the skin with the use of vaccine-coated microneedles.* J Infect Dis, 2010. 201(2): p. 190-8.

51. Gill, H.S., et al., *Cutaneous vaccination using microneedles coated with hepatitis C DNA vaccine.* Gene Ther, 2010. 17(6): p. 811-4.

52. Matriano, J.A., et al., *Macroflux microprojection array patch technology: a new and efficient approach for intracutaneous immunization.* Pharm Res, 2002. 19(1): p. 63-70.

53. Lee, J.W., et al., *Dissolving microneedle patch for transdermal delivery of human growth hormone.* Small, 2011. 7(4): p. 531-9.

54. Ito, Y., et al., *Self-dissolving microneedles for the percutaneous absorption of EPO in mice.* J Drug Target, 2006. 14(5): p. 255-61.

55. Sullivan, S.P., et al., *Dissolving polymer microneedle patches for influenza vaccination.* Nat Med, 2010. 16(8): p. 915-20.

56. Gupta, J., E.I. Felner, and M.R. Prausnitz, *Minimally invasive insulin delivery in subjects with type 1 diabetes using hollow microneedles.* Diabetes Technol Ther, 2009. 11(6): p. 329-37.

57. Davis, S.P., et al., *Hollow metal microneedles for insulin delivery to diabetic rats.* IEEE Trans Biomed Eng, 2005. 52(5): p. 909-15.

58. Gill, H.S., et al., *Effect of microneedle design on pain in human volunteers.* Clin J Pain, 2008. 24(7): p. 585-94.

59. Kaushik, S., et al., *Lack of pain associated with microfabricated microneedles.* Anesth Analg, 2001. 92(2): p. 502-4.

60. Miyano, T., et al., *Sugar micro needles as transdermic drug delivery system.* Biomed Microdevices, 2005. 7(3): p. 185-8.

61. Sivamani, R.K., et al., *Clinical microneedle injection of methyl nicotinate: stratum corneum penetration.* Skin Res Technol, 2005. 11(2): p. 152-6.

62. Donnelly, R.F., et al., *Microneedle arrays allow lower microbial penetration than hypodermic needles in vitro.* Pharm Res, 2009. 26(11): p. 2513-22.

63. Kalluri, H., C.S. Kolli, and A.K. Banga, *Characterization of microchannels created by metal microneedles: formation and closure.* AAPS J, 2011. 13(3): p. 473-81.

64.   Kalluri H, B.A., *Microneedles and transdermal drug delivery.* Journal of Drug Delivery Science and Technology, 2009. 19(5): p. 303-310.

65.   Kalluri, H. and A.K. Banga, *Formation and Closure of Microchannels in Skin Following Microporation.* Pharm Res, 2010.

66.   Lee, S.H., et al., *A role for ions in barrier recovery after acute perturbation.* J Invest Dermatol, 1994. 102(6): p. 976-9.

67.   Lee, S.H., et al., *Calcium and potassium are important regulators of barrier homeostasis in murine epidermis.* J Clin Invest, 1992. 89(2): p. 530-8.

68.   Menon, G.K., et al., *Localization of calcium in murine epidermis following disruption and repair of the permeability barrier.* Cell Tissue Res, 1992. 270(3): p. 503-12.

69.   Badran, M.M., J. Kuntsche, and A. Fahr, *Skin penetration enhancement by a microneedle device (Dermaroller) in vitro: dependency on needle size and applied formulation.* Eur J Pharm Sci, 2009. 36(4-5): p. 511-23.

70.   Bal, S.M., et al., *Influence of microneedle shape on the transport of a fluorescent dye into human skin in vivo.* J Control Release, 2010. 147(2): p. 218-24.

71.   Zhai, H. and H.I. Maibach, *Occlusion vs. skin barrier function.* Skin Res Technol, 2002. 8(1): p. 1-6.

72.   Tsai, J.C., et al., *Metabolic approaches to enhance transdermal drug delivery. 1. Effect of lipid synthesis inhibitors.* J Pharm Sci, 1996. 85(6): p. 643-8.

73.   Elias, P.M., et al., *The potential of metabolic interventions to enhance transdermal drug delivery.* J Investig Dermatol Symp Proc, 2002. 7(1): p. 79-85.

74.   Feingold, K.R., et al., *The lovastatin-treated rodent: a new model of barrier disruption and epidermal hyperplasia.* J Invest Dermatol, 1991. 96(2): p. 201-9.

75.   Menon, G.K., et al., *Structural basis for the barrier abnormality following inhibition of HMG CoA reductase in murine epidermis.* J Invest Dermatol, 1992. 98(2): p. 209-19.

76.   Mauro, T., et al., *Acute barrier perturbation abolishes the Ca2+ and K+ gradients in murine epidermis: quantitative measurement using PIXE.* J Invest Dermatol, 1998. 111(6): p. 1198-201.

77.   Denda, M., S. Fuziwara, and K. Inoue, *Influx of calcium and chloride ions into epidermal keratinocytes regulates exocytosis of epidermal lamellar bodies and skin permeability barrier homeostasis.* J Invest Dermatol, 2003. 121(2): p. 362-7.

78.   Singer, A.J. and R.A. Clark, *Cutaneous wound healing.* N Engl J Med, 1999. 341(10): p. 738-46.

79.   Funk, C.D., *Prostaglandins and leukotrienes: advances in eicosanoid biology.* Science, 2001. 294(5548): p. 1871-5.

80.   Dubois, R.N., et al., *Cyclooxygenase in biology and disease.* FASEB J, 1998. 12(12): p. 1063-73.

81.   Ruzicka, T. and M.P. Printz, *Arachidonic-Acid Metabolism in Skin - a Review.* Reviews of Physiology Biochemistry and Pharmacology, 1984. 100: p. 121-160.

82.   Vaheri, A., et al., *Nemosis, a novel way of fibroblast activation, in inflammation and cancer.* Exp Cell Res, 2009. 315(10): p. 1633-8.

83.   Marie L. Foegh, P.W.R., *The Eicosanoids: Prostaglandins, Thromboxanes, Leukotrienes, & Related Compounds*, in *Basic & Clinical Pharmacology*, B.G. Katzung, Editor 2004, The McGraw-Hill Companies, Inc: New York. p. 298 - 312.

84.   Vane, J.R., *Inhibition of prostaglandin synthesis as a mechanism of action for aspirin-like drugs.* Nat New Biol, 1971. 231(25): p. 232-5.

85.   Lee, J.L., et al., *Cyclooxygenases in the skin: pharmacological and toxicological implications.* Toxicol Appl Pharmacol, 2003. 192(3): p. 294-306.

86. Laulederkind, S.J., et al., *Both constitutive and inducible prostaglandin H synthase affect dermal wound healing in mice.* Lab Invest, 2002. 82(7): p. 919-27.

87. Leong, J., et al., *Cyclooxygenases in human and mouse skin and cultured human keratinocytes: association of COX-2 expression with human keratinocyte differentiation.* Exp Cell Res, 1996. 224(1): p. 79-87.

88. Anton, R.F., et al., *Naltrexone effects on alcohol consumption in a clinical laboratory paradigm: temporal effects of drinking.* Psychopharmacology (Berl), 2004. 173(1-2): p. 32-40.

89. Anton, R.F., et al., *Combined pharmacotherapies and behavioral interventions for alcohol dependence: the COMBINE study: a randomized controlled trial.* JAMA, 2006. 295(17): p. 2003-17.

90. *MICROMEDEX® 2.0.* Accessed July 3, 2012; Available from: <http://www.thomsonhc.com/micromedex2/librarian/%3E.

91. Banks, S.L., et al., *Flux across [corrected] microneedle-treated skin is increased by increasing charge of naltrexone and naltrexol in vitro.* Pharm Res, 2008. 25(7): p. 1677-85.

92. Paudel, K.S., et al., *Transdermal delivery of naltrexone and its active metabolite 6-beta-naltrexol in human skin in vitro and guinea pigs in vivo.* J Pharm Sci, 2005. 94(9): p. 1965-75.

93. Valiveti, S., et al., *Development and validation of a liquid chromatography-mass spectrometry method for the quantitation of naltrexone and 6beta-naltrexol in guinea pig plasma.* J Chromatogr B Analyt Technol Biomed Life Sci, 2004. 810(2): p. 259-67.

94. Curdy, C., et al., *Non-invasive assessment of the effect of formulation excipients on stratum corneum barrier function in vivo.* Int J Pharm, 2004. 271(1-2): p. 251-6.

95. Kalia, Y.N. and R.H. Guy, *The electrical characteristics of human skin in vivo.* Pharm Res, 1995. 12(11): p. 1605-13.

96. Kawai, E., et al., *Skin surface electric potential as an indicator of skin condition: a new, non-invasive method to evaluate epidermal condition.* Exp Dermatol, 2008. 17(8): p. 688-92.

97. Yamamoto, T. and Y. Yamamoto, *Electrical properties of the epidermal stratum corneum.* Med Biol Eng, 1976. 14(2): p. 151-8.

98. Puurtinen, M.M., et al., *Measurement of noise and impedance of dry and wet textile electrodes, and textile electrodes with hydrogel.* Conf Proc IEEE Eng Med Biol Soc, 2006. 1: p. 6012-5.

99. Barbero, A.M. and H.F. Frasch, *Pig and guinea pig skin as surrogates for human in vitro penetration studies: a quantitative review.* Toxicol In Vitro, 2009. 23(1): p. 1-13.

100. Fujii, M., et al., *Evaluation of Yucatan micropig skin for use as an in vitro model for skin permeation study.* Biol Pharm Bull, 1997. 20(3): p. 249-54.

101. Gore, A.V., A.C. Liang, and Y.W. Chien, *Comparative biomembrane permeation of tacrine using Yucatan minipigs and domestic pigs as the animal model.* J Pharm Sci, 1998. 87(4): p. 441-7.

102. Godin, B. and E. Touitou, *Transdermal skin delivery: predictions for humans from in vivo, ex vivo and animal models.* Adv Drug Deliv Rev, 2007. 59(11): p. 1152-61.

103. Gill, H.S. and M.R. Prausnitz, *Coating formulations for microneedles.* Pharm Res, 2007. 24(7): p. 1369-80.

104.   Smart, W.H. and K. Subramanian, *The use of silicon microfabrication technology in painless blood glucose monitoring.* Diabetes Technol Ther, 2000. 2(4): p. 549-59.

105.   Daddona, P.E., et al., *Parathyroid hormone (1-34)-coated microneedle patch system: clinical pharmacokinetics and pharmacodynamics for treatment of osteoporosis.* Pharm Res, 2011. 28(1): p. 159-65.

106.   Milewski, M., N.K. Brogden, and A.L. Stinchcomb, *Current aspects of formulation efforts and pore lifetime related to microneedle treatment of skin.* Expert Opin Drug Deliv, 2010. 7(5): p. 617-29.

107.   *3M Microneedle Technology.* August 16, 2011; Available from: http://solutions.3m.com/wps/portal/3M/en_WW/DrugDeliverySystems/DDSD/technology-solutions/transdermal-technologies/microstructured-transdermal-systems/.

108.   Grubauer, G., P.M. Elias, and K.R. Feingold, *Transepidermal water loss: the signal for recovery of barrier structure and function.* J Lipid Res, 1989. 30(3): p. 323-33.

109.   Lackermeier, A.H., et al., *In vivo ac impedance spectroscopy of human skin. Theory and problems in monitoring of passive percutaneous drug delivery.* Ann N Y Acad Sci, 1999. 873: p. 197-213.

110.   Tagami, H., et al., *Evaluation of the skin surface hydration in vivo by electrical measurement.* J Invest Dermatol, 1980. 75(6): p. 500-7.

111.   Karande, P., A. Jain, and S. Mitragotri, *Relationships between skin's electrical impedance and permeability in the presence of chemical enhancers.* J Control Release, 2006. 110(2): p. 307-13.

112.   Kohli, R., et al., *Impedance measurements for the non-invasive monitoring of skin hydration: a reassessment.* Int J Pharm, 1985. 26: p. 275 - 287.

113.   White, E. and A. Bunge. *Reporting Skin Resistance and Impedance*. in *Barrier Function of Mammalian Skin Gordon Research Conference*. 2009. Waterville Valley, NH.

114.   Milewski, M., *Microneedle-assisted transdermal delivery of naltrexone species: in vitro permeation and in vivo pharmacokientic studies*, 2011, University of Kentucky Doctoral thesis: Lexington, KY.

115.   Fullerton, A., et al., *Guidelines for measurement of skin colour and erythema. A report from the Standardization Group of the European Society of Contact Dermatitis.* Contact Dermatitis, 1996. 35(1): p. 1-10.

116.   Curdy, C., Y.N. Kalia, and R.H. Guy, *Post-iontophoresis recovery of human skin impedance in vivo.* Eur J Pharm Biopharm, 2002. 53(1): p. 15-21.

117.   Gupta, J. and M.R. Prausnitz, *Recovery of skin barrier properties after sonication in human subjects.* Ultrasound Med Biol, 2009. 35(8): p. 1405-8.

118.   Kiptoo, P.K., et al., *In vivo evaluation of a transdermal codrug of 6-beta-naltrexol linked to hydroxybupropion in hairless guinea pigs.* Eur J Pharm Sci, 2008. 33(4-5): p. 371-9.

119.   Schnetz, E., et al., *Multicentre study for the development of an in vivo model to evaluate the influence of topical formulations on irritation.* Contact Dermatitis, 2000. 42(6): p. 336-43.

120.   Brown, M.B. and S.A. Jones, *Hyaluronic acid: a unique topical vehicle for the localized delivery of drugs to the skin.* J Eur Acad Dermatol Venereol, 2005. 19(3): p. 308-18.

121.   *Micromedex® 2.0.* 2011 Available from: http://www.thomsonhc.com/micromedex2/librarian/.

122. Mauro, T., et al., *Barrier recovery is impeded at neutral pH, independent of ionic effects: implications for extracellular lipid processing.* Arch Dermatol Res, 1998. 290(4): p. 215-22.

123. Potts, R.O. and R.H. Guy, *A predictive algorithm for skin permeability: the effects of molecular size and hydrogen bond activity.* Pharm Res, 1995. 12(11): p. 1628-33.

124. Potts, R.O. and R.H. Guy, *Predicting skin permeability.* Pharm Res, 1992. 9(5): p. 663-9.

125. Smith, G., et al., *Regulation of cutaneous drug-metabolizing enzymes and cytoprotective gene expression by topical drugs in human skin in vivo.* Br J Dermatol, 2006. 155(2): p. 275-81.

126. PharmaDerm, *Solaraze® gel package insert.*, 2009.

127. Muller-Decker, K., et al., *Prostaglandin-H-synthase isozyme expression in normal and neoplastic human skin.* Int J Cancer, 1999. 82(5): p. 648-56.

128. Bucks, D. and H. Maibach, *Percutaneous Absorption*, ed. R.L. Bronaugh and H.I. Maibach1999, New York: Marcel Dekker, Inc.

129. Swadley, C.L., *Investigation of Endocannabinoid System Modulators for Percutaneous Drug Delivery*, 2011, University of Kentucky Doctoral thesis: Lexington, KY.

130. Andersen, F., et al., *Comparison of the response to topical irritants in hairless guinea pigs and human volunteers.* J Toxicol-Cutan Ocul Toxicol, 2005. 24: p. 31-43.

131. Ghosh, P., et al. *Microneedle enhanced transdermal delivery using a codrug approach (abstract accepted for presentation).* in *American Association of Pharmaceutical Scientists, Annual meeting.* 2011. Washington D.C.

132. Levin, G., et al., *Transdermal delivery of human growth hormone through RF-microchannels.* Pharmaceutical Research, 2005. 22(4): p. 550-555.

133. Ghosh, P., et al. *Microneedle enhanced transdermal delivery using a codrug approach (abstract accepted for presentation).* in *American Association of Pharmaceutical Scientists, Annual meeting.* 2011. Washington D.C.

134. Swadley, C.L., *Investigation of Endocannabinoid System Modulators for Percutaneous Drug Delivery. ,* in *Pharmaceutical Sciences*2011, University of Kentucky: Lexington, KY.

135. Milewski, M. and A.L. Stinchcomb, *Vehicle composition influence on the microneedle-enhanced transdermal flux of naltrexone hydrochloride.* Pharm Res, 2011. 28(1): p. 124-34.

136. Darlenski, R. and J.W. Fluhr, *Influence of skin type, race, sex, and anatomic location on epidermal barrier function.* Clin Dermatol, 2012. 30(3): p. 269-73.

137. Choi, E.H., et al., *Iontophoresis and sonophoresis stimulate epidermal cytokine expression at energies that do not provoke a barrier abnormality: lamellar body secretion and cytokine expression are linked to altered epidermal calcium levels.* J Invest Dermatol, 2003. 121(5): p. 1138-44.

138. Denda, M., et al., *The epidermal hyperplasia associated with repeated barrier disruption by acetone treatment or tape stripping cannot be attributed to increased water loss.* Arch Dermatol Res, 1996. 288(5-6): p. 230-8.

139. Menon, G.K., et al., *Selective obliteration of the epidermal calcium gradient leads to enhanced lamellar body secretion.* J Invest Dermatol, 1994. 102(5): p. 789-95.

140. Roblin, I., et al., *Topical treatment of experimental hydrofluoric acid skin burns by 2.5% calcium gluconate.* J Burn Care Res, 2006. 27(6): p. 889-94.

141. Robinson, M.K., *Population differences in acute skin irritation responses. Race, sex, age, sensitive skin and repeat subject comparisons.* Contact Dermatitis, 2002. 46(2): p. 86-93.

142. Robinson, M.K., M.A. Perkins, and D.A. Basketter, *Application of a 4-h human patch test method for comparative and investigative assessment of skin irritation.* Contact Dermatitis, 1998. 38(4): p. 194-202.

143. Ahn, S.K., et al., *Functional and structural changes of the epidermal barrier induced by various types of insults in hairless mice.* Arch Dermatol Res, 2001. 293(6): p. 308-18.

144. Birchall, J.C., et al., *Microneedles in clinical practice - an exploratory study into the opinions of healthcare professionals and the public.* Pharmaceutical Research, 2011. 28(1): p. 95 - 106.

<div align="center">**VITA**</div>

Nicole K. Brogden, Pharm.D.

Born: May 21, 1981

Birthplace: Ames, IA USA

EDUCATION AND TRAINING

Doctoral Candidate, University of Kentucky College of Pharmacy   2008 – present

    Clinical and Experimental Therapeutics Program

    Major advisor: Audra Stinchcomb, Ph.D.

Postgraduate Year One (PGY-1) Pharmacy Residency   2007 – 2008

    University of Kentucky HealthCare

    Program director: George A. Davis, Pharm.D., BCPS

Doctor of Pharmacy, The University of Iowa College of Pharmacy   May 2007

Bachelor of Science in Biology, The University of Iowa   May 2003

RESEARCH GRANTS AND FUNDING

1F31DA029374, NIH/NIDA   2010 – 2012

Project title: "Clinical evaluation of novel methods for extending microneedle pore lifetime"

ROLE: Principal Investigator

NIH/NIDA Clinical Loan Repayment Program   2010 – 2012

Project title: "Clinical evaluation of novel methods for extending microneedle pore lifetime" (2010 – 2012)

ROLE: Principal Investigator

Seed Grant, Center for Clinical and Translational Science   2010 – 2012

University of Kentucky

Project title: "Development of impedance spectroscopy as a means of evaluating extended pore lifetime following topical application of diclofenac sodium to microneedle treated skin"

ROLE: Principal Investigator

Pilot Research Program,   2009 – 2011

University of Kentucky Center for Clinical and Translational Science

Project title: "Effects of diclofenac gel on pore lifetime following transdermal microneedle insertion in healthy human subjects"

ROLE: Co-investigator, Research Coordinator

PUBLICATIONS

1. Brogden NK, Mehalick L, Fischer CL, Wertz PW, Brogden KA. (2012) Review - The emerging role of peptides and lipids as antimicrobial epidermal barriers and modulators of local inflammation. *Skin Pharmacology and Physiology.* 25(4): 167 – 81. PMID: 22538862.

2. Brogden NK, Brogden KA. (2011) Review - Will new generations of modified antimicrobial peptides improve their potential as pharmaceuticals? *International Journal of Antimicrobial Agents*. Sep;38(3):217-25. PMID: 21733662

3. Banks SL, Paudel KS, Brogden NK, Loftin CD, Stinchcomb AL. (2011) Diclofenac enables prolonged delivery of naltrexone through microneedle-treated skin. *Pharmaceutical Research*. May;28(5):1211-9. PMID: 21301935

4. Paudel KS, Milewski M, Swadley CL, Brogden NK, Ghosh P, Stinchcomb AL. (2010) Challenges and opportunities in transdermal delivery. *Therapeutic Delivery*. 1(1):109 – 131, July 2010.

5. Banks SL, Pinninti RR, Gill HS, Crooks PA, Brogden NK, Prausnitz MR, Stinchcomb AL. (2010) Transdermal delivery of naltrexol and skin permeability lifetime after microneedle treatment in hairless guinea pigs *in vivo*. *Journal of Pharmaceutical Sciences.* 99(7):3072-80, July 2010. PMID: 20166200

6. Milewski M, Brogden NK, Stinchcomb AL. (2010) Current aspects of formulation efforts and pore lifetime related to microneedle treatment of skin. *Expert Opinion on Drug Delivery.* 7(5):617-29, May 2010. PMID: 20205604

7. Florang VF, Rees JR, <u>Brogden NK,</u> Anderson DG, Hurley TD, and Doorn JA. (2007) Inhibition of mitochondrial aldehyde dehydrogenase-mediated oxidation of 3,4-dihydroxyphenylacetaldehyde. In Enzymology and Molecular Biology of Carbonyl Metabolism 13. (Weiner, E., Maser, E., Lindahl, R. and Plapp, B., Eds.) pp. 33-39, Purdue University Press, West Lafayette, Indiana.

8. Florang VF, Rees JR, <u>Brogden NK,</u> Anderson DG, Hurley TD, and Doorn JA. (2007) Inhibition of the oxidative metabolism of 3,4-dihydroxyphenylacetaldehyde, a reactive intermediate of dopamine metabolism, by 4-hydroxy-2-nonenal. *Neurotoxicology*. 28(1):76-82, January 2007. PMID: 16956664

PUBLICATIONS SUBMITTED

1. Diclofenac delays micropore closure following microneedle treatment in human subjects. Submitted to *Journal of Controlled Release.*

PUBLICATIONS IN PREPARATION

1. Development of *in vivo* impedance spectroscopy techniques for measurement of micropore formation

2. Pharmacokinetic evaluation of microneedle/diclofenac sodium enhanced 7-day transdermal delivery of naltrexone HCl in healthy human volunteers

AWARDS AND HONORS

Pre-Doctoral Fellowship,   2010 – 2012
American Foundation for Pharmaceutical Education (AFPE)

3rd place, Rho Chi Research Day Poster Award,   April 2010
Graduate Student category
University of Kentucky College of Pharmacy

Nomination, Cystic Fibrosis Humanitarian Award   Spring 2008
Lexington, KY

Class of 2007 Excellence in Research Award   Spring 2007
The University of Iowa College of Pharmacy

Best Poster, Pharm.D. Student category,	Spring 2007
8th Annual Research Achievement Day Symposium and Poster Session	
The University of Iowa College of Pharmacy	
President's List, The University of Iowa	Spring 2007
Student Leader Spotlight	2006
The University of Iowa College of Pharmacy 2005-2006 Annual Report	
Best Presentation Award,	Spring 2006
Biological and Health Sciences Division 8th Annual James F. Jakobsen	
Graduate Conference	
The University of Iowa	
Jakobsen Forum Award Winner Spotlight	Fall 2006
The University of Iowa Graduate College	
Poster Session Award	Spring 2006
8th Annual Interdisciplinary Health Research Poster Session	
The University of Iowa	
The University of Iowa College of Pharmacy Scholarship	Spring 2006
APhA-ASP National Patient Counseling Competition local winner	Fall 2006
The University of Iowa College of Pharmacy	
The National Dean's List	2005 – 2006
Iowa Pharmacy Foundation Scholarship	2004 – 2005
The University of Iowa Pharmacy Tuition Scholarship	2006 – 2007, 2003 – 2004

Student Abstract Award Finalist,   May 2003
The American Society for Microbiology

Howard Hughes Research Fellow, The University of Iowa   2001 – 2002

Dean's List, The University of Iowa 9 semesters,   2000 – 2007

Nicole K. Brogden
_____
Student's signature
July 17, 2011
_____
Date